

**POLITECNICO DI MILANO**

Scuola di Ingegneria Industriale e dell'Informazione

Corso di Laurea Magistrale in

Ingegneria Energetica



# Analysis of Electrical Heating Technologies from a Flow Assurance point of View

Relatore: Prof. Luigi Pietro Maria COLOMBO

Correlatore: Dott. Alberto DI LULLO

Tesi di laurea di:

Giovan Battista ZAMBETTI Matr. 852964

Anno accademico 2016/2017



**POLITECNICO DI MILANO**

Scuola di Ingegneria Industriale e dell'Informazione

Corso di Laurea Magistrale in

Ingegneria Energetica



# Analysis of Electrical Heating Technologies from a Flow Assurance point of View

Relatore: Prof. Luigi Pietro Maria COLOMBO

Correlatore: Dott. Alberto DI LULLO

Tesi di laurea di:

Giovan Battista ZAMBETTI Matr. 852964

Anno accademico 2016/2017



## RINGRAZIAMENTI

---

Il primo e il più doveroso ringraziamento va al Professor Colombo, che mi ha aiutato nella realizzazione di questo lavoro e mi ha supportato, e sopportato, nei momenti più critici; senza di lui tutto sarebbe stato molto più difficile. Un ringraziamento speciale va anche ad Alberto Di Lullo, che mi ha guidato durante il mio stage: le sue osservazioni e i suoi suggerimenti hanno reso possibile la stesura di questa tesi. Ringrazio ENI S.p.A. per avermi dato la possibilità di lavorare su questo progetto e per avermi fatto affacciare al mondo del lavoro.

Pensando a questo momento, non posso non ringraziare la mia famiglia che ha sempre creduto in me. Grazie Mamma perché mi hai insegnato l'infinita pazienza della carità e sei la mia sicurezza in momenti in cui mi sembra che vada tutto storto. Grazie Papà perché mi hai fatto capire che l'amore si può donare senza parole ma con tanti piccoli gesti quotidiani. Benny ho sempre sostenuto che tu fossi fortunata ad avere un fratello come me, ma in verità sono io fortunato ad averti come sorella. Grazie per avermi insegnato il valore delle proprie scelte e delle responsabilità che da essere derivano. Grazie Stefano perché in questi anni siamo diventati una famiglia nonostante le incomprensioni e le difficoltà, spero che la vita ti riservi il meglio. Un pensiero va anche alla mia seconda famiglia, Silvano, Catia, Daniele, Marta, Pietro e Agnese: grazie per tutte le risate e i momenti belli che abbiamo passato e che passeremo insieme.

Un grazie anche a tutti i miei i miei compagni di avventura del Politecnico di Milano grazie per le ore passate insieme studiando come se non ci fosse un domani e per tutte le difficoltà che abbiamo superato insieme.

Un pensiero anche ai miei fratelli scout del gruppo Lovere 1 per avermi aiutato a diventare la persona che sono oggi.

Infine, l'ultimo ringraziamento, ma non per importanza: grazie Silvia perché, anche se da poco, tu mi stai rendendo felice. Non ho idea di cosa il futuro ci riservi, ma sono convinto che la strada percorsa insieme sia meno faticosa.



# EXTENDED SUMMARY

---

## **Introduction and Scope**

The increasing demand of liquid fuels drives the Oil&Gas industry towards more challenging scenarios. Furthermore, the so called “easy-to-reach” oil is already exploited. With the term “easy-to-reach” it is indicated the oil from conventional sources as onshore and shallow offshore fields. For this reason, the Oil&Gas industry is focusing its efforts on the exploitation of deep and ultra-deep offshore fields. However, the installation of a production platform is justified only for large or giant fields due to the tremendous economical commitment faced by the Oil&Gas industry. In this context, it is clear the importance of long tie-backs from new oil field to existing facilities. From the point of view of cost perspective long tie-backs are crucial, as they give access to far reserves avoiding the costs of new top-side installations. This can be used for the development of marginal fields that are too small to be economically produced on their own. However, the employment of long tie-back increases the risk of flow assurance issues such as wax and hydrate depositions. Such depositions may reduce or even stop the flow from the reservoir, resulting in an exceedingly high financial loss. The deposition of solids is favoured by high pressure and low temperature. In general, the wellhead conditions are characterized by high pressure and high temperature. However, the temperature of the fluid inside the flowline decreases because heat losses to the surrounding are inevitable. In order to reduce the heat losses, high-performance insulating materials are installed. During normal operating conditions, passive insulation is valid only for limited pipeline lengths because a perfect insulating material does not exist, hence temperature reduction takes place. The situation becomes more critical if for any reason the hot stream from the reservoir decreases. Passive insulation is a temporary solution even during transient scenarios, such as shut-down and start-up. As a matter of fact, during the shut-down phase the hot flow from the reservoir is interrupted and the fluids cool down to the sea water temperature. The operators have no control over the temperature, and so that mitigation methods must be employed. To prevent flow assurance problems, conventional technologies as chemicals injection and dead oil recirculation are employed. Two kinds of chemicals can be used to avoid the formation of hydrates: thermodynamic hydrate inhibitors and low dosage hydrate inhibitors. The former work by shifting the hydrate equilibrium curve to lower the hydrate formation temperature enough to avoid the formation of

solid deposits. The latter are based on a different mechanism as they do not change the hydrate formation curve, but act on the mechanism of formation of the hydrates. However, such technologies are viable only for short pipelines because of their investment and operational costs associated to the looped configuration and pumping constraint. Furthermore, the conventional flow assurance technologies require time to become effective. Hence it is clear that for challenging tie-backs the conventional solutions may not be feasible. In this context, active heating technologies can be employed to allow the production from marginal fields, which otherwise will be not exploited. Active heating is defined as the injection of heat into a production system. In this way, it is possible to control the temperature during transient and normal operating conditions. The benefit of active heating systems is that they allow the pipeline to be heated in order to maintain the temperature above the solid deposition temperature avoiding the employment of conventional flow assurance technologies. In practice different operational modes of the active heating technologies exist, as they can be used to maintain the temperature or to warm-up the fluids especially after a long shut-down. Two types of active heating can be incorporated into a production system: one is based on the circulation of a hot fluid within the system; the other is based on electrical heating. The focus of this work is to compare the different electrical heating technologies from a flow assurance point of view. In such technologies a current is circulated either in the pipe wall or in electrical heaters suitably arranged around the pipe and heat is dissipated according to the Joule effect. Two different technologies have been investigated: direct electrical heating (DEH) and electrical heat traced flowline (EHTF). In the former a current is circulated directly inside the pipe wall, while in the latter electrical cables are laid between the wall of the flowline and the carbon steel layer. The most common application is the open-loop DEH. In the open loop configuration, a single electrical cable is piggy-backed on the flowline and it carries the total current of the system. The current afterward returns through the wall of the pipe generating heat, due to the Joule effect. Heat is transferred to the fluids by conduction in the carbon steel layer.

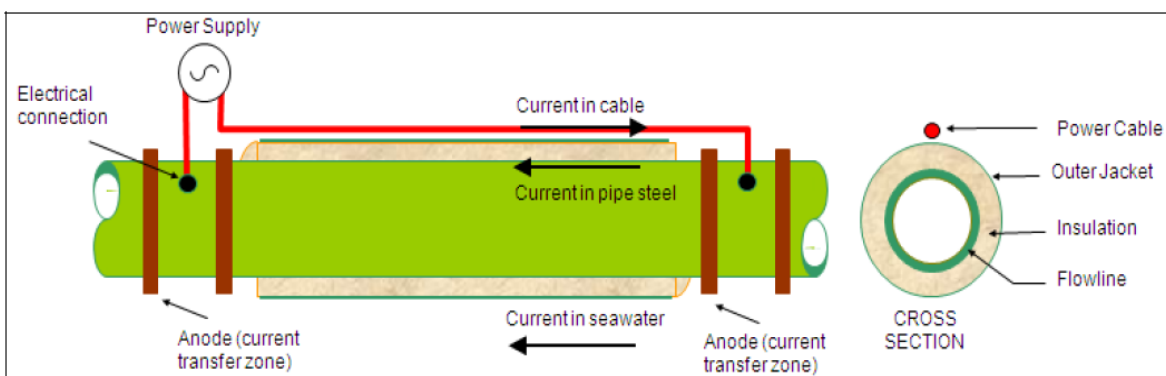


Figure 1. Open Loop DEH

The open-loop DEH is a mature technology that can be used either for preservation and remediation purposes. The EHTF technology is based on the employment of high performance insulation material in combination with a simple, robust and low power consumption electrical heating system within a compact pipe-in-pipe design. As already mentioned, the heating system is composed of copper wires laid between the inner pipe and the insulation material. A schematic of the layout is presented in the figure below.

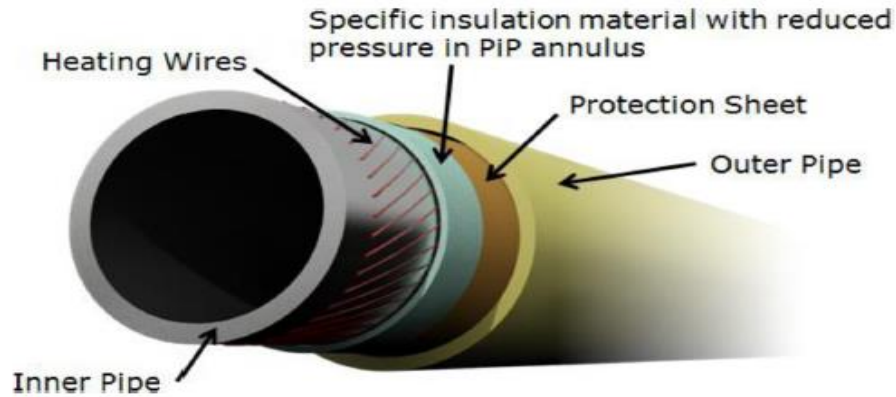


Figure 2. EHTF Pipe-in-Pipe Configuration

In the EHTF technology there is no need for the installation of a return cable for the current because the copper wires are joined in a star configuration.

### **Model Description**

Conjugated models of the fluid dynamics and heat transfer have been implemented in MATLAB® to simulate the steady-state behaviour of the electrical heating technologies. The models discretize the flowline in elements in which the energy equation and the heat transfer problem are solved to calculate the pressure and temperature variation of a multiphase system. The results from one element are used as an input for the following one. The procedure is repeated for the overall length of the line to obtain the trends of the principal thermodynamics variables. Since the fluid properties are a function of both the pressure and the temperature two iterative procedures must be implemented to solve the problem. Initially, the variation of the pressure is calculated using the equation below, which derives from the theory of two-phase systems.

$$-\frac{dP}{dz} = -\frac{dP}{dz}\Big|_a - \frac{dP}{dz}\Big|_g - \frac{dP}{dz}\Big|_f \quad (1)$$

From the equation above is possible to understand that the pressure gradient is the sum of three terms respectively: the acceleration pressure gradient, the gravitational pressure gradient and the frictional pressure gradient. The calculation of the first two contributions is straightforward, while for the evaluation of the frictional pressure drop different approaches can be used. In this work it has been used a separated flow approach that considers the two-phase flow to be artificially separated into two streams, each flowing in its own pipe, with the assumption that the velocity of each phase is constant in the zone occupied by the phase. The method is based on the calculation of the two-phase friction multipliers  $\phi_l^2$ ,  $\phi_g^2$ , which are defined as the ratio between the two-phase frictional pressure drop to the frictional pressure gradient for the liquid/gas phase flowing alone.

$$\phi_l^2 = \frac{\left(\frac{\Delta p}{\Delta z}\right)_{tp}}{\left(\frac{\Delta p}{\Delta z}\right)_l} \quad (2)$$

$$\phi_g^2 = \frac{\left(\frac{\Delta p}{\Delta z}\right)_{tp}}{\left(\frac{\Delta p}{\Delta z}\right)_g} \quad (3)$$

Once the pressure variation of the element has been estimated the models calculate the temperature variation. The temperature variation in the element is calculated as the sum of two contributions.

$$\Delta T = \Delta T_{th} + \Delta T_{JT} \quad (4)$$

The first is associated to the heat flow entering/exiting the element, while the second is related to the Joule-Thompson effect. Such effect describes the temperature change of a real gas or liquid when it is subjected to a pressure variation. In order to calculate the heat flow for each technology the models solve different heat transfer problems. The simplest solution is obtained for the passive insulation configuration, in which there is no power generation inside the pipeline wall and consequently a lumped parameter approach based on the calculation of the thermal resistances can be used. In the figure below are reported the cross section and the equivalent thermal circuit of the flowline.

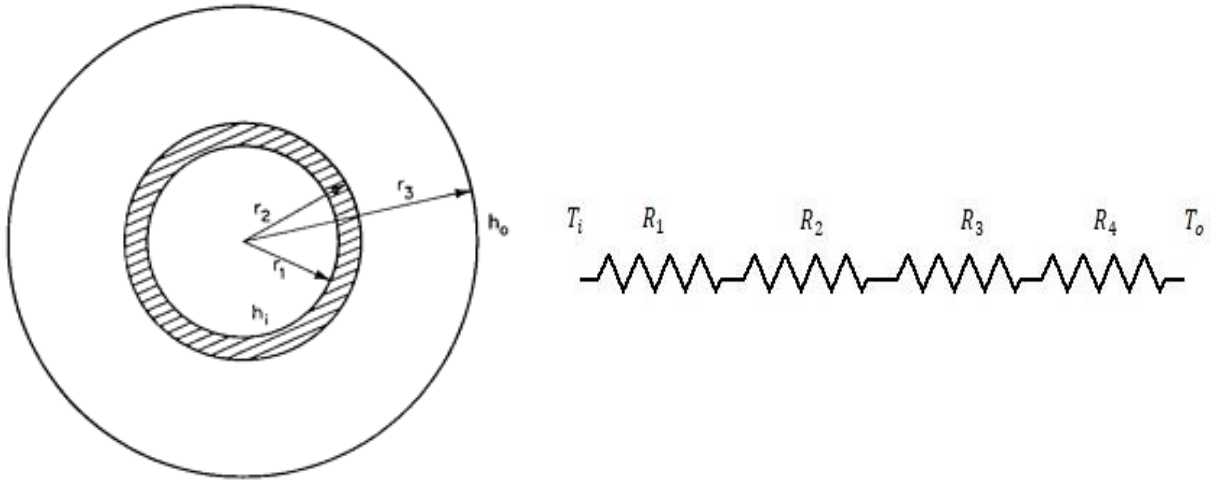


Figure 3. Cross Section and Equivalent Thermal Circuit of the Passive insulation technology

The overall equivalent thermal resistance of the system is computed as the sum of the four resistances which describes the heat transfer from the fluids inside the flowline to the surrounding environment.

$$R_{tot} = R_1 + R_2 + R_3 + R_4 = \frac{1}{h_i A_i} + \frac{\ln\left(\frac{r_2}{r_1}\right)}{2\pi L k_{cs}} + \frac{\ln\left(\frac{r_3}{r_2}\right)}{2\pi L k_{ins}} + \frac{1}{h_o A_o} \quad (5)$$

The lumped parameter approach cannot be used in the other technologies because the concept of thermal resistance is meaningless in the case of active media. Concerning the DEH technology the geometry is the same as for the passive insulation, however in the carbon steel layer there is a generation of heat due to the passage of the current. For this reason, it is necessary to integrate the general steady-state heat conduction equation in cylindrical coordinates and constant thermal conductivity to obtain the heat flow entering/exiting the flowline.

$$\frac{1}{r} \frac{d}{dr} \left( r \frac{dT}{dr} \right) + \frac{S}{k} = 0 \quad (6)$$

Two kinds of current (direct and alternate) can be circulated resulting in a different power generation in the carbon steel layer. The boundary conditions necessary to define the unique solution of the problem must be set according to the different configuration considered. Concerning the EHTF technology a different procedure is adopted due to the geometry of the pipeline cross section. The pipe circumference is divided in several sections, which are dealt with in the same manner owing to the symmetry of the thermal field.

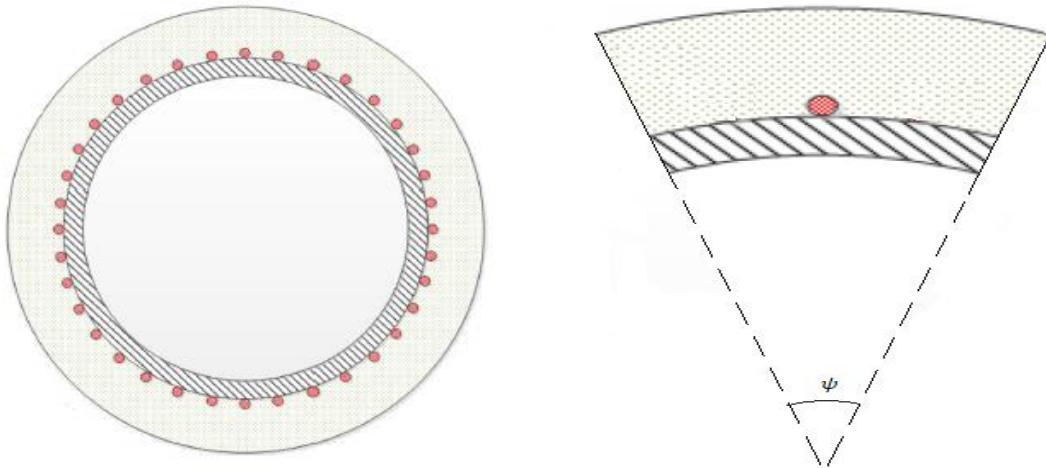


Figure 4. Cross Section and Section of the element considered for the heat transfer problem, EHTF technology

An approximate solution can be obtained by applying the fin theory to the carbon steel layer. However, to apply such a theory it is necessary to neglect the curvature of the considered section and to define an equivalent convective heat transfer coefficient for the carbon steel layer. The governing equation describing the temperature distribution in a fin, under the assumption of one-dimensional heat conduction along the x direction is used to evaluate the heat transfer rate in the flowline. The solution is then carried out element by element.

### **Model Validation**

Validation has been provided by comparison with results of the commercial software OLGA<sup>®</sup>, which is used in the Oil&Gas industry to simulate multiphase flows. OLGA<sup>®</sup> allows to simulate actively heated pipelines. However, it makes no distinctions between the different electrical heating technologies. For this reason, the comparison is performed considering the same conditions in OLGA<sup>®</sup> and in the models implemented in Matlab<sup>®</sup>. The predictions for a 10 km horizontal insulated flowline are reported in the graphs below.

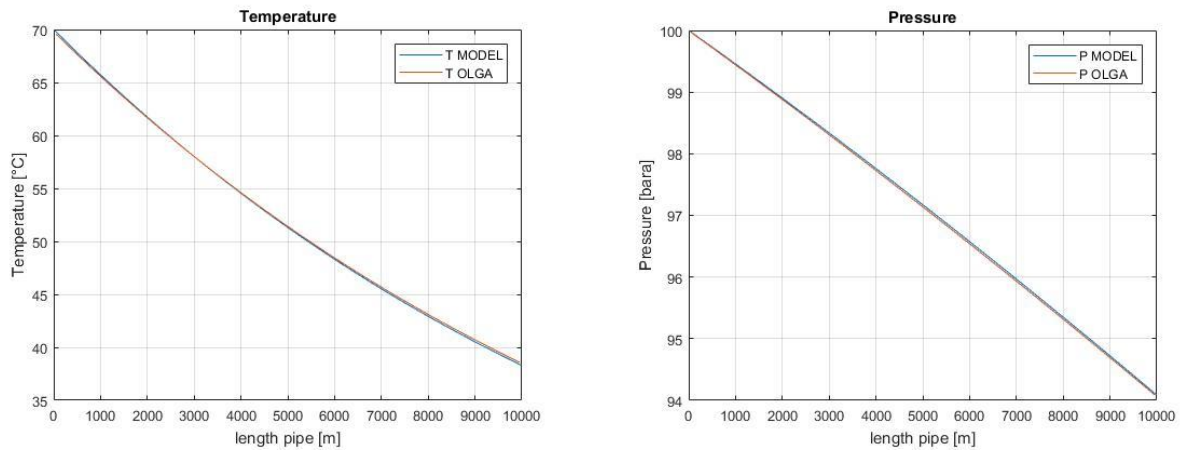


Figure 5. Comparison of the temperature and pressure trends obtained with the model and OLGA®

The maximum relative percentage difference between the trends obtained with OLGA® and with the models implemented in MATLAB® is 0,5% for the temperature and 0,04% for the pressure. Since the difference between the predictions is very small the models have been considered validated.

### Simulation Results

The validated models are used to evaluate the benefits of the electrical heating technologies in a case study of a fictitious production scenario. A poor-insulated 20 km long flowline has been simulated considering the various technologies. The figures 6,7 and 8 report the different trends of the temperature obtained.

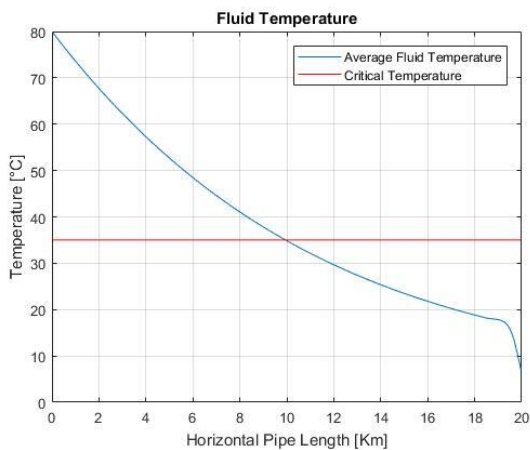


Figure 6 Temperature Variation, Only insulation

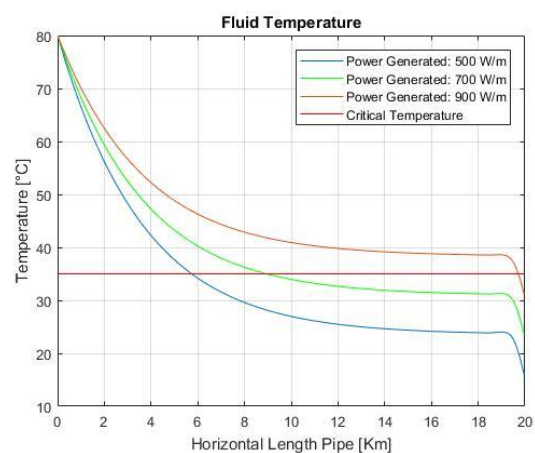


Figure 7 Temperature Variation, DEH

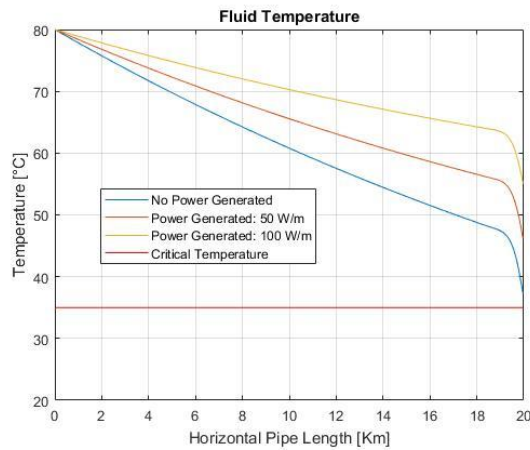


Figure 8 Temperature Variation, EHTF

From the figure 6, it is clear that employing only the passive insulation technology the temperature drops below the critical level for solid depositions leading to the risk of plugging the pipeline. As can be seen from the figures 7 and 8 the employment of the electrical heating technologies allows to maintain the pipeline inside the steady-state operating region. Furthermore, the installation of high performance insulating material, in the EHTF technology, enables the operation of the pipeline without the need of the active heating. However, the real benefits of the active heating technologies are obtained during transient scenarios. A preliminary transient analysis has been performed with the aid of OLGA® on a well-insulated 60 km long flowline. During the shutdown phase the electrical heating technology enables maintaining the flowline above the hydrate formation temperature before the operation is resumed.

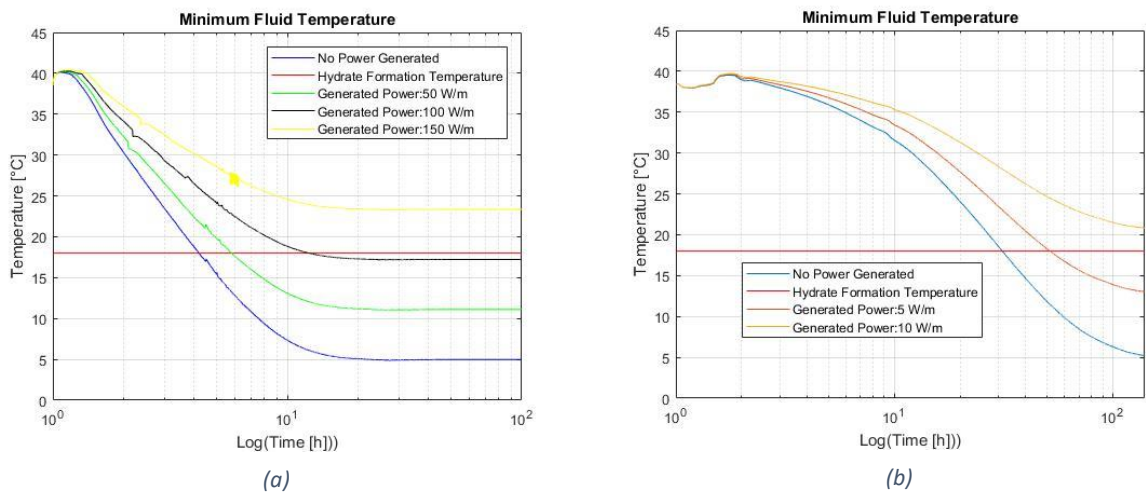


Figure 9. Trend of the minimum temperature during a shutdown, DEH(a) and EHTF(b) technology

It is evident from the graphs above that the required power to maintain the pipeline above the hydrate formation temperature is one order of magnitude smaller for the EHTF technology than

the one of the DEH technology. Furthermore, the higher level of insulation of the EHTF configuration results in a longer “no-touch” time compared to the one of the DEH technology. The “no-touch” time is defined as the period of time from the start of the shutdown until the flowline reaches the hydrate formation temperature. It is the time in which the operators can try to correct the problems without the need to protect the subsea system. During a start-up phase the electrical heating technologies can be employed to warm up the fluids until the minimum temperature exceeds the hydrate formation temperature.

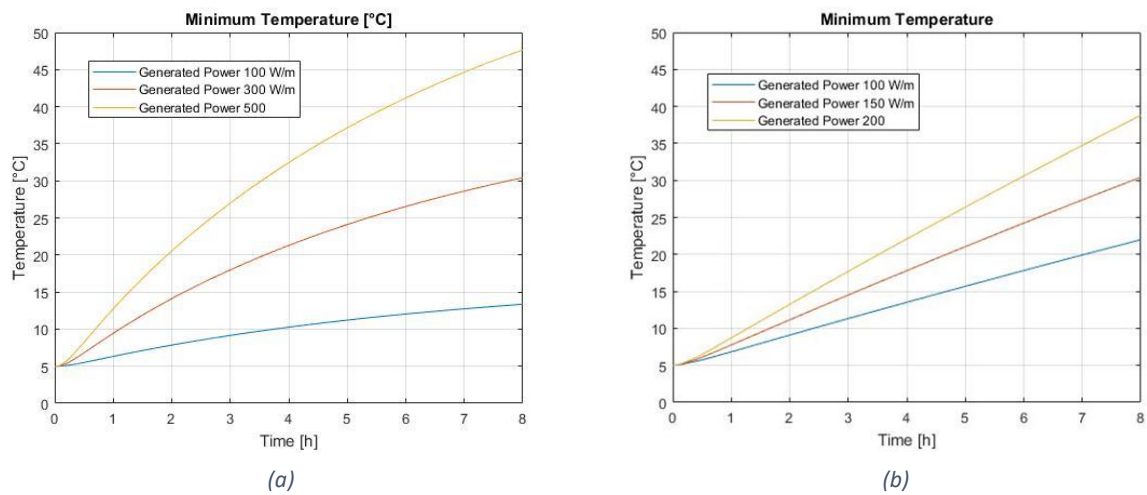


Figure 10. Trend of the minimum temperature during a start-up, DEH (a) and EHT (b)F technology

Considering the trends of the minimum temperature for the different technologies is possible to see that the higher level of insulation provided by the EHTF technology results in a shorter start-up time for a given level of generated power. For this reason, the power required to start the production after 8 hours is smaller for the EHTF configuration than the one for the DEH.

## **Conclusions**

Electrical heating technologies can be used to maintain the temperature above the critical level for wax and hydrates depositions. By providing a solution to these flow assurance challenges, electrical heating technologies enable the production from marginal fields that otherwise will result inconvenient from the economic point of view. Furthermore, the case studies analysed show the advantages of the employment of the EHTF technology over the DEH technology. The benefits derive from the combination of a high-performance insulation material with a simple, robust and low power consumption electrical heating system within a compact pipe-in-pipe design.



# INDEX

---

RINGRAZIAMENTI.....	5
EXTENDED SUMMARY.....	7
ABSTRACT.....	21
SOMMARIO.....	23
1 Chapter 1- Flow Assurance Challenges.....	25
1.1 Introduction to flow assurance.....	25
1.2 Hydrate and Wax formation.....	25
1.2.1 Hydrate.....	26
1.2.2 Wax.....	26
1.3 Flow assurance technologies.....	27
1.3.1 Thermal insulation.....	27
1.3.2 Thermodynamic hydrate inhibitors.....	28
1.3.3 Low Dosage Hydrate Inhibitors (LDHI).....	28
1.3.4 Wax Inhibitors.....	29
1.3.5 During Shutdowns.....	29
2 Chapter 2: Active Heating Technologies.....	31
2.1 Hot water systems.....	31
2.2 Electrical Heating.....	31
2.3 Operational modes.....	32
2.3.1 Maintaining temperature during shutdown.....	32
2.3.2 Heating up from Seabed Temperature.....	32
2.3.3 Continuous use during flowing conditions.....	33
2.4 Direct Electrical Heating (DEH).....	33
2.4.1 Open loop DEH.....	33
2.4.2 End-Fed Pipe-in-Pipe DEH.....	34
2.4.3 Center-Fed Pipe-in-Pipe DEH.....	35
2.5 Electrically heated traced flowline (ehtf).....	36
3 Chapter 3: Steady State Electrical Heating Simulator.....	39
3.1 Introduction to the model.....	39
3.2 Logic of the Simulator.....	39
3.3 Fluid Properties.....	42

3.4	Evaluation of the Pressure drop.....	42
3.4.1	Creation of the equivalent fluid .....	43
3.4.2	Energy Balance .....	43
3.4.3	Kinetic contribute.....	45
3.4.4	Frictional contribute.....	46
3.4.5	Gravitational Contribute .....	48
3.5	Solution Heat Transfer Problem.....	48
3.5.1	Passive Insulation .....	48
3.5.2	Direct Electrical Heating DC .....	51
3.5.3	Direct Electrical Heating AC.....	55
3.5.4	Electrically Heat-Traced Flowline .....	58
3.6	Two-Phase Heat Transfer Coefficient.....	67
3.7	External Heat Transfer Coefficient .....	69
4	Chapter 4: Validation of the model.....	71
4.1	Logic of the validation .....	71
4.2	10 km Horizontal Flowline - Only insulation .....	71
4.3	10 Km Catenary Flowline – Only Insulation .....	73
4.4	10 Km Catenary Flowline – DEH.....	75
5	Chapter 5: Case Study .....	77
5.1	Introduction to the problem .....	77
5.2	Well Insulated Flow Line with Cold Inlet.....	79
5.3	Poor Insulated Flow Line .....	83
5.4	Insulated Flowline .....	85
5.5	Direct Electrically Heated Flowline (DC).....	86
5.6	Direct Electrically Heated Flowline (AC).....	89
5.7	DEH DC VS DEH AC .....	91
5.8	Electrically Heated Traced Flowline .....	93
5.9	Comparison of the different configurations .....	95
6	Chapter 6: Transient Analysis of Active Heating Technologies.....	97
6.1	Introduction to the problem .....	97
6.2	Steady-State Analysis .....	98
6.3	Planned Shut-Down.....	101
6.4	Unplanned Shut-Down.....	104
6.5	Cold Start Up .....	106

6.6	Final Considerations .....	108
7	CONCLUSIONS .....	109
	List of Figures .....	111
	Nomenclature .....	113
	Bibliography .....	115



## ABSTRACT

---

“Easy-to-reach” oil is finished. However, the world demand of liquid fuels is constantly rising. For this reason, Oil&Gas companies are focusing their effort in the exploitation of deep and ultra-deep offshore fields. To justify the economical commitment only large and giant fields can be exploited. Long tie-backs to existing facilities are crucial to exploit small fields, which production otherwise will result uneconomical. However, flow assurance issues, such as wax and hydrate deposition, becomes critical. In this context more cost-effective flow assurance technologies must be employed to enable the production from such fields. One of the most promising technology is Active Heating, which is by definition the injection of heat into a production system. In this work steady-state electrical heating simulators have been implemented in MATLAB® in order to compare the different technologies from a flow assurance point of view. The fluid dynamic validity of the models is verified with the aid of the commercial software OLGA®. The models are then applied to a case study to extract general considerations. A preliminary transient analysis has been also performed to compare the different technologies. From the results, is possible to understand that the employment of the active heating technologies is fundamental to avoid solid depositions during normal flowing conditions. Furthermore, the technologies allow to maintain the temperature during a shut-down and warm-up the fluids during a cold start-up. The installation of high-performance insulating material is necessary to reduce the power requirement of the different active heating technologies.



## SOMMARIO

---

Il petrolio facilmente estraibile è finito, tuttavia la domanda mondiale di combustibili liquidi è in continuo aumento. Per questo motivo le compagnie petrolifere stanno concentrando i loro sforzi nell'esplorazione e sfruttamento di giacimenti in acque sempre più profonde, tuttavia solo grandi giacimenti possono essere sfruttati per via del tremendo impegno economico. Collegare giacimenti marginali con delle infrastrutture già esistenti è fondamentale per ridurre i costi e quindi per produrre da riserve che altrimenti non sarebbero economicamente sfruttabili. La gestione del flusso di idrocarburi, tuttavia, diventa critica per lunghe distanze, per via della deposizione di cere e di idrati che possono completamente ostruire la condotta. In pratica diversi metodi, come ad esempio l'iniezione di inibitori chimici, vengono usati per mantenere il flusso di idrocarburi. Le tecnologie tradizionali tuttavia sono estremamente costose e quindi non possono essere economicamente applicate su condotte lunghe. In questo scenario le tecnologie di riscaldamento attivo possono essere applicate per ridurre i costi e produrre da campi marginali. Lo scopo di questa tesi è di analizzare le varie tecnologie di riscaldamento elettrico dal punto di vista termo-fluido dinamico. Per confrontare le differenti soluzioni diversi modelli sono stati implementati in MATLAB®. I modelli sono stati validati con l'ausilio del simulatore commerciale OLGA. I modelli sono successivamente stati applicati in un caso studio in regime stazionario e per un'analisi preliminare in regime transitorio. Dai risultati ottenuti è possibile capire che l'impiego delle tecnologie di riscaldamento elettrico è fondamentale per evitare la deposizione di cere e idrati e che l'impiego in combinazione con materiali molto isolanti è cruciale per limitare la potenza necessaria per riscaldare la linea.



# 1 CHAPTER 1- FLOW ASSURANCE CHALLENGES

---

## 1.1 INTRODUCTION TO FLOW ASSURANCE

The expression “flow assurance” indicates all the activities performed to ensure a safe flow of hydrocarbons from the reservoir to the process facility. Flow assurance is a multidisciplinary science which encompasses different engineering disciplines. It is sometimes referred to as “cash assurance” because any interruption of the flow would result in a tremendous financial loss. Flow assurance is crucial in deep water scenarios because most of the flowline and riser sections are exposed to a low sea water temperature, which enhances heat losses into the environment. This leads to favourable thermodynamic conditions, high pressures and low temperatures, for the formation of solid deposits, at the risk of degrading or even killing the flow path [1]. Among the potential impediments there may be the formation and deposition of hydrates, paraffins, scales, and asphaltenes in wells, flowlines, or production facilities, as well as corrosive constituents in the flow stream. Under normal operation conditions the thermal insulation of the line is, in general, enough to ensure a safe transportation of the hydrocarbon. However, this solution is effective only for a limited length of the pipe, as a matter of fact a temperature reduction is inevitable because the thermal insulation is not perfect. Furthermore, it has been demonstrated that a pipeline with infinite insulating performance would still experience temperature decrease in the in-field flowlines, but especially in the riser section due to elevation changes. Within the past 10 years, the number of long tie-backs doubled. Long tie-backs to existing infrastructures are certainly strategic from a cost perspective, as they give access to far reserves avoiding new topside installations. The importance of flow assurance is clear; however, for these applications the conventional technologies may be too expensive. For this reason, more cost-effective technologies are required to face the thermal challenges present in deep water and long-distance tie-backs [2].

## 1.2 HYDRATE AND WAX FORMATION

As stated before, operations in deep water and colder climates expose the production fluids to low temperatures. These temperature and pressures may cause the formation of hydrates and wax, solid deposits that can potentially plug the flow line.

### 1.2.1 Hydrate

In oil/gas exploration, production, transportation or processing hydrates represent a potential risk which involves water and molecules smaller than n-pentane. Hydrates are formed when natural gas components occupy empty lattice positions in the water structure. As a matter of fact, when small non-polar molecules contact water at moderate temperature and high pressures, a water crystal form called hydrate may appear [3]. In this case, it seems like water is solidifying at temperatures considerably higher than its normal freezing point. As can be seen from the fig 1.2.1 it is possible to understand the effect of the thermodynamic variables on the hydrate formation.

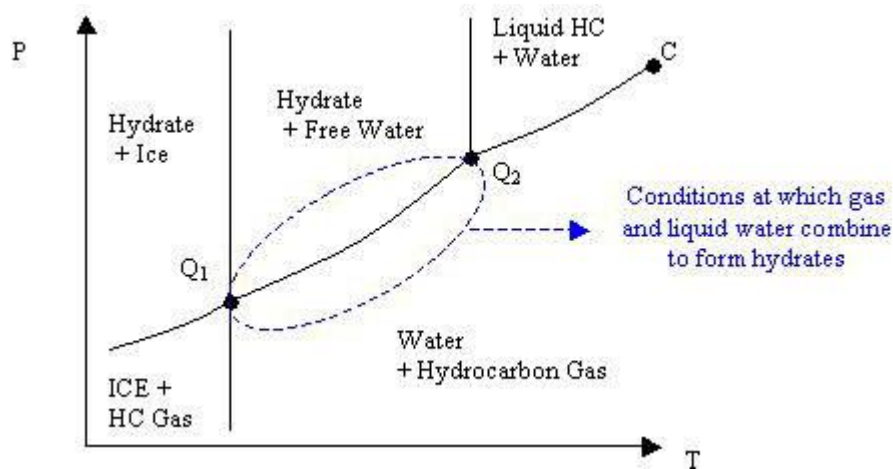


Figure 1.2.1 Phase diagram for water/hydrocarbon system

The three-phase critical point on the diagram is point C that represents the condition where the liquid and gas hydrocarbon merge into a single hydrocarbon phase in equilibrium with liquid water.  $Q_2$  and  $Q_1$  are respectively the upper and the lower quadruple points, where four phases (liquid water, liquid hydrocarbon, gaseous hydrocarbon and solid hydrate) are in equilibrium. However, in case of practical implementation the segment  $Q_1Q_2$  is the most important one, since it represents the thermodynamic conditions for hydrate formation or dissociation. Undoubtedly, the phase diagram of water and hydrocarbon changes according to the different properties of the fluids; nevertheless, it is generally possible to see a common behaviour, which is that hydrates formation is favoured at low temperatures and high pressures. The formation of hydrates is possible only if there is free water.

### 1.2.2 Wax

Paraffin wax produced from crude oil consists primarily of long chains, saturated hydrocarbons (linear alkanes/ n-paraffins) with carbon chain lengths of C18 to C75+, having individual melting points from 40 to 70°C. The deposition process of wax can be divided into two phases: nucleation

and growth. As the temperature drops below a critical level, the dissolved waxes begin to form insoluble crystals which then tend to deposit on the production system. The properties of the wax change according to the different molecules involved, which depend on the composition of the crude. The most important parameter that needs to be assessed is the critical temperature below which the wax nuclei start to form. This temperature is called wax appearance temperature (WAT), and it depends on various parameters, such as oil composition, pressure, paraffin concentration etc.

As with other solids-depositing problems, prevention can be more cost effective than removal. To prevent the formation of solid deposits different technologies have been developed either to maintain the temperature of the produced fluids or to decrease the critical temperature of the formation by injecting chemical inhibitors. In the following different technologies to manage hydrate and wax are presented.

### 1.3 FLOW ASSURANCE TECHNOLOGIES

It is worth noting that not all the field developments require hydrate or wax management. It depends on the production fluid, well characteristic and the surrounding environment. Under normal flowing conditions, in general the pipeline insulation is enough to maintain the produced fluid of the hydrate region. However, especially in the early life of a field, looped lines and periodic pigging of the flowline and riser are required to address the wax deposition. When there is a risk of hydrate or wax deposition, suitable technologies should be employed. These can be classified according to their working principle and maturity level of application. In this comparison only thermal and chemical matured technologies will be considered. Matured technologies, which are well established since they have been employed for a decade or longer, are considered the standard for most applications and are widely available in the market.

#### 1.3.1 Thermal insulation

This technology is based on the installation of high performance materials to maintain the temperature of a production stream to prevent the formation of hydrates. It also allows to extend the cool down period after the shutdown by delaying the hydrate and wax formation. However, for very long distances the solution is inefficient; as a matter of fact a temperature drop, even in the case of perfect insulation is inevitable due to Joule-Thompson effect. This passive solution is interesting, but during a shutdown, the temperature is maintained only for a limited period thus a combination with another technology is required. Furthermore, materials that may have been

sufficient for a certain water depth (1000-1200 m) are not necessarily suitable for deeper water depths and failures can be magnified.

### **1.3.2 Thermodynamic hydrate inhibitors**

Thermodynamic inhibitors, such as methanol and ethylene glycol, work by shifting the hydrate equilibrium curve to lower the hydrate equilibrium temperature enough to keep the system out of the hydrate formation region. To determine the optimum chemical treatment a series of parameters under both steady-state and transient operating conditions must be considered, these parameters are for instance the hydrate structure, the operating conditions, the water composition and cut, the injection points and conditions. In general, thermodynamic inhibitors require a high injection rate, which has to be adjusted over time due to the variation of the system parameters that are not constant during the overall life of the system. The technology is based on a continuous injection strategy, thus regeneration units are employed to recover and regenerate the chemicals in order to reduce the costs associated with the purchase of “fresh” inhibitors. Thermodynamic inhibitors represent an extremely effective solution and they are a common technology in field application. However, exploration and production into deeper waters with harsher conditions, long subsea tieback and high production rates prompted the need for cheaper and more effective inhibition methods [4].

### **1.3.3 Low Dosage Hydrate Inhibitors (LDHI)**

Low dosage hydrate inhibitors differently from the thermodynamic inhibitors do not change significantly the hydrate formation curve because they operate on a completely different mechanism. They can be divided into two categories anti-agglomerates (AAs) and kinetic hydrate inhibitors (KHIs). The first ones are surface molecules which prevent the agglomeration and growth of the hydrate particles, thus they allow to avoid the plugging of the line. The action of the AAs results in the formation of a transportable slurry of tiny hydrate particles in oil. The employment of AAs has two limitations, namely the water cut and the topside emulsion formation. They have a water cut limitation because the system requires an oil layer in which the hydrates are dispersed, furthermore, since AAs are surfactants they may contribute to stabilize the emulsion formation and/or affect the overboard water quality. Kinetic hydrate inhibitors (KHIs) are typically water soluble, low molecular weight polymers whose active groups interfere with the nucleation and growth of hydrate crystals. They delay the hydrate formation for a length of time, which is called “induction time”. Since KHIs operate on a time-dependent mechanism, they are not practical systems which may experience long shutdown mechanism[5].

#### 1.3.4 Wax Inhibitors

Wax inhibitors can be divided into two categories crystal modifiers and dispersants. Paraffin-crystal modifiers are chemicals that interact with the crude-oil waxes to deform the crystal morphology of the crude-oil wax. Once deformed the crystal cannot undergo the normal steps of aggregation. Maleic acid esters, polymeric acrylate and methacrylate esters and ethylene vinyl polymers and copolymers are included among the types of paraffin-crystal modifiers. Dispersants act to prevent the wax nuclei from agglomerating. They are generally surfactants which may also keep the pipe surface wet, minimizing the tendency of wax to adhere to it [6].

#### 1.3.5 During Shutdowns

It is also important to consider the shutdown period, i.e. the period of time during which the flow of the produced fluids is interrupted. More specifically the hot flow from the reservoir ceases consequently the temperature drops because of the heat losses to the environment. A conventional method to remain outside the hydrate formation region consists in depressurising the line to decrease the critical temperatures. Chemicals are then injected during the restart of the line, while the pressure increases. However, this solution is not always feasible. Another solution is the live hydrocarbon displacement, which consists in displacing the production fluids in the flowline using externally threated liquid: such as dead oil or diesel, which have low appearances temperature, hence they allow to avoid solid deposition in the line. This type of solution requires a loop arrangement, which is very costly.

For long distances, in order to avoid costly loop or huge amount of chemicals to be injected others solution have to be exploited. Active heating can be employed to raise the temperature of the produced fluids. The employment of such technologies allows to safely operates the flowlines reducing the investment costs. Furthermore, the fluid information necessary to correctly operate such technologies are less than the ones required for the conventional solutions. In the following chapter, Direct Electrical Heating (DEH) and Electrical Heated Traced Flowline (EHTF) are presented [2].



## 2 CHAPTER 2: ACTIVE HEATING TECHNOLOGIES

---

An efficient way to manage hydrates, wax and viscous production fluid consist of heating the lines to stay above the respective appearance temperatures. Active heating is, by definition, heat injected from some external source into a production system. The benefit of the active heating systems is that they allow heat to be added to the pipeline to maintain the temperature above the solid deposition temperature without the need to depressurize the line. Two types of active heating can be incorporated into a production system; one is based on the circulation of a hot fluid within the system, while the other is based on electrical heat input.

### 2.1 HOT WATER SYSTEMS

This technology can incorporate the benefits of a high-performance insulation system with the circulation of hot fluids. The use of a high-performance insulation system is a necessity as it can significantly reduce the heat load for the active heating. There are two types of hot water circulation one is based on direct heating by annulus circulation and the other on indirect heating from a dedicated hot water line. In the direct hot water circulation technology, the hot water flows in the annulus of the production pipeline, then it can be either injected into an injection well or it can return to the topside through a separated line. The indirect hot water circulation uses the heat provided by a dedicated hot water supply and returns flowlines to maintain the temperature in the production flowlines. The production and the hot water lines are contained within an insulation layer, which is filled with a low-pressure gas such as nitrogen to reduce the losses to the environment [7].

### 2.2 ELECTRICAL HEATING

In these technologies the electrical energy is converted into heat following the principle of Joule heating. As a matter of fact, when an electric current flows through a solid or liquid with finite conductivity, electric energy is converted to heat through the resistive losses in the material. Heat is generated on the microscale when the conduction electrons transfer energy to the conductor's atoms by way of collisions. The electrical heating technologies can supply a uniform heat input along the entire length of the flowline, something which is not possible with the hot water systems.

The pipeline can be heated electrically resorting to two different methods. On one hand, in the Direct electrical heating solution, the current passes through the steel wall of the pipe. The heat thus generated is then transferred to the fluid. To close the electrical circuit the current returns by a cable in the case of a wet insulated pipeline or by the outer pipeline in the case of a pipe in pipe system. On the other hand, in the case of indirect electrical heating solution, external heating devices, such as wires are installed around the pipeline below the insulation layer. This system is suitable for pipe in pipe configurations. The Pipe-in-Pipe technology consists of the production of pipelines which are sleeved into an outer pipe with the annulus which is kept dry and filled with a high-performance material.

In the following paragraph the electrical heating technologies will be analysed from an operation and technological point of view.

### 2.3 OPERATIONAL MODES

The selection and design of an active heating system will be governed by its requirement for different scenarios, for instance temperature maintenance during normal flowing conditions, or planned/unplanned shutdown, or fluid warm up from ambient conditions during restart. In order to maintain the temperature of the hydrocarbon produced in the flowline, the electrical heating system must provide as much heat as the one which is lost into the surroundings through the pipeline steel and insulation. To raise the temperature the system must provide more heat than the one dispersed [8]. In the following paragraphs the three main modes of operation of an active system are presented:

#### 2.3.1 Maintaining temperature during shutdown

Using an active heated technology is possible to maintain the temperature of the flowline during a shutdown. The system can be immediately turned on during the shutdown, in order to avoid the formation of hydrates and/or waxes. Furthermore, there is not a delay for the prevention of the deposition of solids, unlike traditional flow assurance methods which require operations time to circulate dead oil or inject chemicals.

#### 2.3.2 Heating up from Seabed Temperature

The electrical system can be used to bring a flowline's content up to a desired flowing temperature. This is particularly useful, if the system is not activated during the shutdown to restart the flow of the fluids. The power level required to heat up from the seabed temperature is normally greater than the power which is necessary to maintain the temperature, but this depends on the desired heat-up time, the pipe diameter and the U value. It is worth noting that after the initial start-up of

the flowline, the need to heat up a line should be a rare event. So, a relatively long heat-up time may be acceptable and only a small amount of additional power over the maintenance power is required.

### 2.3.3 Continuous use during flowing conditions

The continuous use of the electrical system is necessary for fluids of high viscosity, high pour point or gelation temperature, or long tie-backs where the temperature drop along the line may result in wax and/or hydrates, which may even form during flowing conditions. In this case the electrical heating system is necessary to heat up the fluids above their normal flowing temperatures.

## 2.4 DIRECT ELECTRICAL HEATING (DEH)

Direct electrical heating of flowlines is an alternative to conventional flow assurance techniques it provides heat directly to the flowline by supplying electrical current in the pipe wall. The current causes the steel to warm up because of the electrical resistance of the metal. Then, by thermal conduction the heat is transferred from the pipe wall to the production fluid, thereby maintaining the temperature of the flow above the critical wax and/or hydrate temperatures. In practice different configurations of the DEH based on how the current is transferred to the pipe exist.

### 2.4.1 Open loop DEH

In the open loop configuration, a single electrical cable is piggy-backed on the flowline and it carries the total current of the system. The current afterward returns through the wall of the pipe generating heat, due to the Joules effect. This configuration forms a single-phase circuit which is connected to the power supply of the platform. In figure 2.4.1 a schematic of the technology is presented.

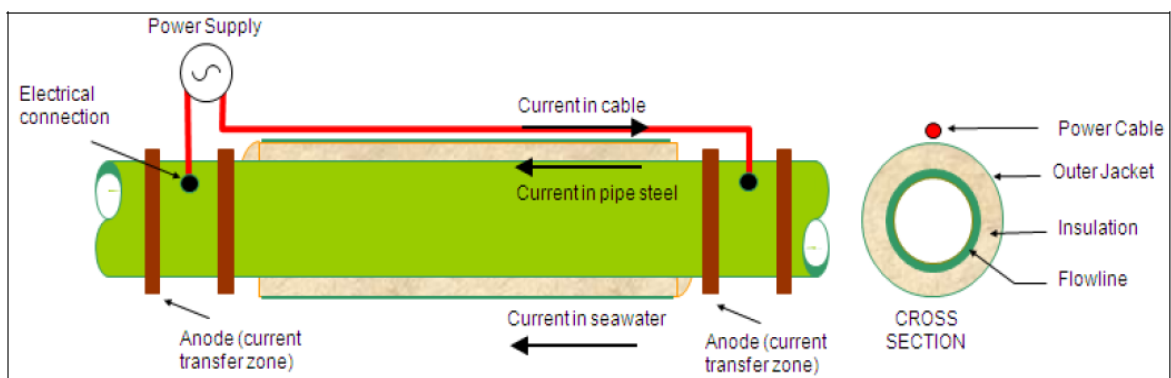


Figure 2.4.1 Schematic Open Loop Direct Electrical Heating

For safety and reliability reasons, the direct electrical heating system is electrically connected (“earthed”) to the surrounding seawater through several sacrificial anodes for a length of about 50

meters at both ends where the cables are connected. These zones are called “current transfer zones”. In this configuration, the seawater functions as a current return path in parallel to the steel pipe, hence the return current is divided between the pipe and the seawater. The repartition of the current depends mainly on the pipe dimensions and magnetic/electrical characteristics of the steel pipe material. In considering the continuous use of the open loop DEH potential corrosion risks from stray currents moving from the pipeline to the seawater particularly in locations of coating damage and premature anode consumption are important factor to be assessed. With properly a designed and engineered cathode protection and an adequate anode surface area, both potential issues should not prevent it from being applied continuously. Open loop Direct Electrical Heating has been identified as a mature and robust technology among the heating technologies [9].

#### 2.4.2 End-Fed Pipe-in-Pipe DEH

In this technology, the current passes through the outer and the inner pipeline, which are electrically connected by a conducting bulkhead. This component allows the current to flow down one pipe and return to the other. At the power supply end an insulating joint is installed, to avoid the possibility to create a short circuit between the electrical supply and the near end bulkhead. An overview of the solution is shown in figure 2.4.2.

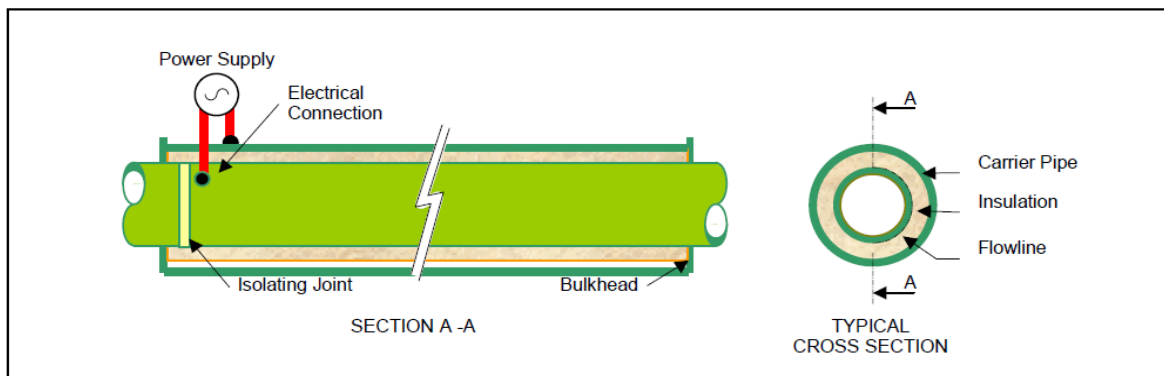


Figure 2.4.2 Schematic End-Fed Pipe-in-Pipe DEH

Since the technology is based on the Pipe-in Pipe configuration and the outer and the inner pipe are the electrical conductors, if the system works using an alternate current (AC), the skin and the proximity effects are present. The skin effect is the tendency of the alternating current to flow mostly near the outer surface of an electrical conductor. The effect becomes more and more apparent as the frequency increases. The proximity effect is the tendency of AC current to move in close proximity to AC current in the opposite directions. The effects are presented in figure 2.2.3.

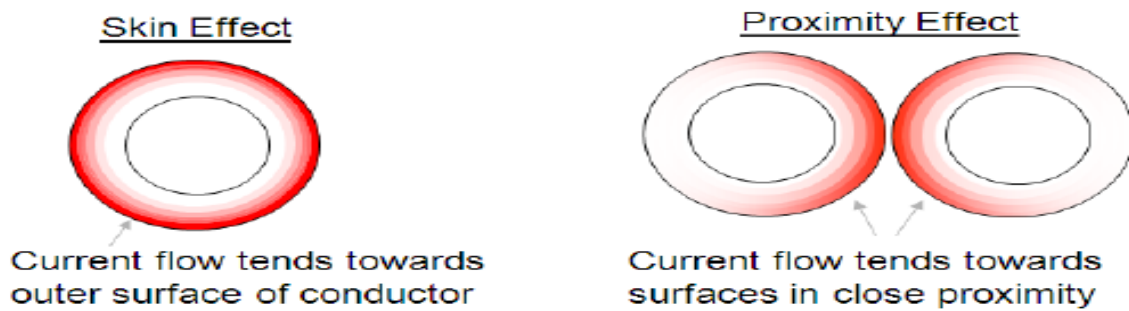


Figure 2.4.3 Skin and Proximity Effects

The combination of both the skin and proximity effect makes the current flow concentrate towards the annulus surfaces, limiting the need for precautions to prevent large stray currents from flowing in the seawater. However, a cathodic protection system is necessary, especially where the conductors are not coaxial, for instance where there are the bulkheads. Although some of the available power is dissipated in the outer pipe, where it doesn't contribute to the heating of the fluid, the absence of the piggyback cable reduces the thermal losses to the environment. Furthermore, there is the possibility to install high performance insulating material in the annulus because of its dry conditions. For these reasons the Pipe-in-Pipe system is considered more efficient than the open loop DEH, even if the technology is more complex and costly.

### 2.4.3 Center-Fed Pipe-in-Pipe DEH

This solution is very similar to the End-Fed Pipe-in-Pipe DEH because also in this case the outer and the inner pipes are used as electrical conductors. However, in the Center-Fed Pipe-in-Pipe technology the power source is connected to the mid-point via the mid line assembly and bulkheads are installed at both ends of the segment. In figure 2.4.4 a schematic of the technology is presented.

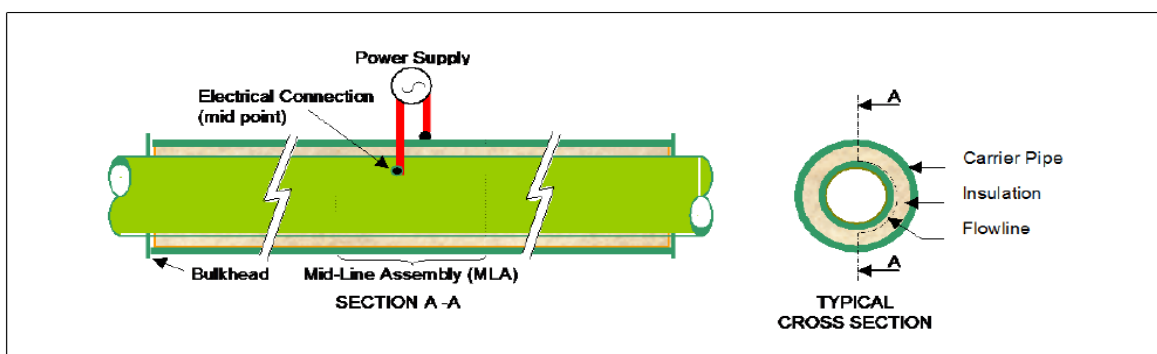


Figure 2.4.4 Schematic Center-Fed Pipe-in-Pipe DEH

In many system, the voltage must be stepped down with a subsea transformer to inject the optimal amount of current into the flowline. The transformer is then connected to the Mid-Line Assembly

(MLA), which is the component that houses the electrical connections to the inner and outer pipes. The system is suitable for application on long flowlines or fragmented subsea developments, where the heated sections can be divided into discrete segments, each with a MLA.

As far as open loop and PiP DEH systems are concerned, quality assurance during the construction and installation phases is critical to the success of the operation, particularly in the initial start-up where there may be risks from DEH short circuiting. Both systems that have been discussed are relatively simple to install. There are several applications in operation in subsea production systems. In addition, the life expectancy of the system components is challenged by the continuous use of DEH. All the insulation and other materials that will be subjected to elevated temperatures, in the annulus and at power connections, should be tested to determine the service life at DEH temperatures.

## 2.5 ELECTRICALLY HEATED TRACED FLOWLINE (EHTF)

This technology is based on the employment of high performance insulation material in combination with a simple, robust and low power consumption electrical heating system within a compact pipe-in-pipe design. The dry conditions of the annulus of the pipe-in-pipe configuration allow the installation of a specific material arrangement, namely mineral/silica based microporous pre-compressed insulation combined with a reduced pressure environment, which provides an excellent thermal insulation. The heating system is composed of copper wires laid between the inner pipe and the insulation material. Heat is generated following the Joule effect as the current flows through the wires. A schematic of the system is presented in figure 2.5.1.

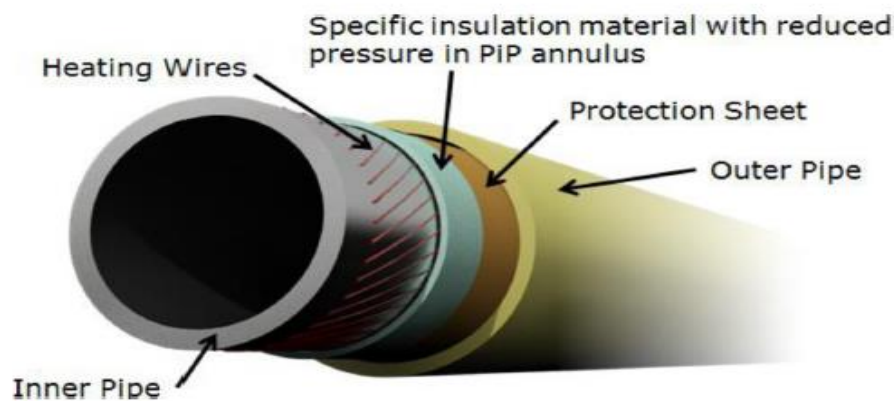


Figure 2.5.1 Schematic of the EHTF Pipe-in-Pipe

With the installation of a high insulation material the thermal losses to the environment are reduced; this results in a lower consumption of the heating system, allowing long tiebacks and operations at reduced voltages compared to alternate heating systems. The electrical cables are connected in a 3-phase circuit, each triplet terminates at the end of the flowline via a star end connection, avoiding the installation of a return umbilical [10]. Two of the main features of the technology are its flexibility and high redundancy. As a matter of fact, with 36 wires organized in 12 independent heating units that can be switched when needed, the reliability of the system increases. Another advantage of the technology is that the electrical cables operate in a dry environment, so standard onshore cables and electrical connectors can be used, thus limiting the need for the new components to be qualified. Besides the installation of the heating system, also fibre optical cables, which allow the monitoring of the temperature are installed. On the down side, the assembly process is more complex and costly, as it requires specific equipment to wind the cables around the inner pipe and attention must be paid to the electrical connections. Moreover, the employment of a pipe-in-pipe configuration limits the dimension of the inner pipe [11].

To deeper understand the characteristics of each technology from a flow assurance point of view in the following chapters a thermo-fluid dynamic model, which allows to simulate the different systems, is presented. The technologies that have been simulated are the open-loop DEH and the electrically heated traced flowline. The former is the most common electrical heating technology, while the latter is the most promising one. The different solutions are then analysed and confronted in a case study, as reported in the respective chapter.



## 3 CHAPTER 3: STEADY STATE ELECTRICAL HEATING SIMULATOR

---

### 3.1 INTRODUCTION TO THE MODEL

The goal of the model is to simulate the trend of the main thermodynamic variables of a steady-state multiphase system flowing inside an electrically heated pipeline. The model, which is implemented in MATLAB®, is based on a finite element approach. As a matter of fact, the simulator divides the flowline in sections in which it solves the conservation of energy and momentum equations. The main inputs for the model are the geometry of the problem, the thermal and electrical properties of the materials of the system, the properties of the fluids as function of pressure and temperature and the inlet conditions of the flowline, namely the inlet pressure, the inlet temperature and the total flow rate. After the discretization of the flowline, the model starts considering the first segment, because the inlet conditions are known, and using an iterative procedure finds the outlet conditions of the segment, which will be used as inlet for the following element. The procedure is repeated for the overall length of the pipeline. The fluid-dynamic validity of the model, in case there is no electrical heating, is validated with OLGA®, which is a commercial dynamic multiphase flow simulator, extensively used in the Oil&Gas industry. OLGA® also simulates an active heated pipeline, but it doesn't make any distinction between the different technologies because it allows only to set a constant generated power. For this reason, the models are needed to evaluate the thermodynamic performances of the different technologies. In the following paragraphs the logic and the different equations that have been implemented in MATLAB® are presented.

### 3.2 LOGIC OF THE SIMULATOR

As stated before the model, once the geometry, the properties of the materials and of the fluids and the inlet conditions are known, implements a finite element approach. The models discretize the line in different elements, as shown in figure 3.2.1, surely the larger the number of sections is the more precise the solution of the problem is, even though the computational time increases.

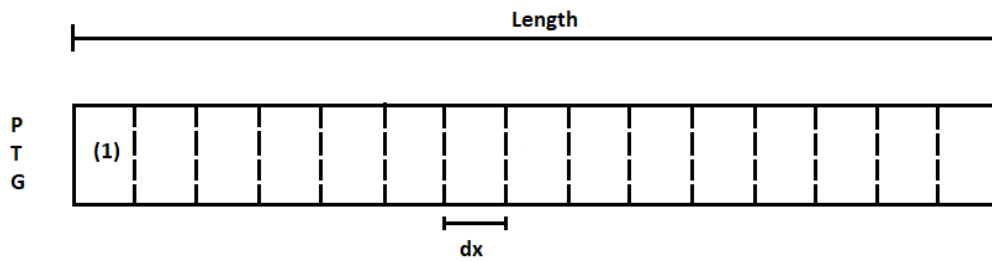


Figure 3.2.1 Example of discretization of the line

The inlet conditions of the pipeline are given, so the programme calculates the temperature and the pressure variation for the first element, the results are used as input for the following section, the procedure is repeated for the overall length of the pipe. Since the fluid properties are a function of both the pressure and the temperature an iterative procedure must be implemented to solve the problem. First of all the model enters an iterative loop to calculate the temperature. The simulator guesses the initial value of temperature at the outlet of the element and calculates the average temperature as the arithmetic average between the inlet and the outlet conditions. Then, it enters a second iterative cycle for calculating the pressure, similarly at what done before, it guesses the first value of the outlet pressure and calculates the average pressure value. In the pressure cycle the fluid properties are evaluated at the mean conditions and the equation of the energy conservation is solved. The solution of such equation is the pressure variation inside the element, which allows to evaluate the outlet pressure. If the calculated value is different from the guessed one, the procedure is repeated assuming the calculated value as the outlet pressure. The cycle is repeated until the convergence between the calculated and the guessed outlet pressure is reached. At this point the model has calculated the actual pressure drop for the wrong temperature variation. To obtain the correct temperature variation the heat transfer problem must be solved. The solution of the equation is the temperature variation in the element. Once again, if the calculated outlet temperature is different from the guessed one the procedure is repeated updating the outlet value with the calculated one. The pressure variation is then calculated according to the new temperature variation, and so on, until the convergence is reached in both the temperature and the pressure cycles. As a result, the element is completely solved as the pressure and temperature variation are calculated. Hence, it is possible to repeat the entire procedure the procedure to the following element considering as inlet conditions the outlet of the previous element. The flow diagram of the model is presented in figure 3.2.2. The heat transfer problem is different for the different technologies.

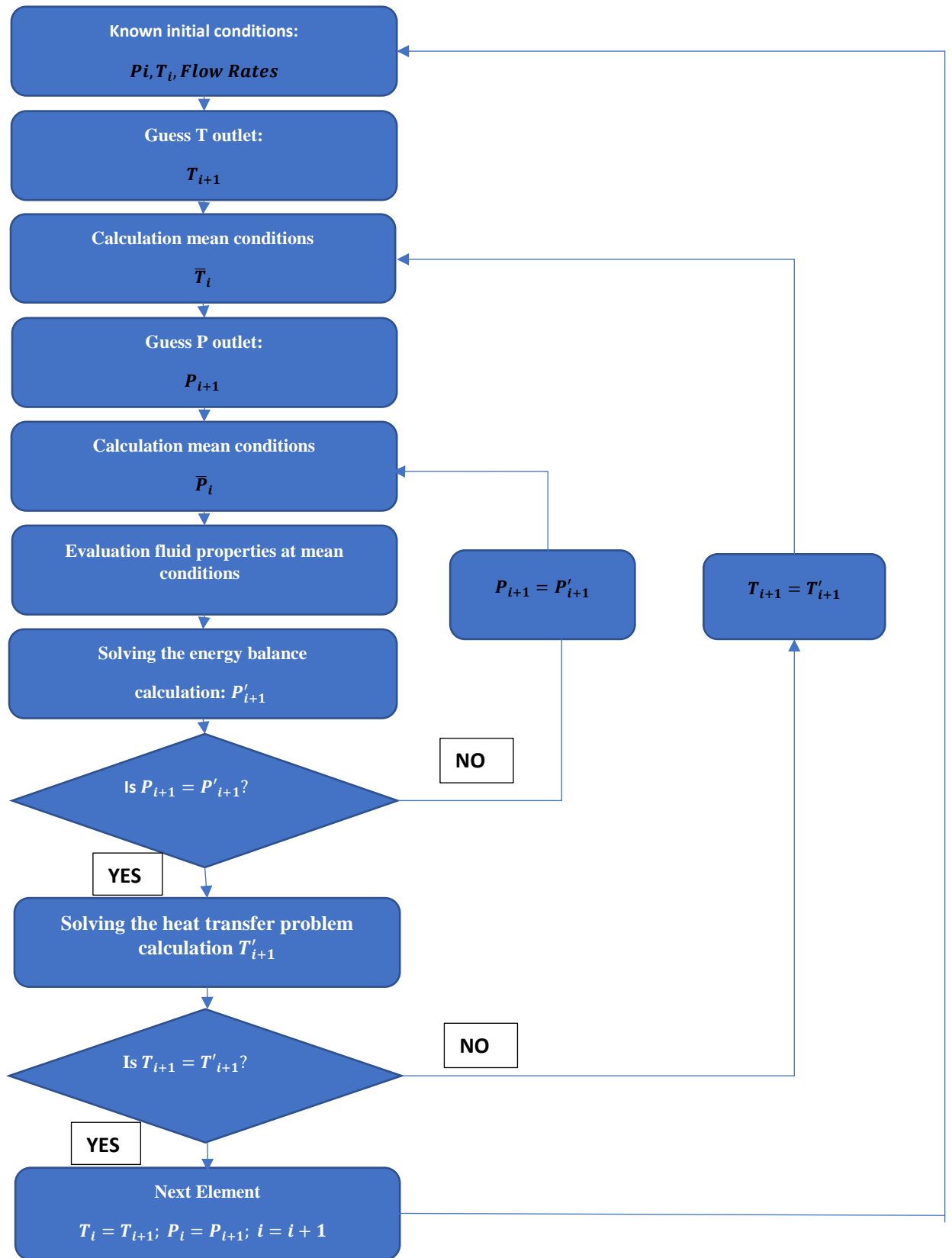


Figure 3.2.2 Flow Diagram of the model

### 3.3 FLUID PROPERTIES

The model requires the phase properties and distributions as a function of pressure and temperature. To obtain these functions another programme must be used, in this case, PVTsim Nova<sup>®</sup> has been employed. PVTsim Nova is a versatile PVT simulation programme developed by Calsep for reservoir engineers, flow assurance specialists, PVT lab engineers and process engineers. Based on an extensive data material collected over a period of more than 30 years, PVTsim Nova carries the information from experimental studies into simulation software in a consistent manner and without losing valuable information. The fluid parameters obtained can be exported to produce high quality input data for simulations [12]. PVTsim Nova requires the molar composition of the fluid and the selected equation of state as an input. In accordance with the purpose of this study the fluid properties have been obtained following the Peng-Robinson equation of state. The outputs of the simulation programme are matrixes which contain the fluid properties. The properties and phase distributions are calculated as functions of pressure and temperature, as a matter of fact along the rows of the matrixes the properties are computed at constant temperature and variable pressure. On the contrary, along the columns the pressure is kept constant and the temperature varies. However, since the matrixes have a finite size, the properties are not calculated for all the possible values of temperature and pressure. To obtain analytical fluid properties functions, the matrixes must be imported in MATLAB<sup>®</sup>. Once, the properties have been imported in MATLAB<sup>®</sup> a linear interpolation is implemented, finally obtaining the properties and the phase distributions as a function of pressure and temperature.

### 3.4 EVALUATION OF THE PRESSURE DROP

Analogously to single-phase flows, two-phase flows are also subjected to pressure variation due to frictions, to velocity variations that could lead to density variations, to the action of gravity and to the exchange of heat and/or work. As already mentioned the model implemented is based on a finite element approach. In this paragraph, the procedure to solve the energy equation will be presented. The solution is the pressure drop in the element considered. The inlet conditions of the segment are given either by the data of the problem, if the first section is considered, or the solution of the problem for the previous elements. Before entering the iterative cycle to evaluate the pressure drop, the model guesses the first value of the outlet pressure and consequently evaluates as a first attempt the mean properties of the fluid. It is important to note that the model is already in another iterative loop for the temperature. Inside the pressure cycle the phases properties and distributions, i.e. the mass fractions of the phases, are evaluated at the mean conditions. The

procedure presented is valid for a two-phase flow, but actually in the majority of the cases, from the reservoir is flowing a three-phase system formed by water, oil and gas. To solve the problem the oil and the water are combined in a pseudo-equivalent liquid phase.

### 3.4.1 Creation of the equivalent fluid

The water and oil properties must be combined to obtain the properties of an equivalent liquid phase, that can afterward be used to evaluate the pressure drop, using the procedure for the two-phase system available in the theory. A homogeneous model has been used to combine the oil and water properties. As a matter of fact, the homogeneous flow model provides the simplest technique to analyse two-phase flows. It assumes that both the phases move at the same velocity, for this reason it is also called the zero-slip model. In the equation 3.4.1 the formula for calculating the properties of the mixture. is presented

$$M_l = \left( \frac{x_w}{M_w} + \frac{1 - x_w}{M_o} \right)^{-1} \quad (3.4.1)$$

Where  $M$  is a generic property, the subscripts refer to the phase and  $x_w$  is the water mass quality defined as follows:

$$x_w = \frac{\Gamma_w}{\Gamma_l} \quad (3.4.2)$$

Where  $\Gamma_w$  and  $\Gamma_o$  are the mass flow rates of the oil and of the water respectively and  $\Gamma_l = \Gamma_o + \Gamma_w$  is the overall liquid flow rate. Applying the equation (3.4.1) to all the properties the equivalent fluid is created.

### 3.4.2 Energy Balance

A general method based on the balance equation is proposed here to determine the pressure drop in the system. To simplify the calculations the following assumptions have been made: steady-state conditions, one-dimensional flow, constant properties, uniform cross section and no flow work. The general control volume for the balance equations is reported in the figure 3.4.1.

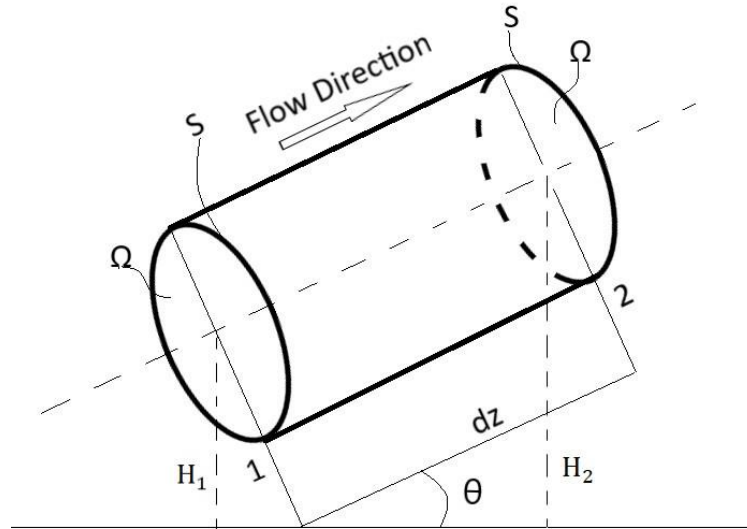


Figure 3.4.1 Control Volume for balance equations

The general structure of the steady-state energy balance is:

$$[\text{flow of energy}]_{\text{out}} - [\text{flow of energy}]_{\text{in}} = \text{work flow} + \text{heat flow}$$

It is possible to write algebraically the terms of the energy balance as presented in the equation (3.4.3).

$$\begin{aligned} \frac{d}{dz} \left( \Gamma_l e_l + \Gamma_g e_g + \Gamma g H + \Gamma_l \frac{\bar{u}_l^2}{2} + \Gamma_g \frac{\bar{u}_g^2}{2} \right) dz \\ = - \frac{d}{dz} (p \Gamma_l v_l) dz - \frac{d}{dz} (p \Gamma_g v_g) dz + d\dot{Q} \end{aligned} \quad (3.4.3)$$

The procedure to obtain the analytical formulation of the energy balance is not reported because it is available in the literature. The left-hand side of the energy balance includes the kinetic, the potential and the internal energy contributions. The right-hand side of the energy balance is the sum of the work flow and heat flow. The contribution of the work flow can be calculated, under the assumption of no flow work in the element, computing the difference between the inlet and outlet conditions. Dividing by the mass flow rate  $\Gamma$  and recalling the definition of the average mass quality  $\bar{x}_g = \frac{\Gamma_g}{\Gamma}$ , it is obtained:

$$\begin{aligned} \frac{d}{dz} \left( (1 - \bar{x}) e_l + \bar{x} e_g + g H + (1 - \bar{x}) \frac{\bar{u}_l^2}{2} + \bar{x} \frac{\bar{u}_g^2}{2} \right) \\ = - \frac{d}{dz} [p(\bar{x} v_g + (1 - \bar{x}) v_l)] + \frac{1}{\Gamma} \frac{d\dot{Q}}{dz} \end{aligned} \quad (3.4.4)$$

It is next possible to define the following bulk quantities, namely the bulk internal energy  $\bar{e}_b$ , the bulk kinetic energy  $\bar{k}_b$  and the bulk specific volume  $\bar{v}_b$ .

$$\bar{e}_b = (1 - \bar{x})e_l + \bar{x}e_g \quad (3.4.5)$$

$$\bar{k}_b = (1 - \bar{x})\frac{\bar{u}_l^2}{2} + \bar{x}\frac{\bar{u}_g^2}{2} \quad (3.4.6)$$

$$\bar{v}_b = \bar{x}v_g + (1 - \bar{x})v_l \quad (3.4.7)$$

Hence, it is possible to rewrite the energy balance in a more compact way, as presented in the equation 3.4.8.

$$\frac{d\bar{e}_b}{dz} + g\frac{dH}{dz} + \frac{d\bar{k}_b}{dz} = -\frac{d}{dz}(p\bar{v}_b) + \frac{1}{\Gamma}\frac{d\dot{Q}}{dz} \quad (3.4.8)$$

$$\text{with } \frac{dH}{dz} = \sin\theta \text{ and } \frac{d}{dz}(p\bar{v}_b) = p\frac{d\bar{v}_b}{dz} + \bar{v}_b\frac{dp}{dz} \quad (3.4.9)$$

Applying the first principle of thermodynamics to the bulk internal energy, it is possible to write:

$$d\bar{e}_b = Td\bar{s}_b - pd\bar{v}_b = \frac{d\dot{Q}}{\Gamma} + d\bar{R}_b - pd\bar{v}_b \quad (3.4.10)$$

Where  $\bar{R}_b$  represents the dissipation of mechanical energy per unit mass due to friction. Dividing the equation 3.4.10 by  $dz$  is possible to obtain:

$$\frac{d\bar{e}_b}{dz} = \frac{1}{\Gamma}\frac{d\dot{Q}}{dz} + \frac{d\bar{R}_b}{dz} - p\frac{d\bar{v}_b}{dz} \quad (3.4.11)$$

Combining the equation 3.4.11 and 3.4.8 the following equation is obtained.

$$\frac{1}{\Gamma}\frac{d\dot{Q}}{dz} - p\frac{d\bar{v}_b}{dz} - \bar{v}_b\frac{dp}{dz} - \frac{d\bar{k}_b}{dz} - g\sin\theta = \frac{1}{\Gamma}\frac{d\dot{Q}}{dz} + \frac{d\bar{R}_b}{dz} - p\frac{d\bar{v}_b}{dz} \quad (3.4.12)$$

Simplifying the equation 3.4.12 and multiplying by the bulk density, an expression for the pressure gradient is obtained.

$$-\frac{dP}{dz} = \bar{\rho}_b\frac{d\bar{k}_b}{dz} + \bar{\rho}_bg\sin\theta + \bar{\rho}_b\frac{d\bar{R}_b}{dz} \quad (3.4.13)$$

From the equation 3.4.22 it is possible to understand that the pressure gradient is the sum of three terms; the first one is related to the kinetic energy variation, the second one to the potential energy variation and the last one is due to friction[13]. In the following paragraphs the three terms are studied to obtain analytical expressions.

### 3.4.3 Kinetic contribute

The kinetic term of the overall pressure drop can be written recalling the definition of the bulk kinetic energy  $\bar{k}_b$ .

$$\bar{\rho}_b \frac{d\bar{k}_b}{dz} = \bar{\rho}_b \frac{d}{dz} \left[ (1 - \bar{x}) \frac{\bar{u}_l^2}{2} + \bar{x} \frac{\bar{u}_g^2}{2} \right] \quad (3.4.14)$$

Recalling the definitions of the actual mass fluxes and of the local velocity, and replacing them in equation 3.4.14, it is possible to obtain:

$$\bar{\rho}_b \frac{d\bar{k}_b}{dz} = \frac{1}{2} \bar{\rho}_b G^2 \frac{d}{dz} \left[ \frac{\bar{x}^3}{\bar{\alpha}^2 \rho_g^2} + \frac{(1 - \bar{x})^3}{(1 - \bar{\alpha})^2 \rho_l^2} \right] \quad (3.4.15)$$

#### 3.4.4 Frictional contribute

The two-phase frictional pressure drop has been a research subject for six decades. The methods developed so far can be divided into two groups: the homogeneous and the separated flow approaches. The former treats a two-phase flow as a pseudo-fluid characterized by suitable averaged properties of the liquid and vapor phase. The latter considers the two-phase flow to be artificially separated into two streams, each flowing in its own pipe, with the assumption that the velocity of each phase is constant in the zone occupied by the phase. In the model a separated flow approach has been implemented. The separated flow approach can be classified into two categories: the  $\phi_l^2, \phi_g^2$  based method and the  $\phi_{lo}^2, \phi_{go}^2$  based method.  $\phi_l^2, \phi_g^2, \phi_{lo}^2$  and  $\phi_{go}^2$  are the two-phase friction multipliers. In accordance with the purpose of this study the  $\phi_l^2, \phi_g^2$  method has been considered, it is based on the theory proposed by Lockhart and Martinelli.  $\phi_l^2$  is defined as the ratio between the two-phase frictional pressure drop to the frictional pressure gradient which would exist if the liquid phase is assumed to flow alone. Analogously,  $\phi_g^2$  is defined as the ratio between the two-phase frictional pressure drop to the frictional pressure gradient which would exist if the gas phase is assumed to flow alone. The analytical expression of the two-phase friction multipliers is presented in the equations below.

$$\phi_l^2 = \frac{\left(\frac{\Delta p}{\Delta z}\right)_{tp}}{\left(\frac{\Delta p}{\Delta z}\right)_l} \quad (3.4.16)$$

$$\phi_g^2 = \frac{\left(\frac{\Delta p}{\Delta z}\right)_{tp}}{\left(\frac{\Delta p}{\Delta z}\right)_g} \quad (3.4.17)$$

The frictional pressure gradients of the gas and the liquid as they are flowing separately are calculated as follows:

$$\left(\frac{\Delta p}{\Delta z}\right)_l = \frac{[G_{tp}(1 - \bar{x})]^2}{2D\rho_l} f_l \quad (3.4.18)$$

$$\left(\frac{\Delta p}{\Delta z}\right)_g = \frac{(G_{tp}\bar{x})^2}{2D\rho_g} f_g \quad (3.4.19)$$

Where the friction factor,  $f$ , is calculated by means of a single-phase correlation using the single-phase properties and mass flux. As far as flow in smooth pipes is concerned, Fang et al. have recently proposed an accurate explicit form to calculate the single-phase friction factor.

$$f = 0.25 \left[ \log \left( \frac{150.39}{Re^{0.98865}} - \frac{152.66}{Re} \right) \right]^{-2} \quad (3.4.20)$$

Lockhart and Martinelli found out that  $\phi_l^2$  and  $\phi_g^2$  are functions of the dimensionless variable  $X$ , which is defined as the square root of the ratio of the frictional pressure gradient which would exist if the liquid phase is assumed to flow alone to the one of the gas.

$$X = \sqrt{\frac{\left(\frac{\Delta p}{\Delta z}\right)_l}{\left(\frac{\Delta p}{\Delta z}\right)_g}} \quad (3.4.21)$$

From several experiments Lockhart and Martinelli have obtained a chart for the calculation of the friction multipliers as a function of the dimensionless variable. However, graphs are inconvenient to employ. Therefore, many investigations have been conducted to generate correlations. The most important one is based on the Chilshom method, in which the  $\phi_l^2$  is expressed as a function of  $X$  and  $C$ .

$$\phi_l^2 = 1 + \frac{C}{X} + \frac{1}{X^2} \quad (3.4.22)$$

However, the Chilshom parameter  $C$  is not constant because it is affected by the flow conditions. A series of experiments have been performed to find correlations of  $C$  for particular applications. As far as viscous liquid and gas flows are concerned, Mishima and Hibiki have developed the following correlation.

$$C = 21[1 - \exp(-0.319D)] \quad (3.4.23)$$

Hence, the two-phase frictional pressure gradient can be evaluated multiplying the single phase frictional pressure drop by the relative two-phase friction multiplier. To compute such quantity the Chilshom method must be used [14].

### 3.4.5 Gravitational Contribute

Recalling the definition of the bulk density as the inverse of the bulk specific volume as expressed in equation 3.4.24.

$$\bar{\rho}_b = \frac{1}{\bar{v}_b} = (\bar{x}v_g + (1 - \bar{x})v_l)^{-1} \quad (3.4.24)$$

It is possible to evaluate the gravitational contribute by simply multiplying 3.4.24 by  $g \sin \theta$ .

$$\bar{\rho}_b g \frac{dH}{dz} = (\bar{x}v_g + (1 - \bar{x})v_l)^{-1} g \sin \theta \quad (3.4.25)$$

## 3.5 SOLUTION HEAT TRANSFER PROBLEM

Once the actual pressure variation is calculated the model computes the temperature distribution of the element. In order to solve the problem, the heat transfer rate entering/exiting the element must be computed. As far as the heat transfer problem is concerned, several solutions deriving from different technologies are implemented. Furthermore, to simplify the problem the heat conduction along the axial direction of the flowline is neglected; in this way a one-dimensional approach can be implemented. Once the heat flow entering/exiting the pipe is calculated, it is then possible to compute the temperature variation of the element considering the specific heat at constant pressure of the mixture, as presented in the equation 3.5.1.

$$\Delta T_{th} = \frac{Q}{\Gamma_{mix} \bar{c} p_{mix}} \quad (3.5.1)$$

Actually, another contribution must be considered. More precisely, it is related to the Joule-Thompson effect, which describes the temperature change of a real gas or liquid when it subjected to a pressure variation.

$$\Delta T_{JT} = \bar{J} T_{mix} \Delta P \quad (3.5.2)$$

The homogeneous model is used to evaluate the average properties of the two-phase mixture.

### 3.5.1 Passive Insulation

As already stated, this is the simplest technology to reduce the temperature variation inside the pipe. In this configuration, there is no power generation in the flowline, consequently a lumped parameter approach can be used, combining both convection and conduction. This method is based on the evaluation of the thermal resistance. For conduction, it is a measure of a temperature difference by which an object or material resists a heat flow. The thermal resistance is a function of the geometry and of the material properties. By employing the definition of the thermal

resistance it is possible to calculate the heat flow knowing the temperature difference of the element considered, as shown in the equation 3.5.3.

$$Q = \frac{T_{out} - T_{in}}{R_{th}} \quad (3.5.3)$$

Where  $Q$  is the heat flow,  $(T_{out} - T_{in})$  is the temperature variation and  $R_{th}$  is the thermal resistance of the layer. In the hypothesis of heat conduction only in the radial direction, for a cylindrical system the thermal resistance can be written as shown in the equation 3.5.4.

$$R = \frac{\ln\left(\frac{r_{out}}{r_{in}}\right)}{2\pi Lk} \quad (3.5.4)$$

Where  $r_{in}$  and  $r_{out}$  are the internal and the external radii of the cylindrical wall,  $L$  is the length of the section considered and  $k$  is the thermal conductivity of the material. The equation 3.5.4 is valid only if the wall is only composed of one material. In fact, if the wall has multiple layers an equivalent thermal resistance must be calculated considering the series of the thermal resistances of each layer. For convection, the concept of thermal resistance is implemented considering the definition of the heat transfer coefficient. As a matter of fact, from the equation 3.5.5 which computes the convective heat flow, it is possible to define the thermal resistance as presented in the equation 3.5.6[15].

$$Q = hA(T - T_{\infty}) = \frac{T - T_{\infty}}{R_{th}} \quad (3.5.5)$$

$$R_{th} = \frac{1}{hA} \quad (3.5.6)$$

To employ the lumped parameter approach is crucial to know the geometry of the problem, in order to create the correct equivalent circuit employing the thermal resistances. In figure 3.5.1 the cross section of the flowline is shown. The carbon steel pipe ( $r_1 < r < r_2$ ) is surrounded by the insulation layer ( $r_2 < r < r_3$ ), which is composed by a material able to work in wet conditions. Inside the pipe ( $r < r_1$ ) a multiphase fluid characterized by a bulk temperature  $T_i$  and by an internal heat transfer coefficient  $h_i$  flows. For simplicity, in this study the insulated pipeline has been considered surrounded by sea water characterized by a temperature  $T_o$  and an external heat transfer coefficient  $h_o$ . The procedure used to calculate the heat transfer coefficients  $h_i$  and  $h_o$  will be presented later on in the study.

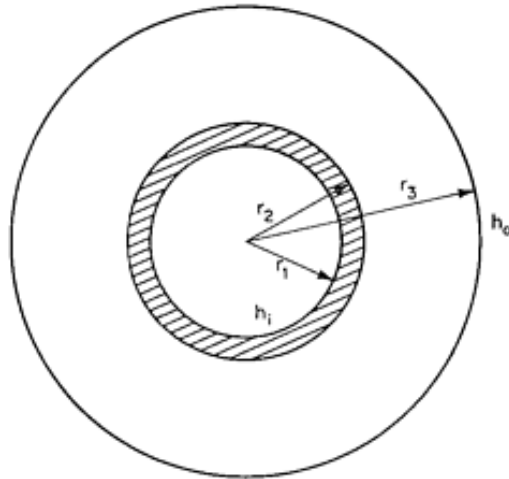


Figure 3.5.1 Cross Section of the pipeline

Since the temperature inside the pipe is higher than the surrounding sea temperature, the heat flows from the inside to the outside passing firstly through the carbon steel and then through the insulation layer. To compute the heat flow it is necessary to build the equivalent thermal circuit, composed of the series of four different thermal resistances, which describe the problem. The equivalent circuit is shown in the figure below.

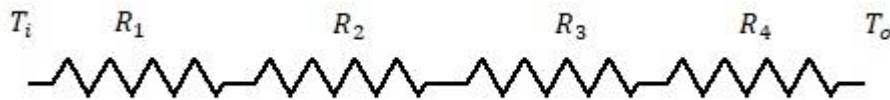


Figure 3.5.2 Thermal Equivalent Circuit

The first resistance considers the heat convection from the fluids to the inner surface of the pipe and the analytical expression is presented in the equation 3.5.7.

$$R_1 = \frac{1}{h_i A_i} \quad (3.5.7)$$

Where  $A_i$  is the internal surface of the pipe, where the heat transfer takes place and can be calculated utilizing the formula to compute the lateral surface of the cylinder. In this case it can be written as  $A_i = 2\pi r_1 L$ , where  $L$  is the length of the element considered. The second and the third resistance take into account the heat conduction respectively in the carbon steel and in the insulation layer; they can be computed recalling the equation 3.5.3.

$$R_2 = \frac{\ln\left(\frac{r_2}{r_1}\right)}{2\pi L k_{cs}} \quad (3.5.8)$$

$$R_3 = \frac{\ln\left(\frac{r_3}{r_2}\right)}{2\pi L k_{ins}} \quad (3.5.9)$$

The fourth resistance considers the convective heat exchange between the outer surface of the insulating layer and the surrounding seawater. Similarly to the first resistance it is possible to write the equation 3.5.10.

$$R_4 = \frac{1}{h_o A_o} \quad (3.5.10)$$

It is then possible to compute the equivalence resistance of the system considering the series of the resistances computed before, as presented in the equation 3.5.11.

$$R_{tot} = R_1 + R_2 + R_3 + R_4 = \frac{1}{h_i A_i} + \frac{\ln\left(\frac{r_2}{r_1}\right)}{2\pi L k_{cs}} + \frac{\ln\left(\frac{r_3}{r_2}\right)}{2\pi L k_{ins}} + \frac{1}{h_o A_o} \quad (3.5.11)$$

Finally, the heat flow can be calculated recalling the equation 3.5.3 using the equivalent resistance of the system and the temperature difference across the pipe.

$$Q = \frac{T_i - T_o}{R_{tot}} \quad (3.5.12)$$

### 3.5.2 Direct Electrical Heating DC

In this technology a direct current (DC) passes through the wall of the pipe generating heat according to the Joule effect. The lumped parameter approach cannot be used, because the concept of thermal resistance is meaningless in case heat is generated. Thus, the heat conduction equation must be solved to compute the temperature distribution in the wall and the heat rate entering in the flowline. The geometry of the problem is equal to the case of the passive insulation, as shown in the figure 3.5.3. The main difference is that in the carbon steel layer ( $r_1 < r < r_2$ ) is circulating the electrical current. Since it is a direct current the current density is constant in the overall cross section of the layer. Hence, it can be considered as a constant volumetric source of heat.

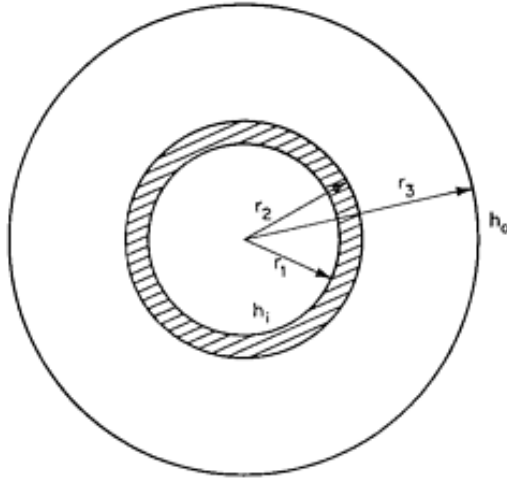


Figure 3.5.3 Cross Section of the Flowline

The general steady-state heat conduction equation in cylindrical coordinates and constant thermal conductivity is presented in equation 3.5.13[16].

$$\frac{1}{r} \frac{d}{dr} \left( r \frac{dT}{dr} \right) + \frac{S}{k} = 0 \quad (3.5.13)$$

Where  $S$  is the volumetric heat generation and  $k$  is the thermal conductivity of the material. Since the current passes only through the carbon steel layer, it is necessary to solve separately the heat conduction equation for each layer and then using the boundary conditions to get the overall temperature distribution of the wall of the flowline. For  $r_1 < r < r_2$  the temperature distribution can be obtained integrating equation 3.5.13. The governing equation is presented in the equation 3.5.14.

$$T_{cs}(r) = -\frac{S}{4k_{cs}} r^2 + C_1 \ln(r) + C_2 \quad (3.5.14)$$

Where  $C_1$  and  $C_2$  are constants of integrations. For  $r_2 < r < r_3$  there is no generation of heat, hence the equation 3.5.13 can be simplified, as presented in equation 3.5.15.

$$\frac{d}{dr} \left( r \frac{dT}{dr} \right) = 0 \quad (3.5.15)$$

Which can be integrated to obtain the temperature distribution in the insulating layer.

$$T_{ins}(r) = C_3 \ln(r) + C_4 \quad (3.5.16)$$

Where  $C_3$  and  $C_4$  are again constants of integration. To find the unique solution of the problem the appropriate boundary conditions must be implemented to find the analytical formula of the constants of integration. Since there are four unknowns ( $C_1, C_2, C_3$  and  $C_4$ ), four different

boundary conditions must be considered. In  $r = r_1$  the pipe exchanges heat with the hydrocarbon mixture by convection, analytically can be written as:

$$-k_{cs} \left. \frac{dT_{cs}}{dr} \right|_{r_1} = h_i [T_i - T_{cs}(r_1)] \quad (3.5.17)$$

Recalling equation 3.5.14 is possible to rewrite equation 3.5.17 in a more explicit form, and after simple mathematical manipulations, is possible to obtain equation 3.5.18.

$$\left( \frac{k_{cs}}{r_1} - h_i \ln(r_1) \right) C_1 - h_i C_2 = \frac{S}{2} r_1 - \frac{h_i S}{4k_{cs}} r_1^2 - h_i T_i \quad (3.5.18)$$

In  $r = r_2$  there is the contact between the carbon steel layer and the insulating one, and the heat exchanged at the interface is the same for both the layers. Such condition can be written analytically as shown in equation 3.5.19

$$-k_{cs} \left. \frac{dT_{cs}}{dr} \right|_{r_2} = -k_{ins} \left. \frac{dT_{ins}}{dr} \right|_{r_2} \quad (3.5.19)$$

Such equation can be manipulated recalling equations 3.5.14 and 3.5.16, so to obtain equation 3.5.20.

$$C_1 \ln(r_2) + C_2 - C_3 \ln(r_2) - C_4 = \frac{S}{4k_{cs}} r_2^2 \quad (3.5.20)$$

Furthermore in  $r = r_2$  the two layers have the same temperature, so the equation 3.5.21 can be written.

$$T_{cs}(r_2) = T_{ins}(r_2) \quad (3.5.21)$$

Analogously to the previous equations also equation 3.5.21 can be manipulated to obtain equation 3.5.22.

$$-\frac{k_{cs}}{r_2} C_1 + \frac{k_{ins}}{r_2} C_3 = -\frac{S}{2} r_2 \quad (3.5.22)$$

The fourth boundary condition consider the convective heat exchange in  $r = r_3$  between the insulated pipe and the surrounding sea water.

$$-k_{ins} \left. \frac{dT_{ins}}{dr} \right|_{r_3} = h_o (T_{ins}(r_3) - T_o) \quad (3.5.23)$$

Such equation can be exploited to obtain a more explicit formulation, as presented in equation 3.5.24.

$$\left( \frac{k_{ins}}{r_3} + h_o \ln(r_3) \right) C_3 + h_o C_4 = h_o T_o \quad (3.5.24)$$

The four equations describing the boundary conditions have been found, it is then possible to solve the problem to obtain the temperature distribution in the pipeline wall. As a matter of fact, a system of four equation in four unknowns have been obtained. The solution of the system can be easily obtained applying the linear algebra theory. In fact, from equations 3.5.18, 3.5.20, 3.5.22 and 3.5.24 is obtained the matrix of the coefficients ( $A$ ) and the vector ( $b$ ) of the constant terms.

$$A = \begin{bmatrix} \frac{k_{cs}}{r_1} - h_i \ln(r_1) & -h_i & 0 & 0 \\ \ln(r_2) & 1 & -\ln(r_2) & -1 \\ -\frac{k_{cs}}{r_2} & 0 & \frac{k_{ins}}{r_2} & 0 \\ 0 & 0 & \frac{k_{ins}}{r_3} + h_o \ln(r_3) & h_o \end{bmatrix} \quad (3.5.25)$$

$$b = \begin{bmatrix} \frac{S}{2} r_1 - \frac{h_i S}{4k_{cs}} r_1^2 + h_i T_i \\ \frac{S}{4k_{cs}} r_2^2 \\ -\frac{S}{2} r_2 \\ h_o T_o \end{bmatrix} \quad (3.5.26)$$

In fact, is possible to write the system as:

$$A * c = b \quad (3.5.27)$$

Where  $c$  is the vectors of the unknowns and it is defined as shown in equation 3.5.28.

$$c = \begin{bmatrix} C_1 \\ C_2 \\ C_3 \\ C_4 \end{bmatrix} \quad (3.5.28)$$

$A$  is a non-singular matrix, because its determinant is different than zero. Hence is possible to find the vector of the unknowns by multiplying the inverse matrix of  $A$  and the vector  $b$  as shown in 3.5.29.

$$c = inv(A) * b \quad (3.5.29)$$

The solution is easily find employing MATLAB® to compute the inverse matrix. Once the problem has been solved, the temperature distribution in the pipe wall is known. The heat flow entering/exiting the pipe is then easily calculated as presented in equation 3.5.30.

$$Q = h_i A_i (T_{cs}(r_1) - T_i) \quad (3.5.30)$$

The heat so formulated is positive if enters in the flowline, i.e.  $T_{cs}(r_1) > T_i$  otherwise is negative and it is the heat loss to the environment.

### 3.5.3 Direct Electrical Heating AC

Also in this configuration the current passes through the carbon steel layer, but in this case, it is alternate. The current density is no more constant in the cross section of the pipe due to the skin effect. Such effect, as defined in the previous paragraphs, is the tendency of an alternate current to become distributed within a conductor such that that the current density is largest near the surface of the conductor, and decreases with greater depths in the conductor. The thickness of penetration of the current inside the conductors is called skin depth. For this reason, the heat generated according to the Joule effect is mainly in the outer ring of the carbon steel layer. A schematic overview of the cross section of the pipe is shown in the figure 3.5.4.

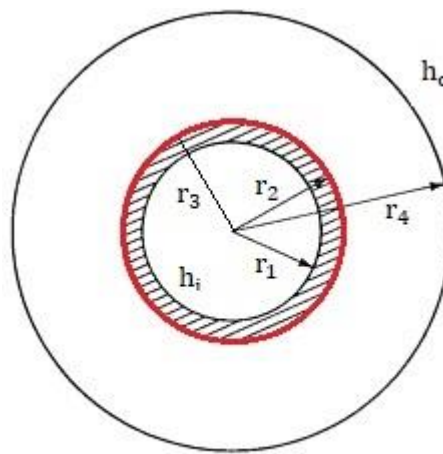


Figure 3.5.4 Cross Section of the Flowline

In the figure above the skin depth is reported in red. The skin depth depends on the properties of the material and of the circulating current. The general formula used to evaluate such thickness is presented in equation 3.5.31.

$$\delta = \sqrt{\frac{\rho_{el}}{\pi\mu_0\mu_r f}} \quad (3.5.31)$$

Where  $\rho_{el}$  is the electrical resistivity of the carbon steel,  $f$  is the frequency of the current,  $\mu_0$  is the permeability of the void and  $\mu_r$  is the relative permeability of the material. Using the definition of the skin depth is possible to divide the carbon steel layer in two regions. In the first one ( $r_1 < r < r_2$ ) there is not heat generation, while in the second one ( $r_2 < r < r_3$ ) yes. Analogously to the case of Direct Electrical Heating DC, the lumped parameter approach cannot be used. Hence the temperature distribution inside each layer must be computed analytically. For  $r_1 < r < r_2$  since there is not heat generation, the heat conduction equation is:

$$\frac{d}{dr} \left( r \frac{dT}{dr} \right) = 0 \quad (3.5.32)$$

Integrating equation 3.5.32 the temperature distribution in the first layer of carbon steel is obtained. The solution, as presented in equation 3.5.33, depends on two constants of integration, namely  $C_1$  and  $C_2$ .

$$T_{cs}(r) = C_1 \ln(r) + C_2 \quad (3.5.33)$$

For  $r_2 < r < r_3$  there is heat generation due to flow of the current and assuming a constant volumetric generation is possible to recall equation 3.5.13. The integration of such equation provides the temperature distribution in the second carbon steel layer. Again, the solution depends on two integration constants, as shown in 3.5.34.

$$T_g(r) = -\frac{S}{4k_{cs}} r^2 + C_3 \ln(r) + C_4 \quad (3.5.34)$$

For  $r_3 < r < r_4$  since there is not heat generation in the insulating layer, the temperature distribution can be found integrating equation 3.5.32. The solution is presented in equation 3.5.35.

$$T_{ins}(r) = C_5 \ln(r) + C_6 \quad (3.5.35)$$

To solve the problem six boundaries conditions must be considered. For  $r = r_1$  the pipe exchanges heat through convection with the convection fluids. Analytically this can be written according to equation 3.5.36.

$$-k_{cs} \left. \frac{dT_{cs}}{dr} \right|_{r_1} = h_i (T_i - T_{cs}(r_1)) \quad (3.5.36)$$

Such formulation can be rearranged to obtain an equation containing the constants of integrations. After replacing 3.5.33 and some mathematical calculation is obtained 3.5.37.

$$\left( h_i \ln(r_1) - \frac{k_{cs}}{r_1} \right) C_1 + h_i C_2 = h_i T_i \quad (3.5.37)$$

In  $r = r_2$  there is the interface between the two carbon steel layers. In such point the temperature is the same for the two layers.

$$T_{cs}(r_2) = T_g(r_2) \quad (3.5.38)$$

Recalling 3.5.33 and 3.5.34 and manipulating 3.5.38 is possible to obtain a second expression containing a relation between the constants of integration.

$$C_1 \ln(r_2) + C_2 - C_3 \ln(r_2) - C_4 = -\frac{S}{4k_{cs}} r_2^2 \quad (3.5.39)$$

Furthermore, in such interface also the flow rate of heat is the same for the two different layers. Such condition is expressed as equation 3.5.40.

$$-k_{cs} \frac{dT_{cs}}{dr} \Big|_{r_2} = -k_{cs} \frac{dT_g}{dr} \Big|_{r_2} \quad (3.5.40)$$

Which then becomes:

$$\frac{1}{r_2} C_1 - \frac{1}{r_2} C_3 = -\frac{S}{2k_{cs}} r_2 \quad (3.5.41)$$

In  $r = r_3$  there is the interface between the carbon steel layer and the insulating one. Analogously, to the interface in  $r = r_2$  the temperature and the heat flow are constant across the different layers. These conditions are respectively written in 3.5.42 and 3.5.43.

$$T_g(r_3) = T_{ins}(r_3) \quad (3.5.42)$$

$$-k_{cs} \frac{dT_g}{dr} \Big|_{r_3} = -k_{ins} \frac{dT_{ins}}{dr} \Big|_{r_3} \quad (3.5.43)$$

Such expressions can be manipulated to obtain two equations depending on the constants of integration. They became respectively:

$$C_3 \ln(r_3) + C_4 - C_5 \ln(r_3) - C_6 = \frac{S}{4k_{cs}} r_3^2 \quad (3.5.44)$$

$$\frac{k_{cs}}{r_3} C_3 - \frac{k_{ins}}{r_3} C_5 = \frac{S}{2} r_3 \quad (3.5.45)$$

The system of six equations in six unknowns is solved using MATLAB®. From the boundary conditions is possible to find the matrix of the coefficient ( $A$ ) and the vector of the constant ( $b$ ).

$$A = \begin{bmatrix} h_i \ln(r_1) - \frac{k_{cs}}{r_1} & h_i & 0 & 0 & 0 & 0 \\ \ln(r_2) & 1 & -\ln(r_2) & -1 & 0 & 0 \\ \frac{1}{r_2} & 0 & -\frac{1}{r_2} & 0 & 0 & 0 \\ 0 & 0 & \ln(r_3) & 1 & -\ln(r_3) & -1 \\ 0 & 0 & \frac{k_{cs}}{r_3} & 0 & -\frac{k_{cs}}{r_3} & 0 \\ 0 & 0 & 0 & 0 & \frac{k_{ins}}{r_4} + h_e \ln(r_4) & h_e \end{bmatrix} \quad (3.5.46)$$

$$\mathbf{b} = \begin{bmatrix} h_i T_i \\ \frac{S}{4k_{cs}} r_2^2 \\ -\frac{S}{2k_{cs}} r_2 \\ \frac{S}{4k_{cs}} r_3^2 \\ \frac{S}{2} r_3 \\ h_e T_e \end{bmatrix} \quad (3.5.47)$$

With the definition of the matrix of the coefficients and of the vector of constant is possible to write the system as shown in equation 3.5.48.

$$\mathbf{A} * \mathbf{c} = \mathbf{b} \quad (3.5.48)$$

Where  $\mathbf{c}$  is the vector of the unknowns, which can be obtained by multiplying both sides for the inverse matrix of A.

$$\mathbf{c} = \text{inv}(\mathbf{A}) * \mathbf{b} \quad (3.5.49)$$

Solving equation 3.5.49 the integration constants are found and so the temperature distributions in each layer are obtained. The heat flow entering the pipe is then computed recalling the definition of the convective heat transfer coefficient.

$$Q = h_i A_i (T_{cs}(r_1) - T_i) \quad (3.5.50)$$

According to 3.5.50 the heat flow is positive if it is entering in the flowline, i.e. when the wall temperature is higher than the fluid one. Otherwise it is negative, and it represents the heat loss to the environment.

#### 3.5.4 Electrically Heat-Traced Flowline

The current, in this configuration, doesn't pass through the wall of the flowline, but in cables laid between the carbon steel layer and the insulating material. The system is installed in a Pipe-in-Pipe configuration which allows the employment of high performance materials. The cables are connected in triplets, so to avoid the installation of a return circuit for the current. Furthermore, to increase the reliability of the system 12 triplets are mounted on the flowline. During continuous operating conditions not all the cables are activated, so in case of failure of a triplet, is possible to immediately switch on another one. A cross section of the flowline is shown in the figure 3.5.5.

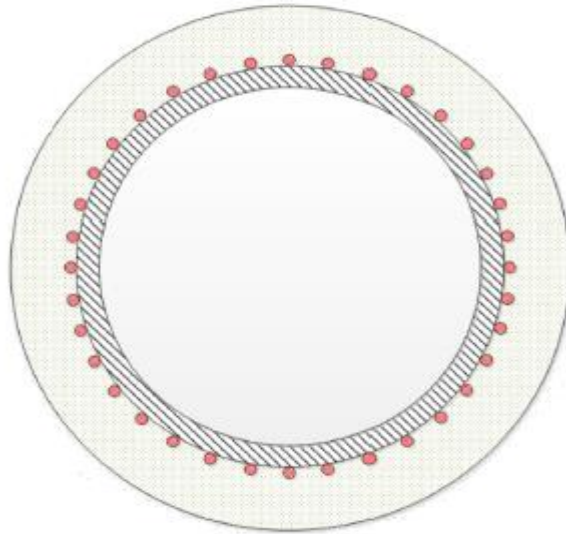


Figure 3.5.5 Cross Section EHTF

To determine the heat flow entering inside the pipe a model describing the heat transfer must be employed. According to the symmetry of the problem the circumference can be divided in many sections having the same solution. The number of sections is equal to the number of activated cables. In figure 3.5.6 is presented the cross section of the considered element.

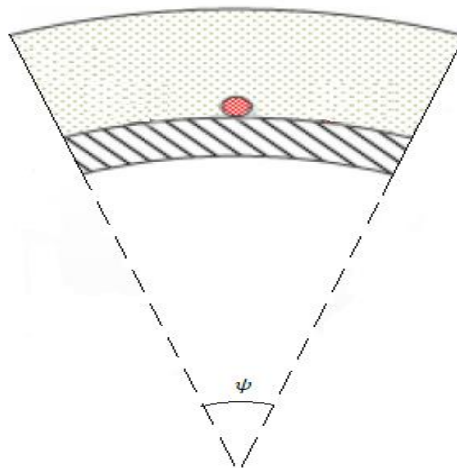


Figure 3.5.6 Section of the element considered for the heat transfer

The central angle  $\psi$  is calculated by simply dividing  $2\pi$  by the number of activated wires. To simplify the problem, the curvature of the arc of circumference has been neglected so to obtain a flat plane as shown in the figure 3.5.7.

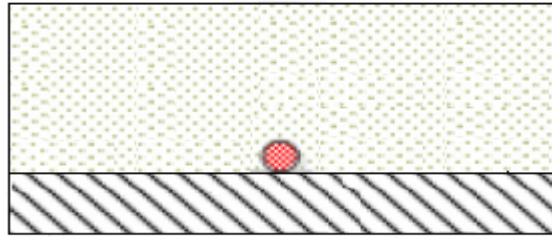


Figure 3.5.7 Section neglecting the curvature radius

The length of the section can be calculated using the formula for the arc of the circumference considering the average radius.

$$l = \frac{2\pi\bar{r}\psi}{2\pi} = \bar{r}\psi \quad (3.5.51)$$

The current passing through the cable is generating heat according to the Joule effect. A fraction of the heat generated is lost to the environment, while the remnant passes through the carbon steel layer to heat up the fluids. To calculate the fractions an iterative process must be employed, because the solution depends on the temperature of the cable, which as first attempt is guessed. The symmetry of the flat plane, as shown in figure 3.5.6, allows to further simplify the problem. The heat entering in the flowline can be approximated using simple heat conduction considerations. In fact, is possible to apply the fin theory to calculate the temperature distribution inside the carbon steel layer. In the figure 3.5.8 is presented the half plane with fundamental quantity necessary to solve the problem.

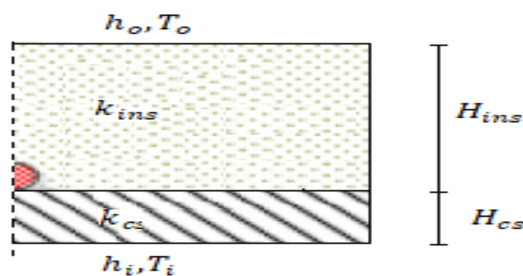


Figure 3.5.8 Geometry of the simplified problem

Looking at the geometry in figure 3.5.7 is possible to see an analogy between the carbon steel layer and a fin. However, to determine the temperature distribution using the fin theory some assumptions are necessary. It is necessary to define an equivalent convective heat transfer coefficient for the overall carbon steel layer. First the conduction in the insulating layer and the convection to the surrounding water are considered to determine a fictitious external heat transfer

coefficient. This is possible computing the heat loss from an infinitesimal section  $dx$  of the fin. The equivalent thermal circuit is presented in the image below.

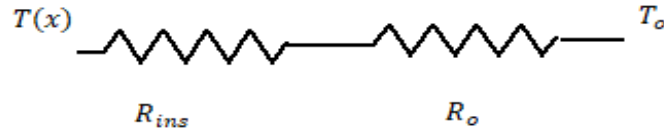


Figure 3.5.9 Equivalent thermal circuit of the insulating layer and convective heat transfer with the surrounding water

Recalling the theory of the lumped parameter approach is possible to analytically write the expression of the thermal resistances.

$$R_{ins} = \frac{H_{ins}}{k_{ins} dA} \quad (3.5.52)$$

$$R_o = \frac{1}{h_o dA} \quad (3.5.53)$$

Where  $H_{ins}$  is the thickness of the insulating layer,  $dA$  is the infinitesimal area,  $k_{ins}$  is the thermal conductivity of the insulating layer and  $h_o$  is the outer convective heat transfer coefficient. It is then possible to define the overall equivalent resistance by simply summing the equations 3.5.52 and 3.5.53.

$$R_{tot} = R_{ins} + R_o = \frac{1}{dA} \left( \frac{H_{ins}}{k_{ins}} + \frac{1}{h_o} \right) \quad (3.5.54)$$

Using the definition of the equivalent resistance is possible to calculate the infinitesimal heat loss to the environment knowing the temperature difference  $(T(x) - T_o)$ .

$$\delta Q_{out} = \frac{T(x) - T_o}{R_{tot}} = \frac{T(x) - T_o}{\frac{1}{dA} \left( \frac{H_{ins}}{k_{ins}} + \frac{1}{h_o} \right)} \quad (3.5.55)$$

Equation 3.5.55 can be easily rearranged as shown in 3.5.56.

$$\delta Q_{out} = dA \left( \frac{H_{ins}}{k_{ins}} + \frac{1}{h_o} \right)^{-1} (T(x) - T_o) \quad (3.5.56)$$

From such equation the outer equivalent convective heat transfer coefficient can be easily extrapolated, and its formulation is presented in 3.5.57.

$$h_{o,eq} = \left( \frac{H_{ins}}{k_{ins}} + \frac{1}{h_o} \right)^{-1} \quad (3.5.57)$$

To better visualize the problem in the figure 3.5.10 is shown the carbon steel layer and the outer equivalent convective heat transfer coefficient.

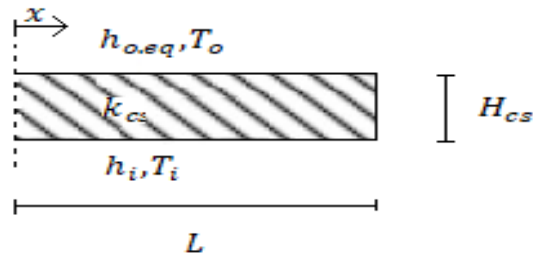


Figure 3.5.10 Geometry of the carbon steel layer and relative properties

The lengths of the fin is easily calculated as half of the arc of circumference computed in equation 3.5.51.

$$L = \frac{\bar{r}\psi}{2} \quad (3.5.58)$$

There is a difference between the inner conditions of the fin which are described by an internal heat transfer coefficient ( $h_i$ ) and a bulk temperature of the fluids ( $T_i$ ) and the outer conditions described by  $h_{o,eq}$  and  $T_o$ . Hence, is necessary to define equivalent properties valid overall for the fin. Such quantities are defined calculating the heat loss for an infinitesimal fraction  $dx$  of the fin. The heat loss is computed as shown in equation 3.5.59.

$$\delta Q_{loss} = h_{o,eq}(T(x) - T_o)p_1 dx + h_i(T(x) - T_i)p_2 dx \quad (3.5.59)$$

Where  $p_1$  and  $p_2$  represent respectively the outer and the inner wetted perimeters of the fin. According to the geometry of the problem the inner and the outer wetted perimeter are equal and equivalent to the width of the fin (i.e. of the length of the finite element considered in the heat transfer problem). Hence, is possible to collect some terms in equation 3.5.59 as shown in 3.5.60.

$$\delta Q_{loss} = [h_{o,eq}(T(x) - T_o) + h_i(T(x) - T_i)]p dx \quad (3.5.60)$$

Manipulating 3.5.60 is possible to obtain:

$$\delta Q_{loss} = (h_{o,eq} + h_i) \left[ T(x) - \left( \frac{h_{o,eq}T_o + h_iT_i}{h_{o,eq} + h_i} \right) \right] p dx \quad (3.5.61)$$

From such equation is finally possible to define an equivalent convective heat transfer coefficient and an equivalent temperature.

$$h_{eq} = h_{o,eq} + h_i \quad (3.5.62)$$

$$T_{eq} = \frac{h_{o,eq}T_o + h_iT_i}{h_{o,eq} + h_i} \quad (3.5.63)$$

It is finally possible to apply the fin model to determine the temperature distribution in the carbon steel layer. The governing equation describing the temperature distribution in a fin, under the assumption of one-dimensional heat conduction in the  $x$  direction is presented in equation 3.5.64[17].

$$\frac{d^2T}{dx^2} - \frac{h_{eq}p}{k_{cs}A_c}(T - T_{eq}) = 0 \quad (3.5.64)$$

Where  $A_c$  is the area of the cross section and  $p$  as stated before is the wetted perimeter which coincides with the width of the fin. It is useful to define a new quantity called excess temperature ( $\vartheta$ ) because allows to simplify the problem. The excess temperature is defined as follow

$$\vartheta(x) = T(x) - T_{eq} \quad (3.5.65)$$

Deriving equation 3.5.65 in  $dx$  is then possible to obtain 3.5.66.

$$\frac{d\vartheta(x)}{dx} = \frac{dT(x)}{dx} \quad (3.5.66)$$

Using the definition of excess temperature and equation 3.5.66 is easy to manipulate the governing equation 3.5.64 obtaining:

$$\frac{d^2\vartheta}{dx^2} - \frac{h_{eq}p}{k_{cs}A_c}\vartheta = 0 \quad (3.5.67)$$

Defining the fin parameter ( $m^2$ ) as shown in equation 3.5.68 is possible to further simplify 3.5.67, the result is the expression in 3.5.69.

$$m^2 = \frac{h_{eq}p}{k_{cs}A_c} \quad (3.5.68)$$

$$\frac{d^2\vartheta}{dx^2} - m^2\vartheta = 0 \quad (3.5.69)$$

Equation 3.5.69 is a linear, homogeneous second-order differential equation with constant coefficients thus is easily solvable. Its solution is presented in 3.5.70.

$$\vartheta(x) = C_1e^{mx} + C_2e^{-mx} \quad (3.5.70)$$

Where  $C_1$  and  $C_2$  are the constants of integration. Thus, to determine the actual temperature distribution in the carbon steel layer two boundary conditions must be set. According to the assumptions made regarding the division of the pipe cross section in many segments is possible to consider the tip of the fin as adiabatic. Because the heat flow exiting from the tip is compensated by the one flowing from the adjacent element. For this reason, in  $x = L$  is possible to write:

$$\left. \frac{d\vartheta}{dx} \right|_{x=L} = 0 \quad (3.5.71)$$

Recalling the solution of the governing equation and manipulating the boundary condition is obtained:

$$(C_1 e^{mL} - C_2 e^{-mL})m = 0 \quad (3.5.72)$$

The second boundary condition is found by setting the temperature at the base of the fin ( $T_b$ ) equal to the one of the electrical cable, which is not known but guessed as a first approximation. Hence, for  $x = 0$  the condition is:

$$\vartheta(x = 0) = \vartheta_b = T_b - T_{eq} \quad (3.5.73)$$

That can be rewritten using 3.5.70.

$$\vartheta_b = C_1 + C_2 \quad (3.5.74)$$

Equations 3.5.75 and 3.5.72 form a linear system, that allows to determine the two integrating constants.

$$C_1 = \vartheta_b \frac{e^{-mL}}{e^{mL} + e^{-mL}} \quad (3.5.75)$$

$$C_2 = \vartheta_b \frac{e^{mL}}{e^{mL} + e^{-mL}} \quad (3.5.76)$$

Finally, the governing equation can be obtained replacing the formulations of the constants of integration and recalling the definitions of the hyperbolic functions.

$$\vartheta(x) = \vartheta_b \frac{\cosh[m(L-x)]}{\cosh(mL)} \quad (3.5.77)$$

Knowing the temperature distribution is possible to evaluate either the heat transfer rate at the base of the fin and the heat flow to the hydrocarbon fluids. The heat entering at the base of the fin can be calculated applying the Fourier law as shown in 3.5.78.

$$Q_b = -k_{cs} A_c \left. \frac{dT}{dx} \right|_{x=0} = -k_{cs} A_c \left. \frac{d\vartheta}{dx} \right|_{x=0} \quad (3.5.78)$$

Replacing the derivate of the temperature distribution evaluated at  $x = 0$ , it is found:

$$Q_b = \sqrt{k_{cs} A_c h_{eq} p} \vartheta_b \tanh(mL) \quad (3.5.79)$$

Since the temperature is varying along the  $x$  direction to determine the heat flow is necessary to apply the Fourier law for an infinitesimal portion of the lateral surface of the fin. The analytical expression is shown in 3.5.80.

$$\delta Q = h_i(T(x) - T_i)pdx \quad (3.5.80)$$

The heat flow is calculated integrating 3.5.80 on the internal lateral surface of the fin. Recalling the definition of excess temperature and its distribution, the following expression is obtained:

$$Q = \int_0^L h_i \left\{ T_{eq} + (T_b - T_{eq}) \left[ \frac{\cosh[m(L-x)]}{\cosh(mL)} \right] - T_i \right\} p dx \quad (3.5.81)$$

Which leads to the heat flow been calculated as follow:

$$Q = h_i p L (T_{eq} - T_i) + \left( \frac{h_i (T_b - T_{eq}) p}{\cosh(mL)} \right) \frac{\sinh(mL)}{m} \quad (3.5.82)$$

Since the solution is found guessing the temperature at the base of the fin ( $T_b$ ), as stated before, an iterative procedure must be implemented. To solve the problem is worth to note that the heat entering at the base of the fin ( $Q_b$ ) is only a fraction of the heat generated by the cable. As a matter of fact, a portion of the generated heat is directly lost to the environment. This quantity can be calculated by simply subtracting  $Q_b$  from the generating heat.

$$Q_{loss} = Q_{gen} - Q_b \quad (3.5.83)$$

Using such information is possible to calculate a new temperature at the base of the fin. This is done considering a lumped parameter approach defining the thermal resistance from the electrical cable to the environment. To simplify the problem, it is assumed that due to the installation process there is a small gap between the electrical cable and the insulating layer. This gap ensures only a small area of contact between the cable and the insulation. The heat is transferred initially by conduction and afterward by convection. Thus, the equivalent circuit is composed of two thermal resistances in series. The first accounts for the conduction in the insulating layer, while the second for the convection with the surrounding water. The schematic of the circuit is presented in figure 3.5.11.

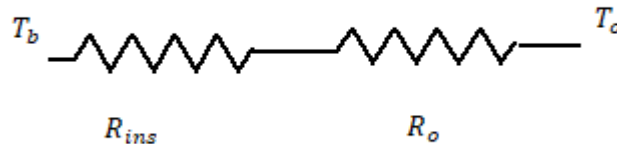


Figure 3.5.11 Equivalent thermal circuit from the cable to the surrounding water

The outer resistance can again be defined according to equation 3.5.7. using the outer convective heat transfer coefficient and the actual area where the heat transfer takes places. The analytical expression is presented in the equation 3.5.84.

$$R_o = \frac{1}{h_o A_o} \quad (3.5.84)$$

The energy conservation equation must be solved to determine the analytical expression of the thermal resistance in the insulating layer. This is necessary because the area through which the heat passes is not constant. Since there is not heat generation in the insulating layer, the one-dimensional steady state governing equation can be expressed as shown in equation 3.5.85.

$$\frac{d}{dx} \left( -k_{ins} A(x) \frac{dT_{ins}}{dx} \right) = 0 \quad (3.5.85)$$

That is equivalent to say that the heat flow is constant in the insulating layer, such condition can be also written as

$$-k_{ins} A(x) \frac{dT_{ins}}{dx} = C \quad (3.5.86)$$

Where  $C$  is a constant value, its expression is necessary to compute the thermal resistance. The variation of the area can be described using the equation 3.5.87, which is obtained considering the formula for the arc of a circumference.

$$A(x) = p \tau \frac{x}{2} \quad (3.5.87)$$

Rearranging the equation 3.5.86 and integrating across the insulating layer the formulation of the constant  $C$  is obtained. The integral solved and the formulation of the constant are presented below.

$$\int_{T_b}^{T_e} dT = \int_{x_i}^{x_e} \frac{2C}{p\tau x} dx \quad (3.5.88)$$

$$C = \frac{p\tau}{2 \ln\left(\frac{x_e}{x_i}\right)} (T_e - T_b) \quad (3.5.89)$$

Since the left-hand side of the equation 3.5.87 according to the Fourier law is the heat flow through the layer, it is possible to write:

$$Q_{loss} = k_{ins} \frac{p\tau}{2 \ln\left(\frac{x_e}{x_i}\right)} (T_e - T_b) \quad (3.5.90)$$

Recalling the definition of the thermal resistance as presented in the equation 3.5.3, the expression of the thermal resistance of the insulating layer is easily found from 3.5.90.

$$R_{ins} = \frac{2 \ln\left(\frac{x_e}{x_i}\right)}{k_{ins} p \tau} \quad (3.5.91)$$

Finally, the equivalent thermal resistance can be found considering the series of the resistances which are presented in equation 3.5.91 and 3.5.84.

$$R_{eq} = \frac{2 \ln\left(\frac{x_e}{x_i}\right)}{k_{ins} p \tau} + \frac{1}{h_o A_o} \quad (3.5.92)$$

Using the definition of the thermal resistance is then possible to evaluate the heat loss to the environment. According to the assumptions made on the geometry of the problem, the actual loss is the double of the one calculated using the thermal resistance as defined in the equation 3.5.92.

$$Q_{loss} = 2 \frac{(T_o - T_b)}{R_{eq}} \quad (3.5.93)$$

From the formulation of the heat loss is possible to obtain the value of the base of the fin  $T_b$  as shown in equation 3.5.94.

$$T_b = T_o - \frac{R_{eq} Q_{loss}}{2} \quad (3.5.94)$$

The value of the temperature so calculated is then confronted with the value used for solving the governing equation in the carbon steel layer. If the two temperatures are different the procedure is repeated considering as an input the value of the temperature calculated in equation 3.5.94. The procedure is repeated till the convergence is reached. The overall heat entering in the flowline is then computed multiplying the equation 3.5.82 by the number of activated wires.

### 3.6 TWO-PHASE HEAT TRANSFER COEFFICIENT

To solve the heat transfer problem the internal heat transfer coefficient ( $h_i$ ) must be calculated. Correlations have been proposed according to the geometry of the problem. However, due to the complex nature of the two-phase gas-liquid flow, the accessible heat transfer data and applicable correlations for non-boiling two-phase flow in horizontal and inclined pipes covering various flow patterns and inclined positions are limited in the literature. Furthermore, most of the available heat transfer correlations are often limited by specific flow pattern and flow orientation. In this paragraph a general heat transfer correlation for non-boiling two-phase with different flow patterns and pipe is presented. The correlation is based on the work of Kim et. Al (2000). In their work they assumed that the total gas-liquid two-phase heat transfer is the sum of the individual single-phase heat transfers of the gas and liquid, weighted by the volume of each phase present as shown in equation 3.6.1.

$$h_i = h_{tp} = (1 - \alpha)h_L + \alpha h_G \quad (3.6.1)$$

Where  $\alpha$  is the void fraction, which is defined as the volume fraction of the gas-phase in the tube cross-sectional area. Equation 3.6.1 can be rewritten as presented in equation 3.6.2.

$$h_i = (1 - \alpha)h_L \left[ 1 + C \left\{ \left( \frac{x}{1-x} \right)^m \left( \frac{\alpha}{1-\alpha} \right)^n \left( \frac{Pr_G}{Pr_L} \right)^p \left( \frac{\mu_G}{\mu_L} \right)^q \right\} \right] \quad (3.6.2)$$

The void fraction, however, does not fully account for the effect for the different flow patterns and inclinations angles. Therefore, in order to handle such effects with only one correlation, Ghajar and Kim (2005) introduced the flow pattern factor ( $F_p$ ) and the inclination factor ( $I$ ). As a matter of fact, the void fraction does not reflect the actual wetted-perimeter in the tube with respect to the corresponding flow pattern. Therefore, an effective wetted-perimeter relation is necessary, such formulation is presented in equation 3.6.3.

$$F_p = (1 - \alpha) + \alpha F_s^2 \quad (3.6.3)$$

The term  $F_s$  in the equation 3.6.3 is the shape factor which in essence is a modified and normalized Froude number. The definition of the shape factor is presented in the equation 3.6.4

$$F_s = \frac{2}{\pi} \tan^{-1} \left( \sqrt{\frac{\rho_G (u_G - u_L)^2}{gD(\rho_L - \rho_G) \cos(\theta)}} \right) \quad (3.6.4)$$

The shape factor represents the shape changes of the gas-liquid interface by the force acting on the interface due to the relative momentum and gravitational forces. Due to the density difference between gas and liquid, the liquid phase is much more affected by the orientation of the flow. In order to account for the effect of inclination, the inclination factor,  $I$ , is introduced and defined as follow.

$$I = 1 + \frac{gD(\rho_L - \rho_G) \sin(\theta)}{\rho_L u_{SL}^2} \quad (3.6.5)$$

Considering the terms defined above the heat correlation then becomes:

$$h_i = F_p h_L \left\{ 1 + C \left[ \left( \frac{x}{1-x} \right)^m \left( \frac{1-F_p}{F_p} \right)^n \left( \frac{Pr_G}{Pr_L} \right)^p \left( \frac{\mu_G}{\mu_L} \right)^q (I)^r \right] \right\} \quad (3.6.6)$$

The heat transfer coefficient as if liquid is flowing alone were flowing ( $h_L$ ) is calculated using the Sieder and Tate correlation for turbulent flow.

$$h_L = 0.027 Re_L^{\frac{4}{5}} Pr_L^{\frac{1}{3}} \left( \frac{k_L}{D} \right) \left( \frac{\mu_b}{\mu_w} \right)_L^{0.14} \quad (3.6.7)$$

The relationship used to evaluate the Reynolds number is presented in the equation 3.6.8. For this formulation the in-situ Reynolds number is calculated rather than the superficial one.

$$Re_L = \left( \frac{\rho u D}{\mu} \right)_L = \frac{4\dot{\Gamma}_L}{\pi \sqrt{1 - \alpha} \mu_L D} \quad (3.6.8)$$

As can be understood from the above equations the void fraction is a crucial parameter, that needs to be carefully evaluated. For the purpose of this work the correlation provided by Lockhart and Martinelli has been used [18].

$$\alpha = \left[ 1 + 0.28 \left( \frac{1-x}{x} \right)^{0.64} \left( \frac{\rho_G}{\rho_L} \right)^{0.36} \left( \frac{\mu_L}{\mu_G} \right)^{0.07} \right]^{-1} \quad (3.6.9)$$

### 3.7 EXTERNAL HEAT TRANSFER COEFFICIENT

In this project the pipeline has been considered laid out on the sea floor. Hence, to determine the external heat transfer coefficient ( $h_o$ ) the sea water properties must be used. The thermophysical properties of seawater are given as functions of temperature, pressure and salinity [19][20]. Not only the sea water properties are necessary but also the geometry of the pipeline is required. It has been assumed that when the flowline is on the sea floor, there aren't sea currents. Under this hypothesis the heat transfer is governed by natural convection. The correlation used to estimate the heat transfer coefficient is the one valid for long horizontal cylinder. The formulation for an isothermal cylinder proposed by Morgan is presented in the equation 3.7.1[21].

$$\overline{Nu}_D = \frac{\bar{h}D}{k} = C Ra_D^n \quad (3.7.1)$$

The constants of equation 3.7.1 for free convection on a horizontal circular cylinder are reported in the table 3.7.1.

$Ra_D^n$	$C$	$n$
$10^{-10} - 10^{-2}$	0.675	0.058
$10^{-2} - 10^2$	1.02	0.058
$10^2 - 10^4$	0.850	0.188
$10^4 - 10^7$	0.48	0.25
$10^7 - 10^{12}$	0.125	0.333

Table 3.7.1 Constants for free convection on a horizontal circular cylinder

Where  $Ra_D$  is the Rayleigh number evaluated at the film temperature. The analytical formulation of the Rayleigh number is presented in the equation 3.7.2.

$$Ra_D = \frac{g\beta}{v\alpha_{th}}(T_s - T_\infty)D^3 \quad (3.7.2)$$

However, the relation presented above is valid only when the flowline is horizontal and laid on the sea floor. As a matter of fact, for the other conditions it is necessary to employ a different correlation. Under the assumption that there is a sea current with constant velocity and direction is possible to employ the correlation valid for circular cylinder in cross flow. The empirical correlation due to Hilpert is presented in the equation 3.7.3.

$$\overline{Nu}_D = \frac{\bar{h}D}{k} = CRe_D^m Pr^{1/3} \quad (3.7.3)$$

The constants  $C$  and  $m$  used in equation 3.7.3 are listed in the table 3.7.2[22].

$Re_D$	$C$	$m$
0.4 – 4	0.989	0.33
4 – 40	0.911	0.385
40 – 4000	0.683	0.466
4000 – 400000	0.193	0.618
40000 – 400000	0.027	0.805

Table 3.7.2 Constants of equation 3.7.3 for the circular cylinder in crossflow

## 4 CHAPTER 4: VALIDATION OF THE MODEL

---

### 4.1 LOGIC OF THE VALIDATION

Before applying the models to any production scenario, it is necessary to evaluate their fluid dynamic validity. The results of the models implemented in MATLAB® are confronted with the ones obtained using the commercial software OLGA®. As already presented OLGA® models the multiphase flow behaviour. Since OLGA® allows only a constant generation per unit length, it is not possible to simulate all the technologies, but only passive insulation and direct electrical heating. Actually, it would be possible to simulate in OLGA® also the electrical heated traced flowline. As a matter of fact, this is done creating a fictitious layer placed between the carbon steel and the insulating material. Such component fakes the behaviour of the electrical cables. However, it is an approximation and for this reason it is employed only in the chapter regarding the transient of the technologies. The fluid dynamic validity of the models is obtained for the passive insulation configuration and the direct electrical heating one. As already presented in the previous chapters the main difference of the models is the solution of the heat transfer problem. As a matter of fact, the fluid dynamic laws used are the same for the different models. Different productions scenarios have been analysed using the simulators implemented in MATLAB® and OLGA®.

### 4.2 10 KM HORIZONTAL FLOWLINE - ONLY INSULATION

It is the easiest case considered. The thermodynamic variables, i.e. temperature and pressure, are simulated for a 10 Km horizontal flowline. The inlet conditions, the geometry and the materials of the pipeline are known. Also, the conditions of the surrounding sea water are given as a data of the problem. Furthermore, it has been assumed a constant value for the external heat transfer coefficient. In this way the only variables to be investigated are the relations describing the fluid dynamic properties of the multiphase system inside the flowline. The thermophysical characteristics of the materials employed are reported in the table 4.2.1.

MATERIAL	DENSITY $\left[\frac{Kg}{m^3}\right]$	CONDUCTIVITY $\left[\frac{W}{mK}\right]$	CAPACITY $\left[\frac{J}{KgK}\right]$
Carbon Steel	7850	43	470
Polypropylene	960	0.4	2200

Table 4.2.1 Properties of the materials

In the figure 4.2.1 the temperature trend predicted from the model and the one obtained from OLGA® are presented.

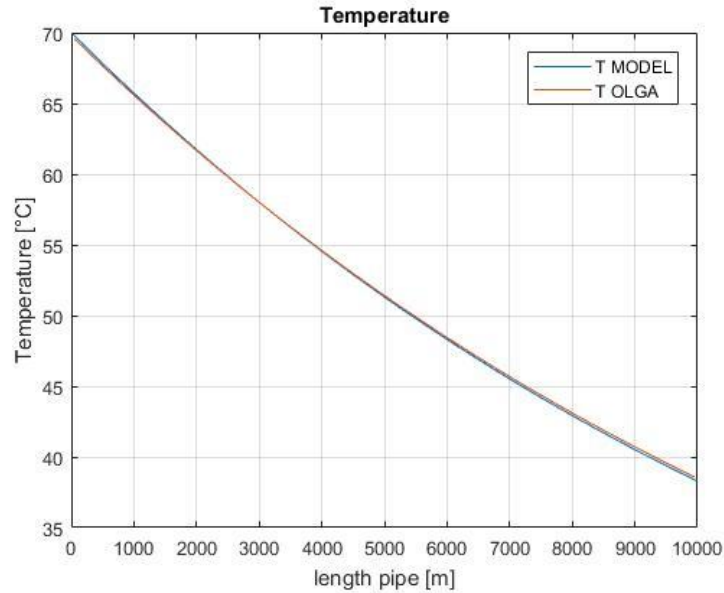


Figure 4.2.1 Temperature variation inside the flowline

As can be seen from the figure 4.2.1 the temperature prediction of the models is very close to the one obtained using OLGA®. As a matter of fact, the maximum percentage variance between the two trends is 0,5%. However, the temperature alone is not enough to completely validate the model. For this reason, also the pressure must be considered. The trend of the pressure is presented in the figure 4.2.2.

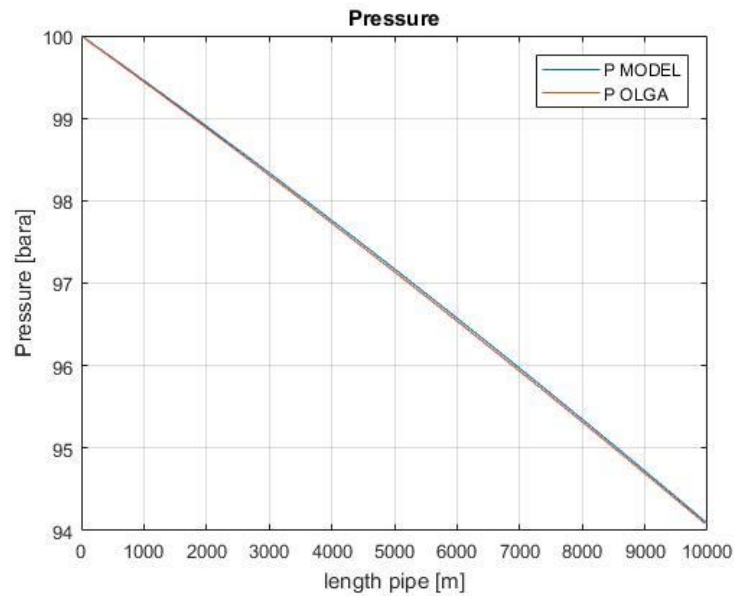


Figure 4.2.2 Pressure variation inside the flowline

From the figure 4.2.2 is possible to see that the trend of the pressure computed from the model is almost overlapping the one computed by OLGA®. The maximum relative percentage difference is calculated equal to 0,04%. From the above charts it is possible to understand the validity of the model. However, due to the horizontal configuration the gravity effect on the pressure is not considered. In order to include all the possible effects a different scenario has been investigated.

### 4.3 10 KM CATENARY FLOWLINE – ONLY INSULATION

The only difference with the horizontal configuration is the geometry of the flowline. The new geometry is presented in the figure 4.3.1.

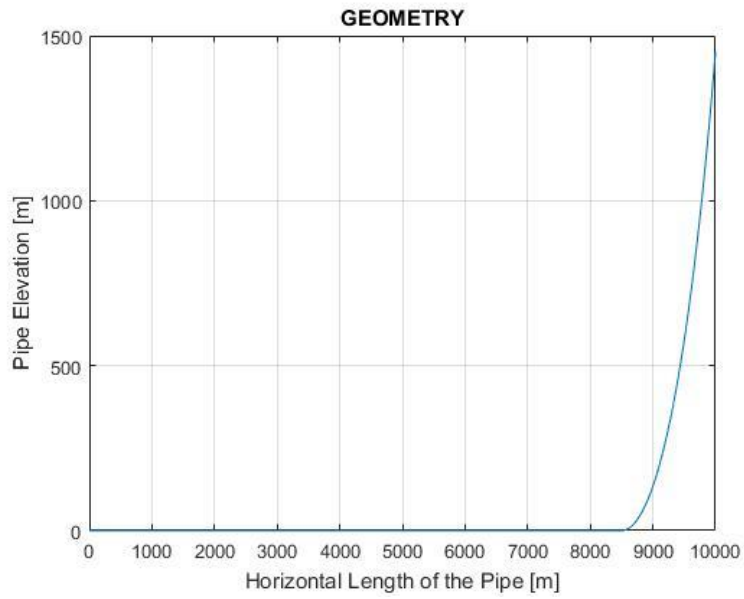


Figure 4.3.1 Geometry of the Flowline

As can be understood from the figure 4.3.1 the flowline initially is horizontal and then it rises. In this way it is possible to include also the gravity effect in the evaluation of the pressure drop. The variation of the temperature is presented in the figure 4.3.2. The prediction obtained from the model is almost overlapping the one computed from OLGA®.

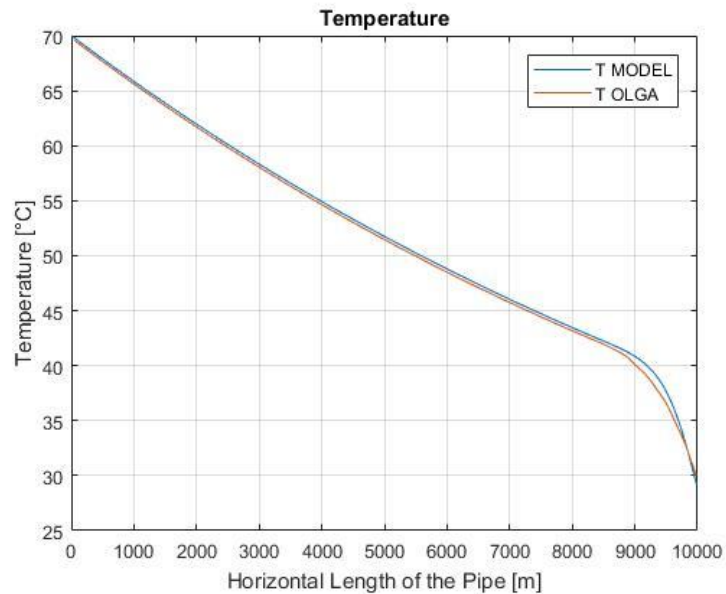


Figure 4.3.2 Temperature variation of the flowline

The maximum relative percentage difference is of the 3%. Also, the pressure variation computed from the model is almost the same as the one obtained from OLGA®. The trends are presented in the figure 4.3.3.

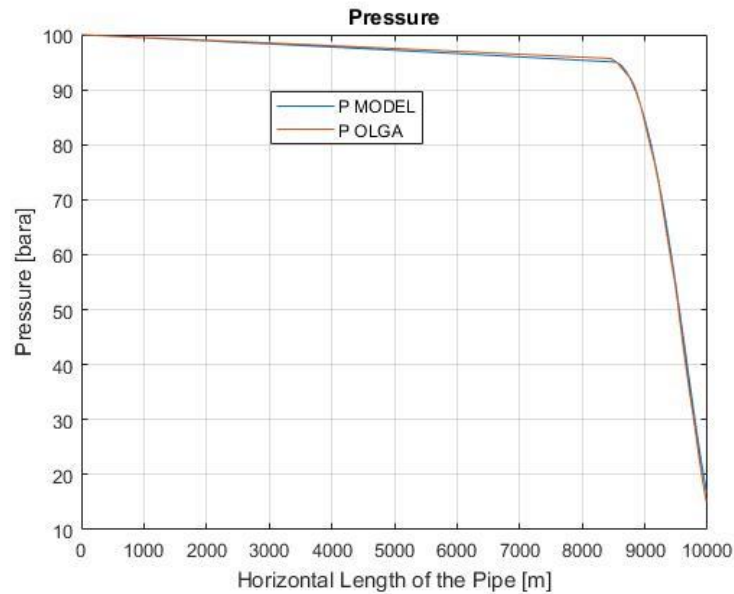


Figure 4.3.3 Pressure variation inside the flowline

The maximum relative percentage difference is of the 9%. It is worth to note that the gravity effect as a major impact on the pressure variation inside the flowline. This can be seen comparing the figures 4.3.3. and 4.2.2, in which the only difference is due to the change in elevation of the pipe in the second case. From the above imagines is possible to state that the models simulate well the fluid dynamic conditions inside the flowline. However, it is necessary also to consider the configuration with the electrical heating turned on.

#### 4.4 10 KM CATENARY FLOWLINE – DEH

The geometry and the material properties are the same of the configuration with only the passive insulation. The simulations are performed considering a generated power of  $800 \frac{W}{m}$ . The temperature distributions are reported in the figure 4.4.1.

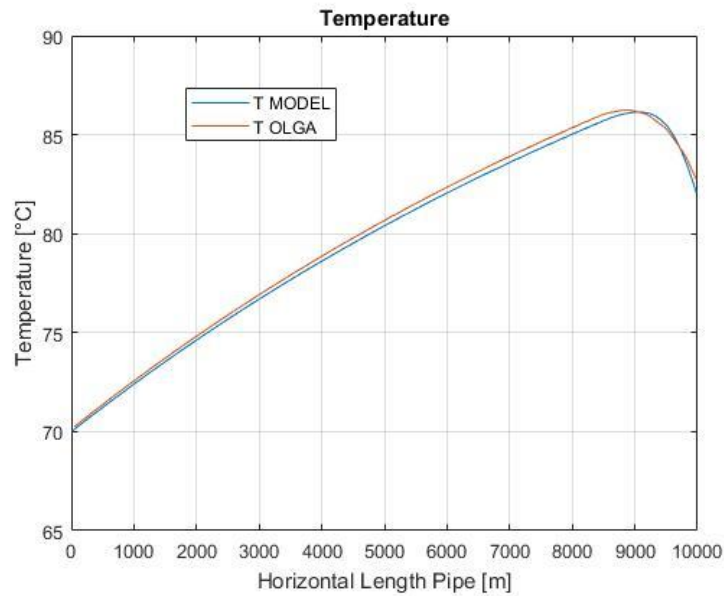


Figure 4.4.1 Comparison of the Temperature distributions obtained with OLGA and with the Steady-State model

The two temperature distributions are almost identical, as can be seen from the figure above. As a matter of fact the maximum relative percentage difference is 2%. It is worth to note that the temperature is increasing along the flowline. In practice during normal flowing conditions this is not necessary, because it is enough to maintain the temperature above the critical temperature for solid deposition. The only application in which the temperature of the produced fluid must increase is during the start-up phase. Such phase will be analysed with the aid of OLGA® in the respective chapter.

## 5 CHAPTER 5: CASE STUDY

---

### 5.1 INTRODUCTION TO THE PROBLEM

In this chapter the models implemented in MATLAB® are used to compare the different technologies from a flow assurance point of view. In order to compare the different solutions a fictitious production scenario has been considered. A new well have been successfully drilled in the Angola's sea and the nearest platform is distant 20 km. From a sensitivity analysis a 10 inches pipeline has been chosen as the optimal solution. The flowline is laid on the sea floor for 18 km and then it rises to the platform. The geometry of the problem is presented in the figure 5.1.1.

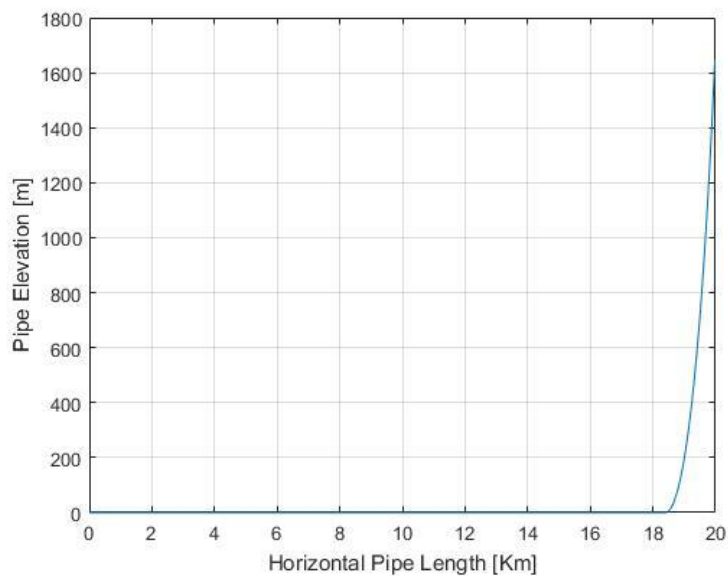


*Figure 5.1.1 Geometry of the Case Study*

The wall of the pipeline is composed by carbon steel and it is externally surrounded by an insulating layer. The material of the insulating layer changes according to the different technologies considered. Since confident information regarding the fluid properties aren't available because of errors during sampling, the fluid properties of a nearby field have been used. The phase envelope of the fluid is reported in the figure 5.1.2.

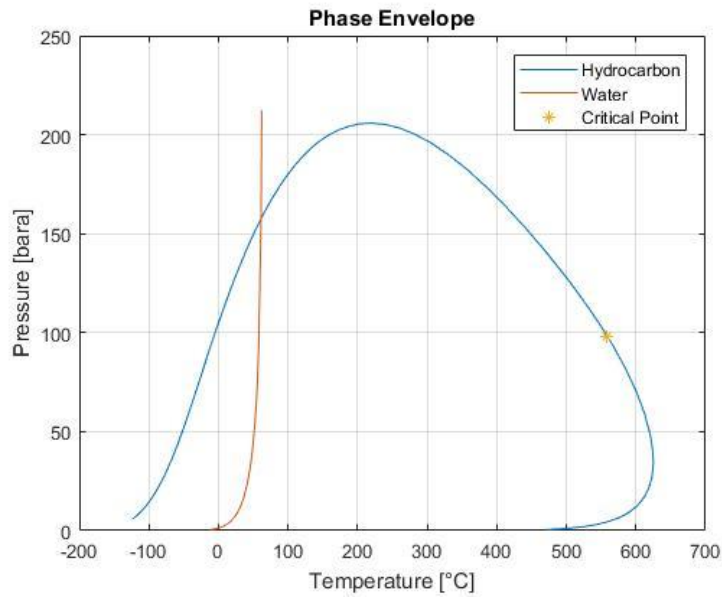


Figure 5.1.2 Phase Envelope

The phase envelope is a useful chart which allows to determine the number and the nature of the phases of a system by knowing the thermodynamic conditions. However, it may be difficult to understand all the possible problem that may arise. For this reason, it is necessary to plot a more complete chart which takes into account also the hydrate equilibrium curve (HEC) and the wax appearance temperature (WAT). Such graph is called operating phase envelope and it is reported in the figure 5.1.3.

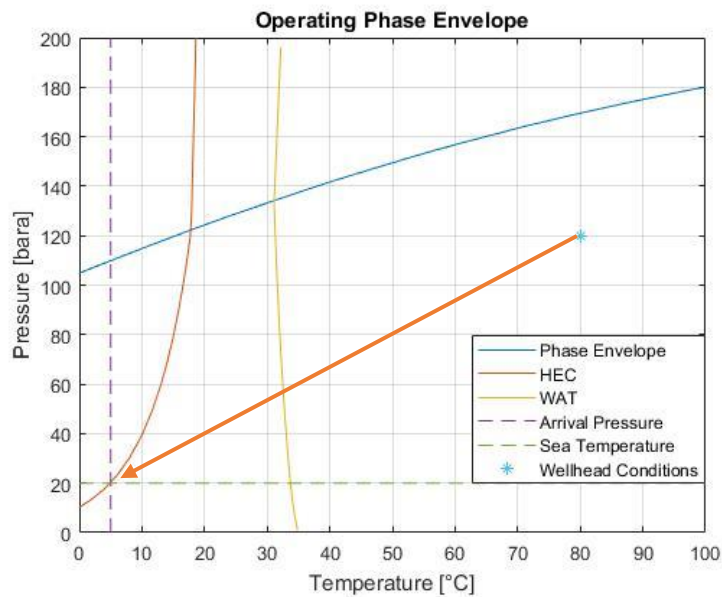


Figure 5.1.3 Operating Phase Envelope

The wellhead conditions, the guessed arrival pressure and the sea water temperature are also reported in the operating envelope, as can be seen from the figure above. It is worth to note that for a given pressure the wax appearance temperature is higher than the hydrate equilibrium curve. The stream from the reservoir conditions would reach the arrival pressure losing heat to the environment. But, as can be seen from the red arrow in the figure 5.1.3. the flowline may risk to get plugged. Hence, technologies are employed to maintain the flowline inside the steady-state operating region. Such region is reported in the figure 5.1.4.

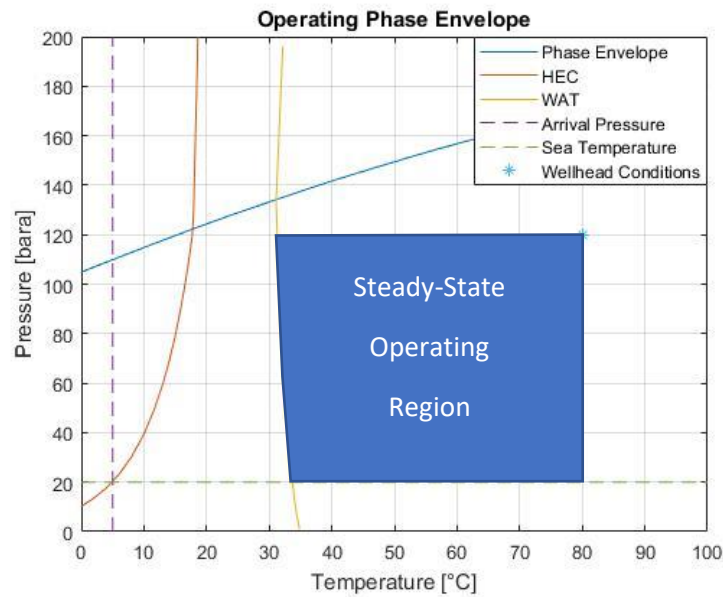


Figure 5.1.4 Steady-State Operating Region

From the above figure it has been assumed a critical temperature for solid deposition of 35°C. If the fluid temperature drops below 35°C the flowline may risk getting plugged. Furthermore, the total flow rate from the reservoir has been assumed equal to  $40 \frac{Kg}{s}$ . As a first approximation the water cut is considered zero. The surrounding sea water temperature have been chosen equal to 5°C. The different technologies investigated are passive insulation, direct electrical heating (DC and AC) and electrically heated traced flowline. The comparison is performed initially using the nominal flow rate and then a reduced value.

## 5.2 WELL INSULATED FLOW LINE WITH COLD INLET

In this configuration the thickness of the insulation layer is 2 inches and it is composed by polypropylene. The properties of the materials considered are reported in the table 4.2.1.

MATERIAL	DENSITY $\left[\frac{Kg}{m^3}\right]$	CONDUCTIVITY $\left[\frac{W}{mK}\right]$	CAPACITY $\left[\frac{J}{KgK}\right]$
Carbon Steel	7850	43	470
Polypropylene	960	0.4	2200

Table 5.2.1 Properties of the materials

The model is applied to determine the relevant thermodynamic variables inside the flowline. As already stated before the temperature is the most important quantity that must be evaluated. The trend of the temperature obtained from the model considering the nominal flow rate is presented in the figure 5.2.1.

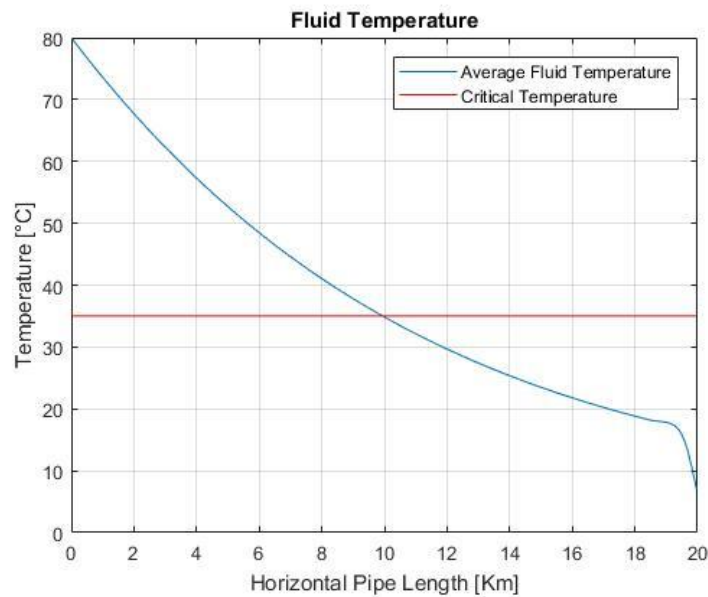


Figure 5.2.1 Fluid Temperature of the 2 inches insulated flowline, nominal flowrate

As can be seen from the figure 5.2.1 at a distance of 10 Km from the wellhead the temperature inside the flowline drops below the critical value, leading to the risk of plug the line. In order to avoid the solid deposition, the conventional flow assurance technologies must be applied, but, as already stated before they are very expensive. It is worth to note that in the last part of the flowline the temperature drop is more significant. This peculiar trend is related to the Joule-Thomson effect. Such effect becomes relevant when the gas fraction increases inside the flowline. As can be seen from the figure 5.2.2 the fluid pressure suddenly drops because the gravity contribution in the equation 3.4.33 becomes more relevant as the pipe elevation changes.

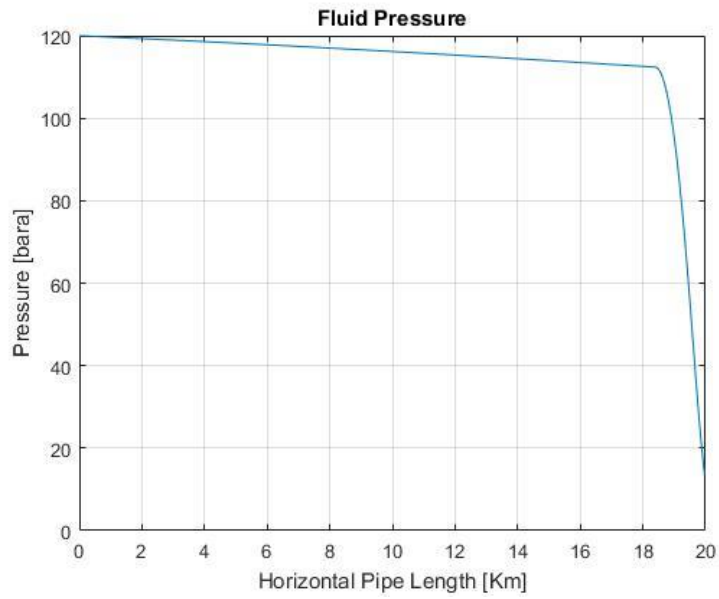


Figure 5.2.2 Fluid Pressure of the 2 inches insulated flowline, nominal flowrate

Because of the pressure reduction the gas fraction increases as shown in the figure 5.2.3. According to the increase of the gas fraction also the Joule-Thompson contribution increases, leading to a further reduction of the temperature.

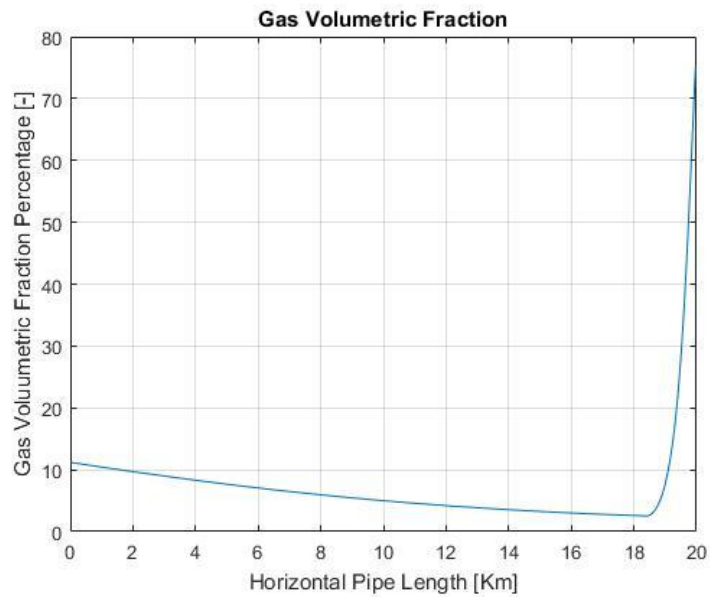


Figure 5.2.3 Gas Volumetric fraction of the 2 inches insulated flowline, nominal flow rate

Not only the Joule-Thompson effect plays a role on the temperature variation. As a matter of fact, the pressure drop changes also the average fluid properties inside the flowline. Furthermore, the situation becomes more critical if for any reason the flow rate from the reservoir reduces. This can

be seen in the figure 5.2.4, where the temperature variation is computed considering a reduced flow rate (30% of the nominal).

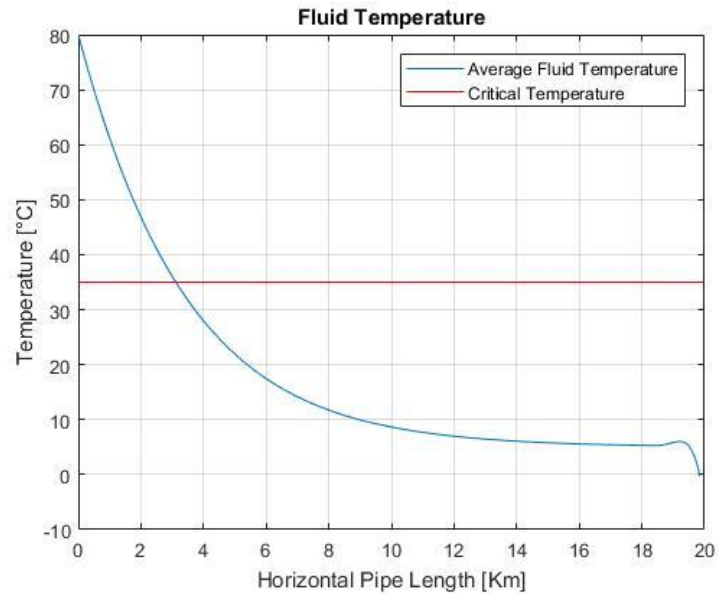


Figure 5.2.4 Fluid Temperature of the 2 inches insulated flowline, reduced flowrate

From the above diagram it seems that the temperature slightly increases before dropping in the final sections of the pipe. Such behaviour doesn't have any physical interpretation. As a matter of fact, such peculiar trend is related to the approximation introduced with the definition of the Joule-Thompson coefficient for the mixture. In order to have a more significant comparison the two trends are plotted on the same chart, as presented in the figure 5.2.5. As can be seen from the figure the configuration with the reduced flow rate is more critical than the one with the nominal flow rate. This is because the hot stream from the reservoir is reduced, hence the heat losses to the environment are more significant. The risk of plugging the line is in any case unavoidable, for this reason conventional flow assurance technologies must be implemented.

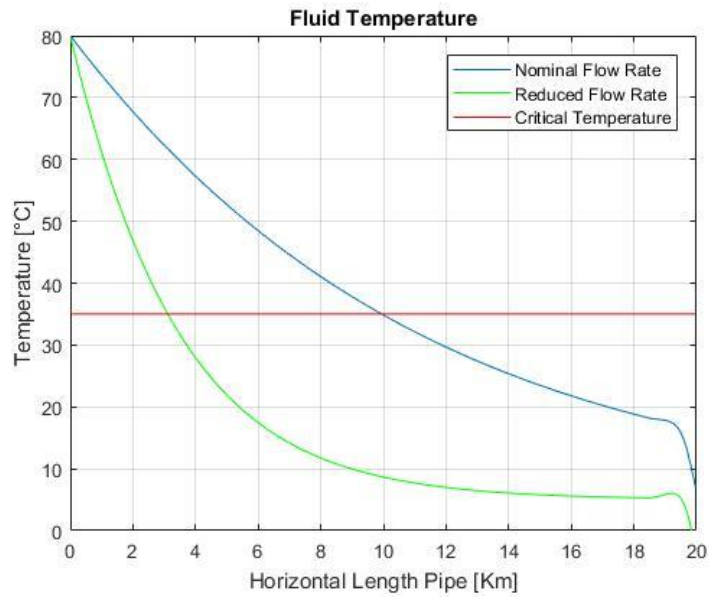


Figure 5.2.5 Fluid Temperature of the 2 inches insulated flowline

### 5.3 POOR INSULATED FLOW LINE

This configuration is very similar to the one considered in the previous paragraph. The initial conditions and the materials of the flowline are the same of the previous case. However, the thickness of the insulation layer is limited to half inch. The temperature variation is obtained considering both the nominal and the reduced flow rate. The trend considering the nominal flow rare is shown in the figure 5.3.1.

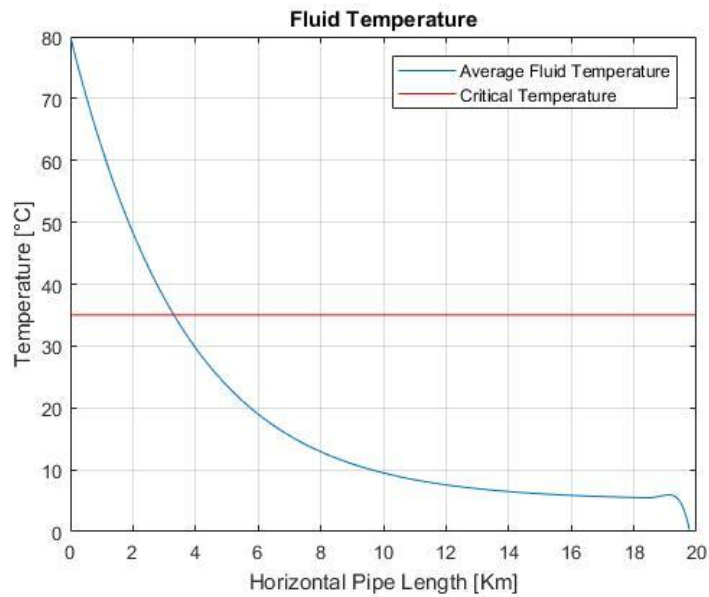


Figure 5.3.1 Fluid Temperature of the 1/2 inches insulated flowline, nominal flowrate

As can be expected, reducing the insulating level the heat losses to the environment increases. This can be seen from the figure 5.3.1, where the average fluid temperature drops below the critical level at 3 km from the wellhead. Meaning that the solid deposition is possible almost for the entire length of the flowline. The situation is even more critical if the reduced flowrate is considered. The trend of the temperature considering the reduced flow rate is presented in the figure 5.3.2.

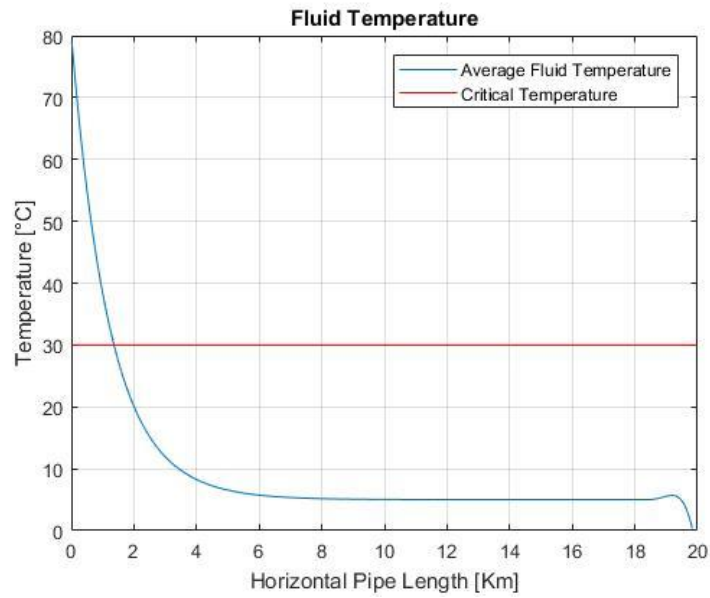


Figure 5.3.2 Fluid Temperature of the 1/2 inches insulated flowline, reduced flowrate

Again, it is worth to note that a reduction of the flow the reservoir results in a lower temperature inside the flowline. Furthermore, using the reduced flowrate the flowline reaches the thermal equilibrium with the surrounding sea water. This can be seen in the horizontal section of the temperature trend in the figure 5.3.2. The fact that the temperature drops below 5°C, i.e. the sea temperature, it is associated with the Joule-Thompson effect. In order to have a more significant comparison the two trends are plotted on the same graph, which is reported in the figure 5.3.3. From the graph is possible to understand that the conventional flow assurance technologies are necessary if this configuration is employed.

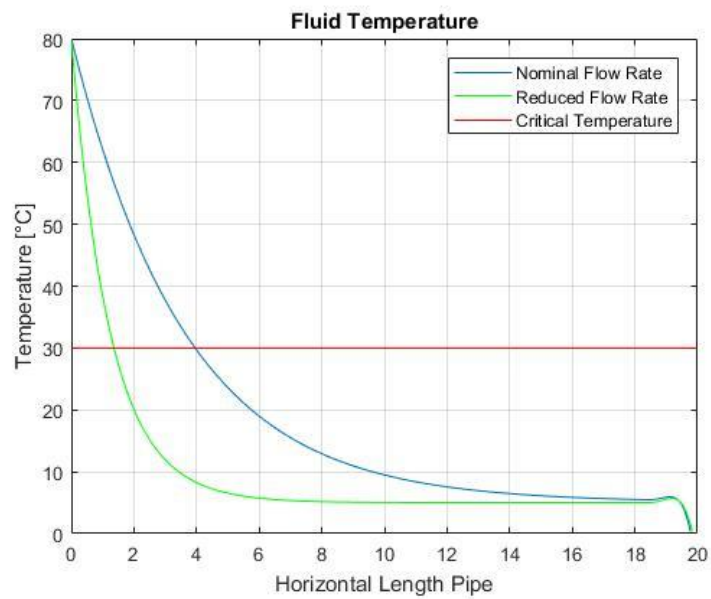


Figure 5.3.3 Fluid Temperature of the 1/2 inch insulated flowline

#### 5.4 INSULATED FLOWLINE

The model is used to understand the effect of the level of insulation on the temperature distribution inside the flowline. The results have been obtained considering the nominal flow rate. The temperature distributions are reported in the figure 5.4.1.

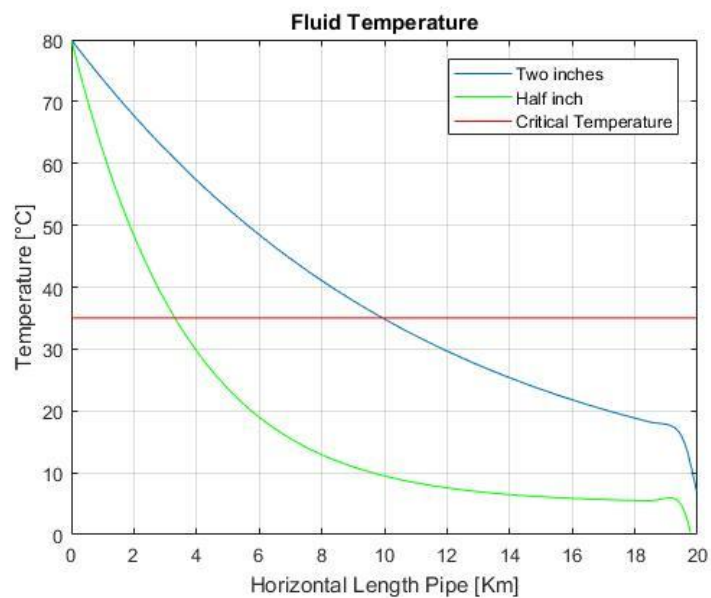


Figure 5.4.1 Effects of the level of insulation on the temperature distribution

As can be seen from the chart above, the higher the level of insulation the lower are the heat losses to the environment. However, it is worth to note that also the costs of the flowline increase with

the level of insulation. Employing this technology, a compromise must be found between the thickness of the insulating layer and the investment costs. Furthermore, a temperature reduction is inevitable even considering a perfect insulating layer because of the Joule-Thompson effect.

## 5.5 DIRECT ELECTRICALLY HEATED FLOWLINE (DC)

The flowline is actively heated to reduce the heat losses to the environment. A direct current passes through the carbon steel layer generating heat according to the Joule effect. The materials and the geometry are the same of the one considered in the insulated configurations. The thickness of the insulating layer is limited to half inch. The fluid temperature is obtained considering different levels of power generation. The results are reported in the figure 5.5.1.

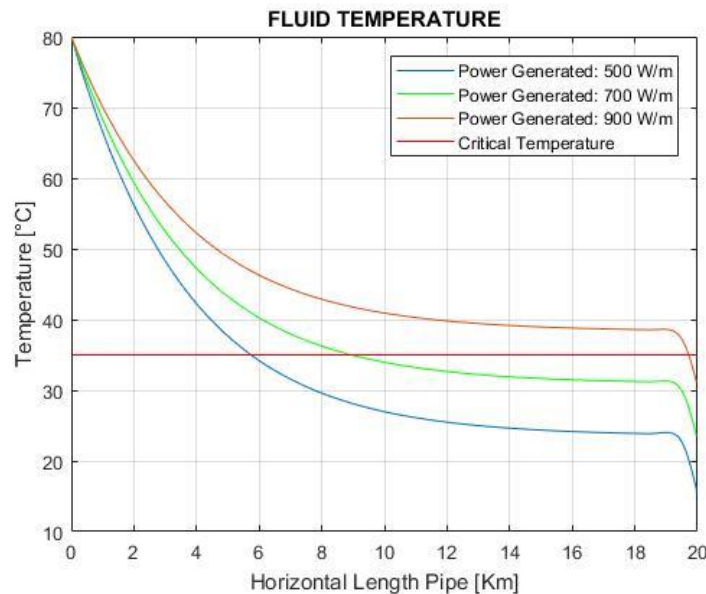


Figure 5.5.1 Fluid Temperature of the pipeline with DEH technology, nominal flow rate

Naturally the higher the power generated the lower the heat losses to the environment. From the above graph is possible to see that a generated power higher than  $900 \frac{W}{m}$  is required to safely operating the flowline. As already mentioned the power is generated by the passage of the current in the carbon steel layer. Hence is possible to evaluate the required current according to the equation 5.5.1[23].

$$I = \sqrt{\frac{A_c * S}{\rho_{el}}} \quad (5.5.1)$$

Where  $S$  is the power generated per unit volume,  $A_c$  is the cross-sectional area through which the current passes and  $\rho_{el}$  is the electrical resistivity of the material. Hence, inevitably the higher the

power generated the higher the current needed. A very useful chart can be obtained from the temperature trends reported in figure 5.5.1. As a matter of fact, it is possible to plot the outlet temperature as a function of the generated power as shown in the figure 5.5.2.

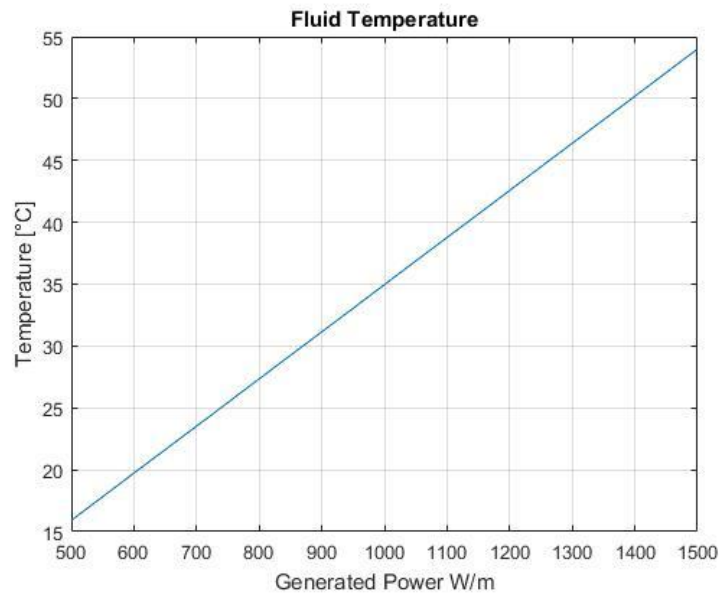


Figure 5.5.2 Outlet Temperature as a function of the generated power

It is worth to note that in this theoretical study the flowline is poorly isolated. For this reason, the required power is very high. As a matter of fact, in real applications the level of insulation is high enough to safely operate the flowline under normal operating conditions. Hence the required power is smaller than the one obtained. However, to properly compare the different configurations from a flow assurance point of view a low level of insulation has been considered. The simulations are performed also to consider the configuration with a reduced flow rate. The results are reported in the figure 5.5.3.

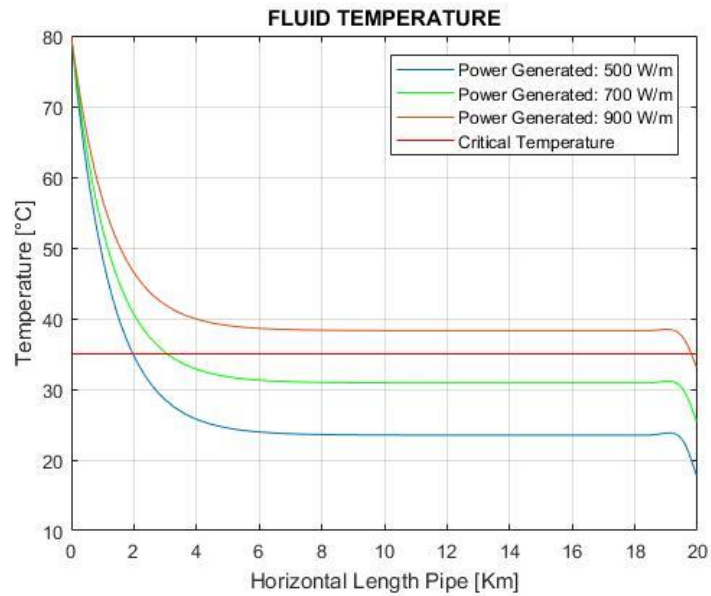


Figure 5.5.3 Fluid Temperature of the pipeline with DEH (DC) technology, reduced flow rate

It is worth to note that for each level of power generated is possible to obtain a constant fluid temperature inside the flowline. This implies that the heat provided by the technology is equivalent to the one lost to the environment. As already explained in the previous paragraphs in the last section of the flowline the change elevation of the pipe leads to a temperature reduction. Actually, also considering the nominal flow rate it would be possible to find stable operating conditions; however, the limited length of the pipe doesn't allow to reach such situations. In order to evaluate the effect of the flow rate on the fluid temperature, the model is applied considering a constant level of generation of  $700 \frac{W}{m}$ . The results are reported in the figure 5.5.3. The reduction of the mass flow rate from the reservoir results in a faster temperature drop inside the flowline. However, the employment of the DEH technology allows to reach the same equilibrium conditions, resulting in the same outlet temperature. The employment of the DEH allows the production without the need of the traditional flow assurances technologies. As a matter of fact, to avoid the temperature drop below the critical value is enough to increase the provided current. Furthermore, it allows to safely operates the line regardless the composition of the fluid considered.

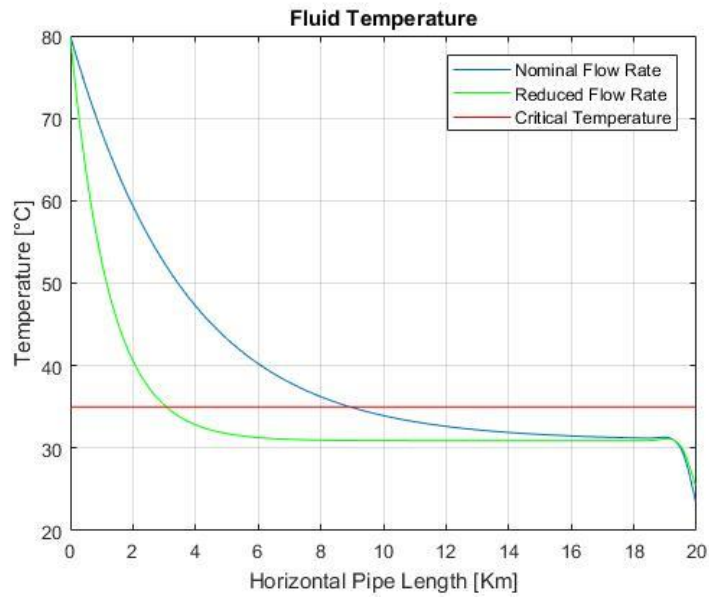


Figure 5.5.4 Fluid Temperature considering different flow rates, Power generated 700 W/m

## 5.6 DIRECT ELECTRICALLY HEATED FLOWLINE (AC)

The only difference with the previous case is the fact that in this configuration an alternating current is employed. Hence, both the skin effect and the proximity effect must be considered. The temperature variation is computed at fixed mass flow rate and current frequency for different levels of generated power, as shown in the figure 5.6.1.

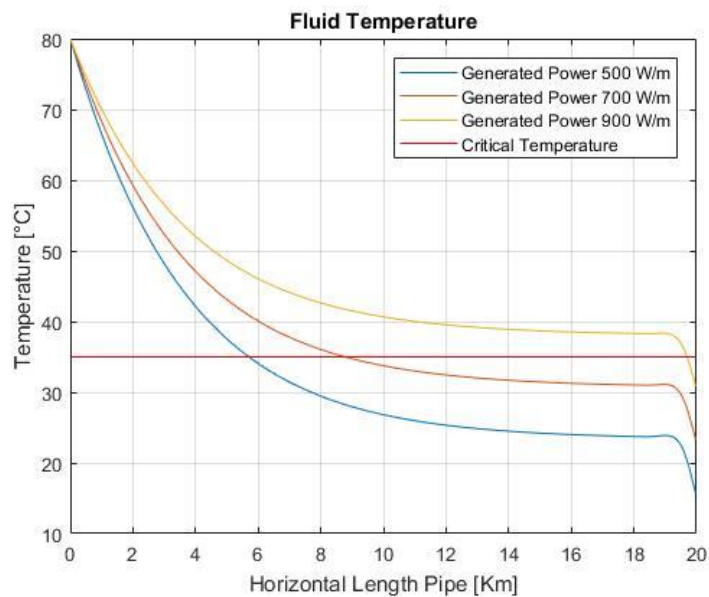


Figure 5.6.1 Fluid temperature, nominal flow rate and 50 Hz alternating current

Analogously to what done in the previous paragraphs is possible also to consider the reduced flow rate. The results are reported in the figure 5.6.2.

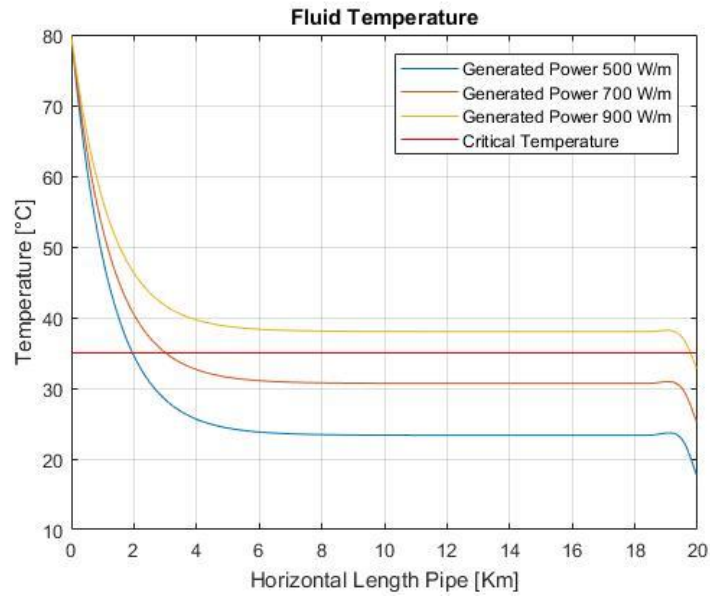


Figure 5.6.2 Fluid temperature, reduced flow rate and 50 Hz alternating current

It is also possible to consider the effects of the frequency on the temperature distribution. As a matter of fact, the skin depth depends on the frequency of the current, as previously shown in equation 3.5.31. The skin depth is evaluated for two different values of frequency. The results are reported in the table 5.6.1.

<i>Frequency [Hz]</i>	<i>Skin Depth [mm]</i>
50	1.35
500	0.43

Table 5.6.1 Skin Depth at different frequencies

The simulations are performed considering the nominal flow rate and a generated power of  $700 \frac{W}{m}$ . The results are reported in the figure 5.6.3.

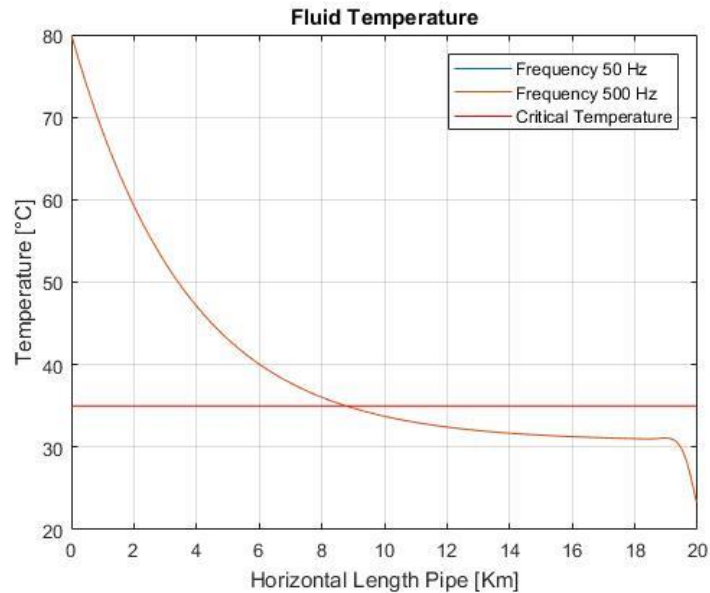


Figure 5.6.3 Fluid Temperature considering different frequencies

As can be seen from the graph above the variation of the frequency has not an effect on the temperature distribution from a thermodynamic point of view. This is true because the carbon steel has a very high thermal conductivity, hence the effects of the reduction of the generating thickness are negligible. However, from an electrical point of view the reduction of the skin depth results in an increase of the alternating resistance of the material, according to the equation 5.6.1.

$$R_{ac} = \frac{\rho_{el} l}{\pi \delta D} \quad (5.6.1)$$

The equation 5.6.1 is valid under the assumptions that the wall thickness is greater than the skin depth and that only the skin effect determines the current distribution (i.e. concentric current distribution). Hence the main advantage of the increased frequency is the reduction in the required current for achieving the same heat developed in the steel pipe.

## 5.7 DEH DC VS DEH AC

The models are used to compare the two configurations from a thermodynamic point of view. As already stated before the only difference is the current, which determines the generation in the carbon steel layer. In order to have a fair comparison the same level of generation has been considered. The results are reported in the figure 5.7.1.

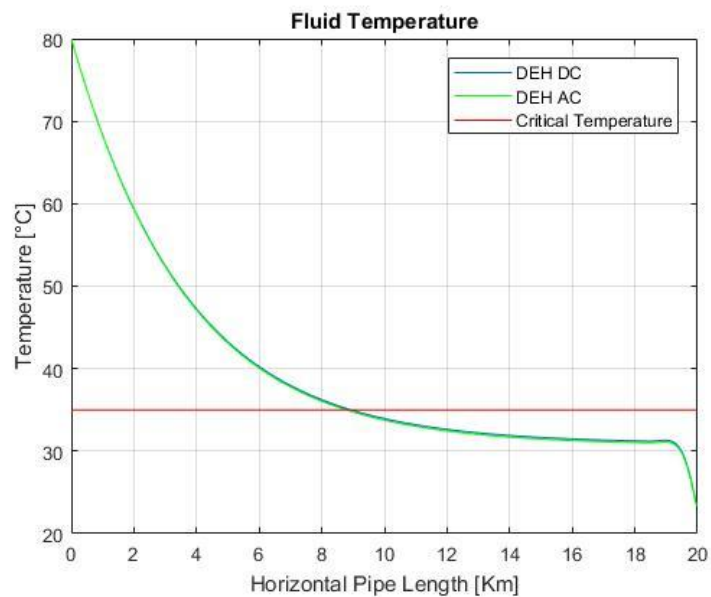


Figure 5.7.1 Fluid Temperature according different current distributions

The temperature distribution is almost the same considering either an alternating current and a direct current. Again, this is related to the high thermal conductivity and limited thickness of the carbon steel layer. However, it is possible to calculate the temperature difference between the two configurations. The difference is reported in the figure 5.7.2. As can be seen the employment of the direct current results in a slightly higher fluid temperature compared to the one obtained with the alternating current. Such result is related to the current density distribution in the carbon steel layer. As already stated, the direct current passes through the overall cross section of the conductor. Hence, the heat generated is transmitted directly into the flowline. Instead, the alternating current is subjected to the skin effect. For this reason, the heat generated by the current before entering in the flowline has to pass through a carbon steel layer. Accordingly, a small fraction of heat is dissipated. However, as already mentioned, due to the high thermal conductivity and limited thickness of the carbon steel layer the difference is almost negligible.

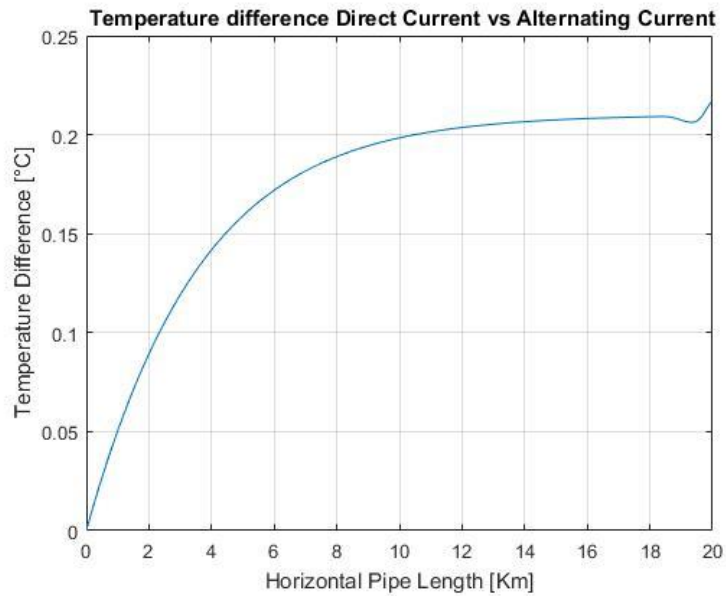


Figure 5.7.2 Temperature difference between direct current and alternating current

### 5.8 ELECTRICALLY HEATED TRACED FLOWLINE

In this configuration, a very high-performance insulating material has been employed in combination with the electrical heating technology. The properties of the materials considered are reported in the table 5.8.1. The thickness of the insulating material is limited to half inch.

MATERIAL	DENSITY $\left[\frac{Kg}{m^3}\right]$	CONDUCTIVITY $\left[\frac{W}{mK}\right]$	CAPACITY $\left[\frac{J}{KgK}\right]$
Carbon Steel	7850	43	470
Poly-ethylene foam	32	0.04	2300

Table 5.8.1 Properties of the materials

The temperature distribution is obtained considering initially the nominal flow rate. As can be seen from the figure 5.8.1. the level of insulation is enough to safely operates the flowline above the critical temperature. As expected increasing the fluid temperature increases as the level of generated power increases.

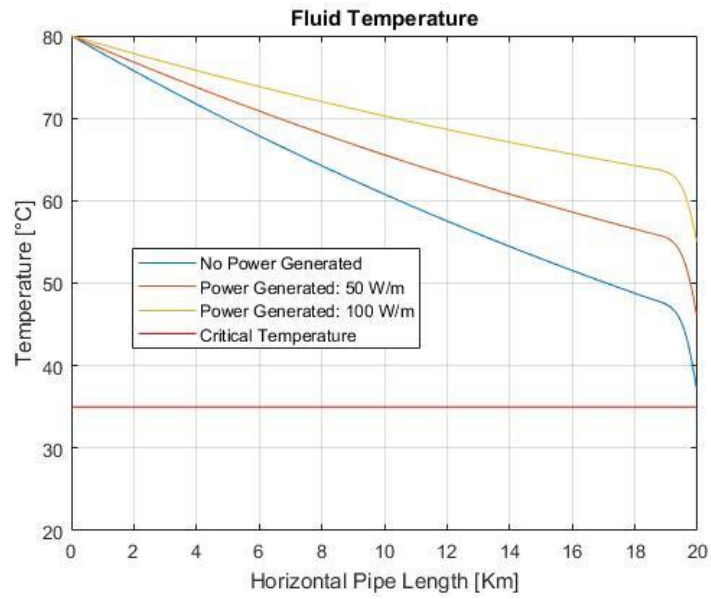


Figure 5.8.1 Fluid Temperature of the pipeline with EHTF technology, nominal flow rate

The simulations are repeated considering a reduced flow rate. The reduction of the warm stream from the reservoir results in a higher heat loss to the environment, as shown in the graph 5.8.2.

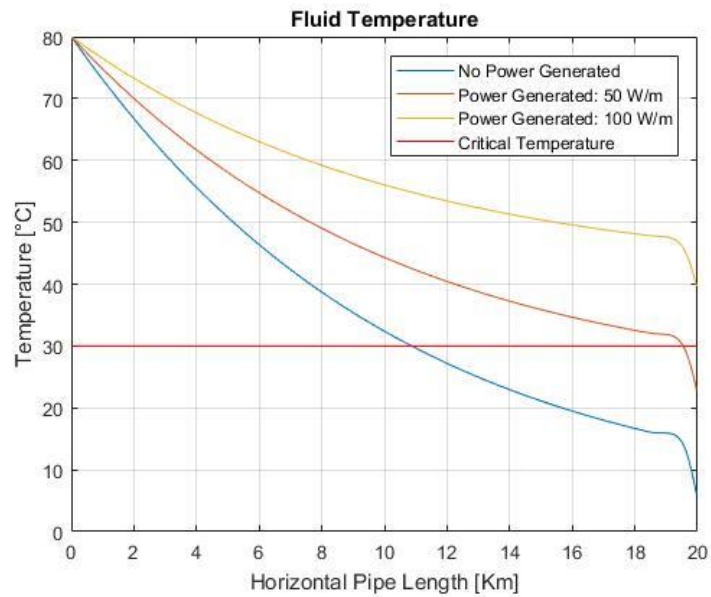


Figure 5.8.2 Fluid Temperature of the pipeline with EHTF technology, reduced flow rate

In this case the heating system must be turned on to avoid the solid depositions inside the flowline. It is worth to note that the required power is lower than the one necessary using the direct electrically heated technology. Such result is in accordance with the higher level of insulation adopted in the electrically heated traced flowline. Furthermore, it is possible to investigate the

effect of the number of the activated wires on the temperature distribution. The results are reported in the figure 5.8.3.

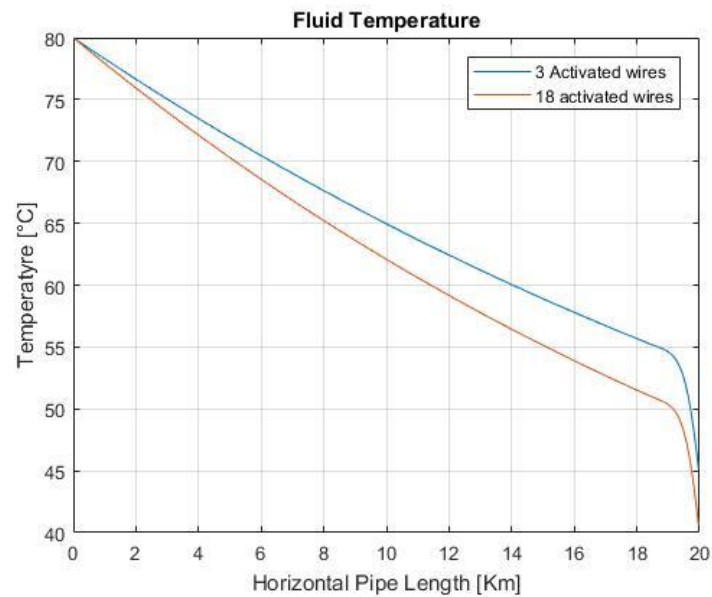


Figure 5.8.3 Fluid Temperature of the pipeline with EHTF technology, nominal flow rate, different activated wires

As can be seen from the above chart, the fluid temperature decreases as the number of activated wires increases. As a matter of fact, the heat losses to the environment described by the equation 3.5.93 increase as the number of heating elements increases.

## 5.9 COMPARISON OF THE DIFFERENT CONFIGURATIONS

In the above paragraphs the different technologies have been simulated to obtain the average temperature distribution inside the flowline. Looking at the different chart is possible to note that the case with only passive insulation must be employed with other conventional flow assurance technologies to avoid problems during the operating conditions. The employment of the direct electrical heating technology allows to operate the flowline inside the steady state operating region. From a thermal point of view, the direct current is more effective than the alternating current. However, the difference is minimal due to the high thermal conductivity and the limited thickness of the carbon steel layer. From the figure 5.5.4, is possible to see that the employment of the direct electrical heating technology allows to reach an equilibrium, which seems independent of the flow rate considered. Meaning that the temperature at the outlet of the flowline is independent from the energy of the produced fluid. However, the energy contained in the stream determines the distance at which the equilibrium is reached. The energy is related to the total flow rate from the reservoir. As a matter of fact, the higher the flow rate the higher the energy of the

stream. The high level of insulation provided by the Pipe-in-Pipe configuration of the electrical heat traced flowline to maintain the flowline inside the steady-state operating region under the nominal operating conditions, as can be seen from the figure 5.7.1. However, active heating is necessary as the flow rate from the reservoir decreases. The power required for the EHTF is lower than the one required by the DEH by one order of magnitude, because of the high level of insulation. Furthermore, for the EHTF the temperature at the end of the flowline depends on the flow rate from the reservoir. As a matter of fact, the required power decreases with hotter fluids and increasing flowrate. The combination of high-performance materials and electrical heating technologies is crucial for the operability of long tie-backs.

## 6 CHAPTER 6: TRANSIENT ANALYSIS OF ACTIVE HEATING TECHNOLOGIES

---

### 6.1 INTRODUCTION TO THE PROBLEM

In this chapter a more realistic production scenario has been considered. The analysis is initially performed using the steady-state electrical heating simulator implemented in MATLAB®. Afterward, OLGA® is employed to analyse the cool down time and start-up of the different technologies. As already mentioned, OLGA® doesn't allow to properly simulate the different electrical heating technologies, however it is still useful to obtain a preliminary analysis of the different solutions. The geometry of the problem is reported in the figure 6.1.1.

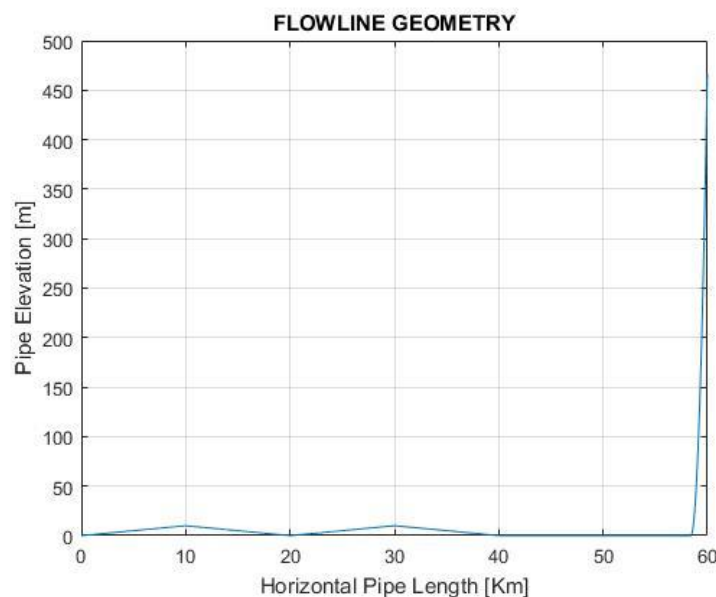


Figure 6.1.1 Geometry of the Problem

As can be seen from the figure above, the horizontal length of the flowline is 60 km. To simulate the irregularity of the sea bottom the first part of the flowline is not perfectly horizontal. The fluid simulated is the same as the one used in the case study presented in the previous chapter. For this reason the critical temperature for solid deposition has been assumed equal to 35°C. The inlet conditions of the flowline are 50°C and 150 bara. The thickness and the materials of the pipe depends on the technology considered. For the DEH, the materials and their relative properties are reported in the table 6.1.1.

MATERIAL	THICKNESS [inch]	DENSITY $\left[\frac{Kg}{m^3}\right]$	CONDUCTIVITY $\left[\frac{W}{mK}\right]$	CAPACITY $\left[\frac{J}{KgK}\right]$
Carbon Steel	0,768	7850	43	470
Polypropylene	2	960	0.4	2200

Table 6.1.1 Material Properties of DEH wall

For the EHTF, the thickness and the properties of the materials are reported in the table 6.1.2.

MATERIAL	THICKNESS [inch]	DENSITY $\left[\frac{Kg}{m^3}\right]$	CONDUCTIVITY $\left[\frac{W}{mK}\right]$	CAPACITY $\left[\frac{J}{KgK}\right]$
Carbon Steel	0,768	7850	43	470
Aspen Aereogel	0,787	110	0,0155	1097
Air	1,095	1,127	0,1	1006,43
Carbon Steel	0,5	7850	45	470
FBE	0,006	1450	0,3	1500
Adhesive	0,006	900	0,3	2100
3LPP	0,102	900	0,3	1700

Table 6.1.2 Material Properties of EHTF wall

## 6.2 STEADY-STATE ANALYSIS

In this paragraph the models implemented in MATLAB® are used to evaluate the temperature distribution inside the flowline. Only the Direct Electrical Heating and Electrical Heat Traced technology have been investigated. The temperature distribution employing the DEH technology is reported in the figure 6.2.1. As can be seen from the figure, the active heating is necessary to avoid the solid deposition inside the flowline. Of course, the higher the power of generation the higher the outlet temperature.

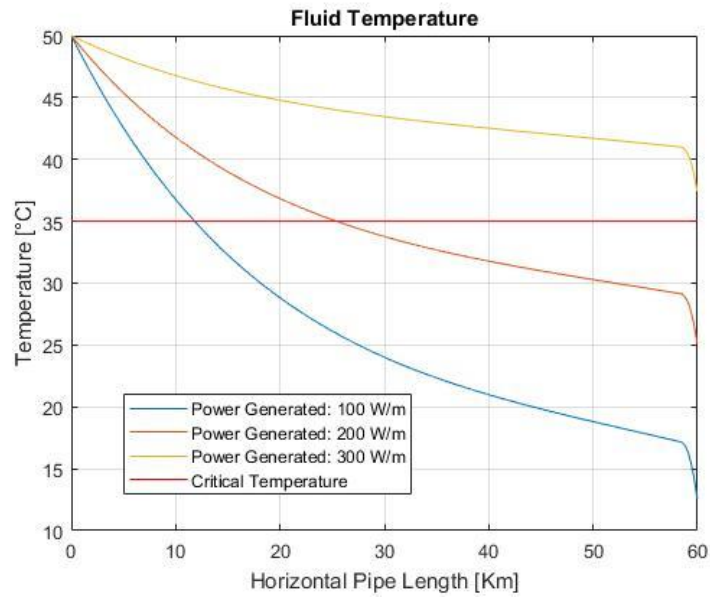


Table 6.2.1 Temperature Distribution DEH

From the above figure a more useful chart can be obtained. This is done plotting the flowline outlet temperature versus the generated power. In this way, it is possible to determine the required power necessary to obtain the desired outlet temperature. Such graph is reported in the figure 6.2.2.

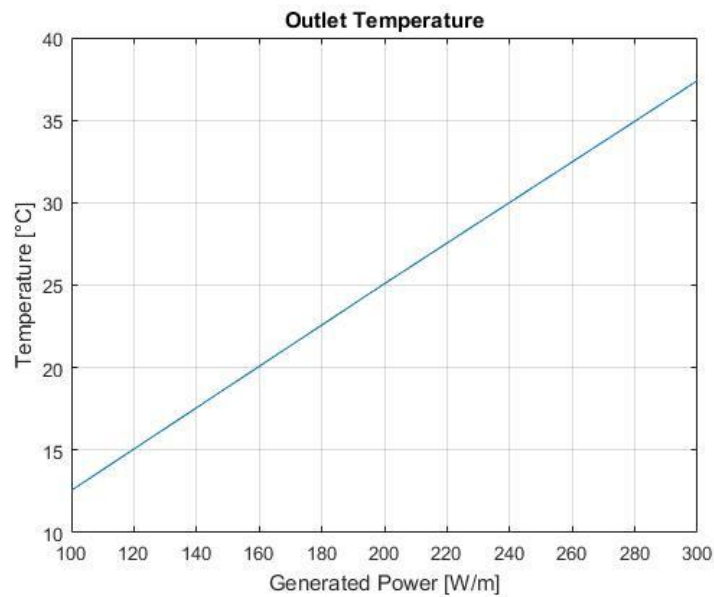


Table 6.2.2 Outlet Temperature VS Generated Power for DEH technology

According to the figure 6.2.2, it is possible to understand that a generated power of  $280 \frac{W}{m}$  is necessary to avoid the risk of solid deposition inside the flowline.

The temperature distribution obtained employing the EHTF technology is reported in the figure 6.2.3.

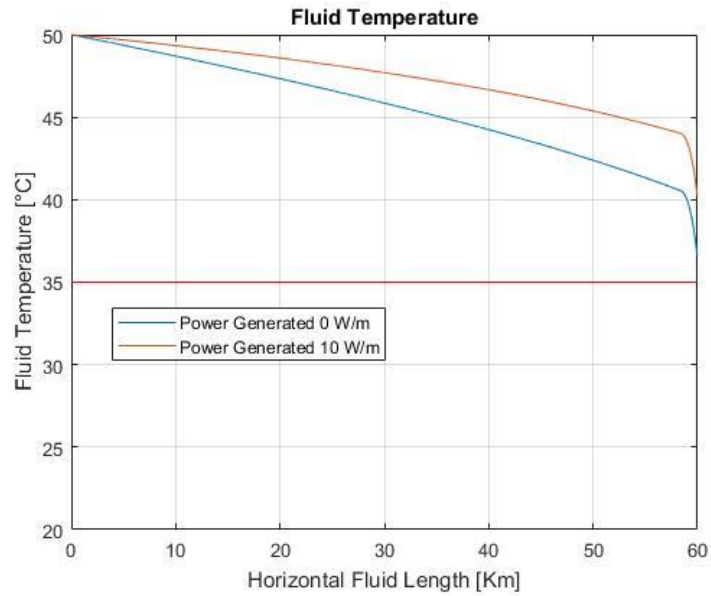


Table 6.2.3 Temperature Distribution EHTF

In this configuration the high level of insulation is enough to maintain the flowline inside the operating steady-state region as can be seen from the figure above. Also, for the EHTF technology is possible to plot the outlet temperature as a function of the generated power. The results are reported in the figure 6.2.4.

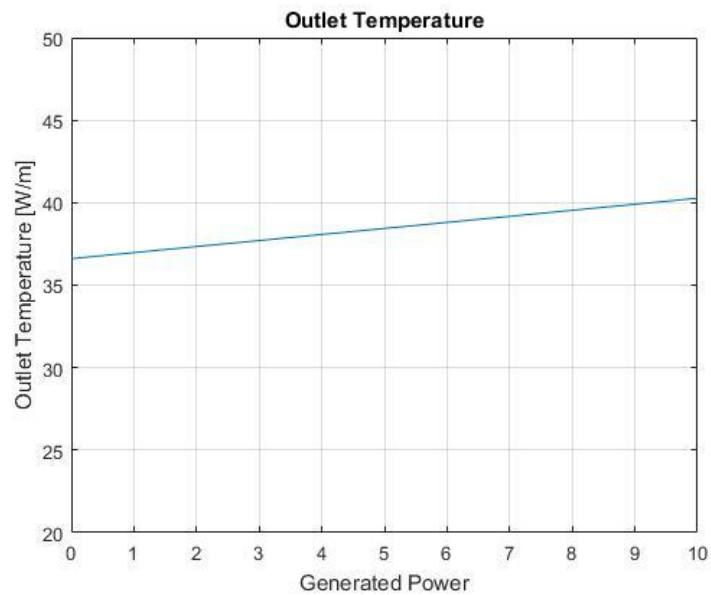


Table 6.2.4 Outlet Temperature Vs Generated Power for EHTF technology

In this scenario the high level of insulation provided by the Pipe-in-Pipe configuration is enough to ensure a safe transportation of hydrocarbon from the wellhead to the receiving facility. However, it is necessary to evaluate also the effect of the technology during the shut-down and start-up of the technology.

### 6.3 PLANNED SHUT-DOWN

In this paragraph the cool down times of the different technology have been analysed. In particular the “no-touch time” has been estimated. The “no-touch time” is defined as the time in which the operators can try to correct the problems without having to take any action to protect the subsea system from hydrates. Certainly, the longer the “no-touch time” the better. It is worth to note that during the shut-down phase there is no flow from the reservoir. Since there is not flow inside the flowline, the critical temperature for solid deposition is the one for the formation of hydrates. It is possible to define a shut-in operating region, i.e. a region where there is no risk of formation of hydrates. In this configuration, the shut-in operating region is reported in the figure 6.3.1.

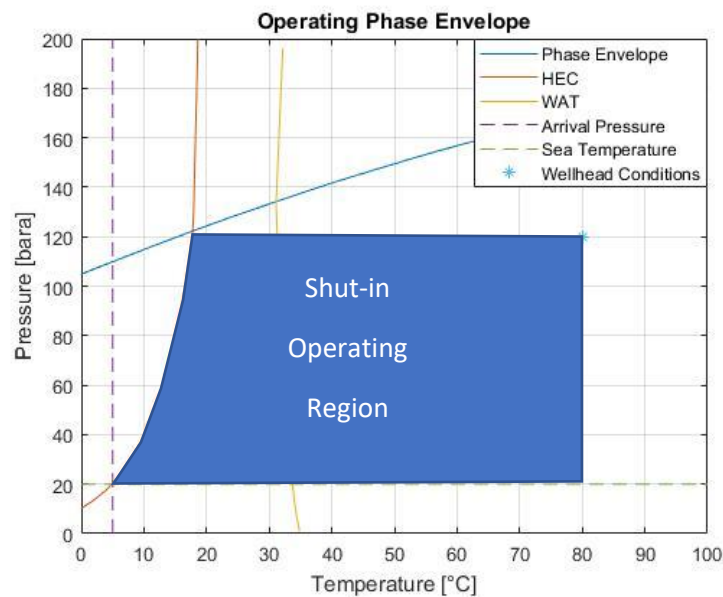


Figure 6.3.1 Shut-in Operating Region

Since the thermal insulation is not perfect heat losses to the environment are inevitable. Active heating technologies can be employed either to increase the “no-touch time” or to maintain the flowline temperature above the hydrate formation temperature. Certainly, the level of generated power changes according to the different applications. In this comparison, a steady-state production has been initially simulated in order to obtain the phase distributions inside the flowline.

Then the flowrate from the reservoir has been stopped and the trend over time of the average minimum temperature inside the flowline has been investigated. The results employing the DEH technology are reported in the figure 6.3.2.

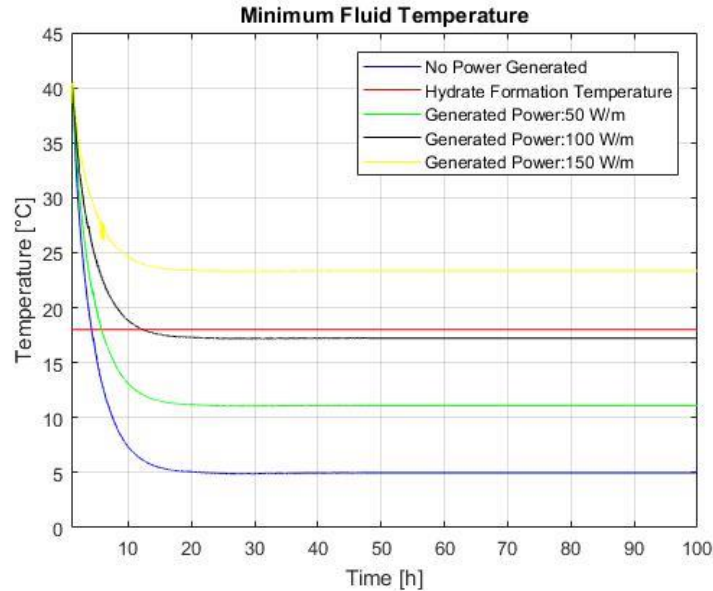


Figure 6.3.2 Variation of the minimum fluid temperature considering different level of generation, DEH technology

As can be seen from the blue line in the above figure, if the electrical heating is turned off the flowline reaches the thermal equilibrium with the surrounding sea water. In this scenario, the flowline risks to get plugged five hours after the shutdown. For this reason, conventional flow assurance technologies must be employed to maintain the system inside the shut-in operating region. As already stated, electrical heating technologies can be applied to increase the “no-touch” time. Obviously, the “no-touch” time increases as the generated power increases, as shown in the figure 6.3.2. Furthermore, it is possible to provide enough power to obtain an infinite “no touch” time. In order to better visualize the effects of the level of generation on the minimum fluid temperature the trends are reported in a logarithmic graph, as presented in the figure 6.3.3.

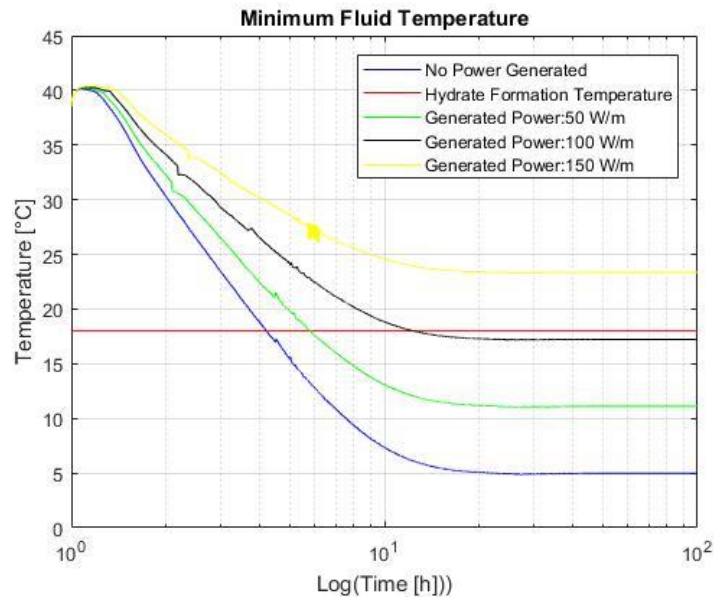


Figure 6.3.3 Logarithmic variation of the minimum temperature inside the flowline, DEH technology

From the charts is possible to see that a generated power slightly higher than  $100 \frac{W}{m}$  is enough to avoid the formation of the hydrates. Obviously, the required power depends on the level of insulation of the flowline. As a matter of fact, the higher the level of insulation the smaller the power required. The planned shutdown phase is simulated also for the EHTF technology. The results are reported in the figure 6.3.3. Analogously, to the previous case if the generated power increases the “no-touch” time increases.

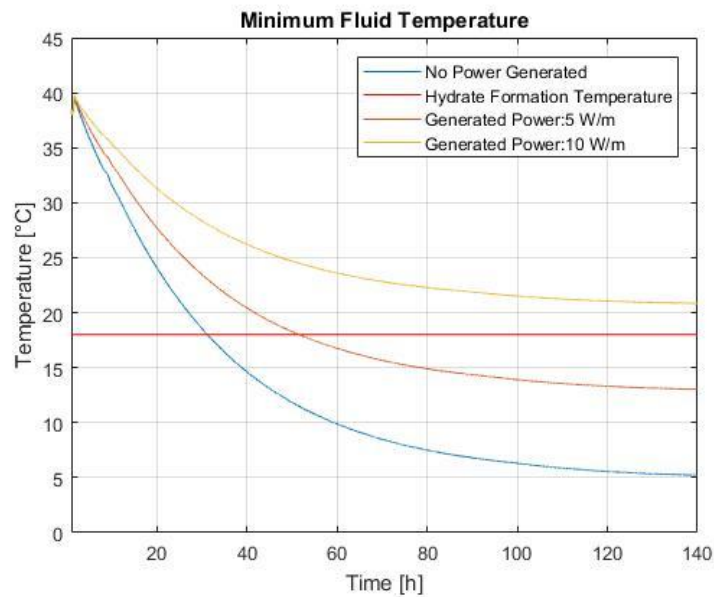


Figure 6.3.4 Variation of the minimum fluid temperature considering different level of generation, EHTF technology

As expected the higher level of insulation results in a longer “no-touch” time compared to the DEH technology. However, also in this configuration hydrates may form if there is no generation of power in the flowline. For this reason, the EHTF technology must be employed to maintain the flowline inside the shut-in operating region.

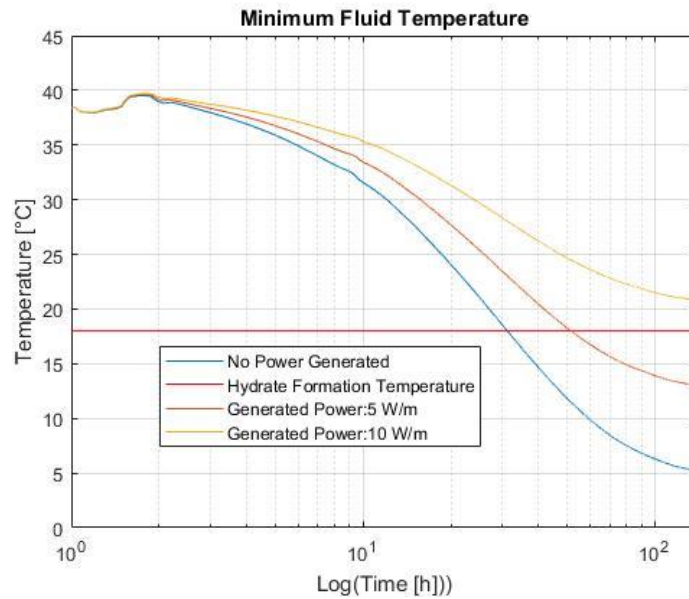


Figure 6.3.5 Logarithmic variation of the minimum temperature inside the flowline, EHTF technology

As can be seen from the above figure the required power for the EHTF technology is one order of magnitude lower than the one required for the DEH technology.

#### 6.4 UNPLANNED SHUT-DOWN

In this paragraph a different scenario has been investigated. The cool down time has been evaluated considering the electrical heating technologies turned off. This is done to evaluate the effects of the level of insulation on the minimum fluid temperature inside the flowline. A steady-state production has been initially simulated to obtain the phases distribution inside the flowline. The flow from the reservoir is then suddenly stopped and the minimum temperature is plotted as a function of time. The trends of the minimum temperature inside the flowline are reported in the figure 6.4.1.

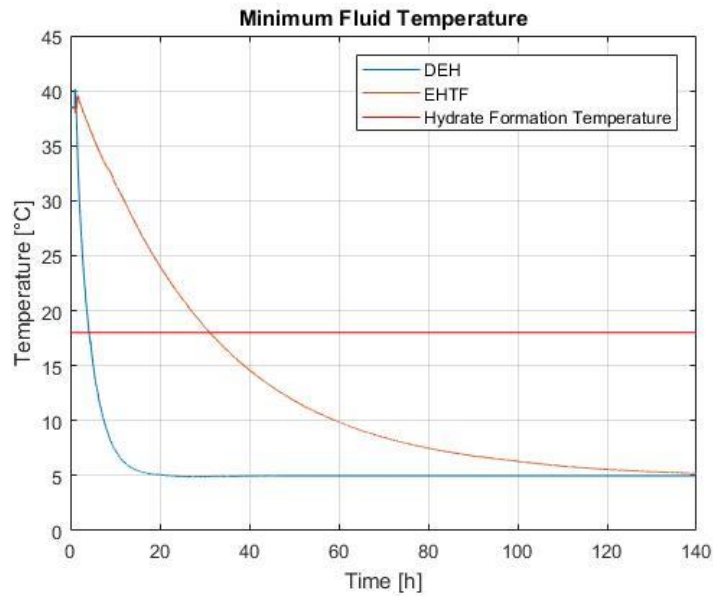


Figure 6.4.1 Minimum Temperature Inside the flowline during a shutdown

As can be expected the high level of insulation provided by the Pipe-in-Pipe configuration of the EHTF results in a longer “no-touch” time than the one obtained applying the DEH technology. In order to better visualize the difference, the results are reported on a logarithmic chart, which is reported in the figure 6.4.2.

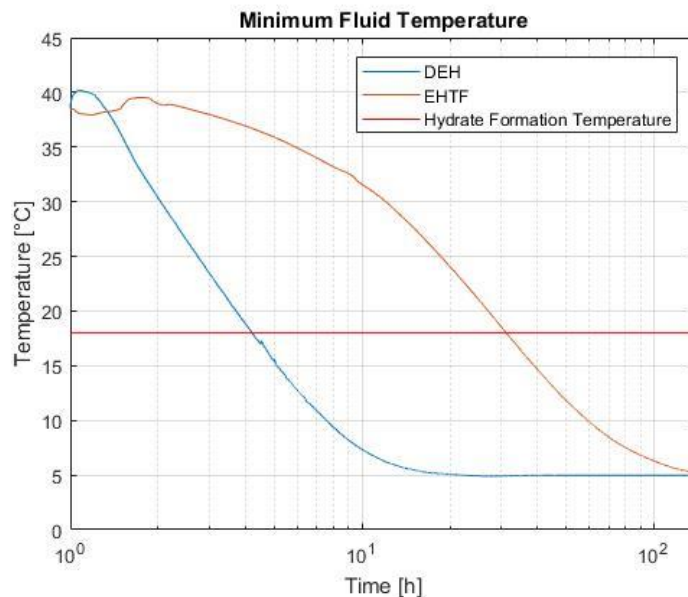


Figure 6.4.2 Minimum Temperature Inside the flowline during a shutdown, logarithmic chart

The higher level of insulation of the EHTF compared to the one of the DEH results in a smaller heat loss to the environment. Hence, the employment of the EHTF technology provides more time to the operator to solve the problem, without the need to perform operation on the flowline.

## 6.5 COLD START UP

The electrical heating technologies can be applied to warm up the flowline during the start-up phase. It is worth to note that the start-up phase should be a rare event as the hydrocarbon flows from the reservoir should be continuous. In this analysis, it has been assumed that the flowline is initially in thermal equilibrium with the surrounding sea water. In order to have the phase distribution inside the flowline at the beginning of the start-up a production scenario has been simulated beforehand. The steady-state production has been simulated for 24h before stopping the flowrate and waiting the flowline to reach the thermal equilibrium with the surrounding sea water. During the start-up phase there is no flow inside the flowline. The simulations are performed for both the DEH and EHTF technologies. The trends of the minimum temperature for the DEH are reported in the figure 6.5.1.

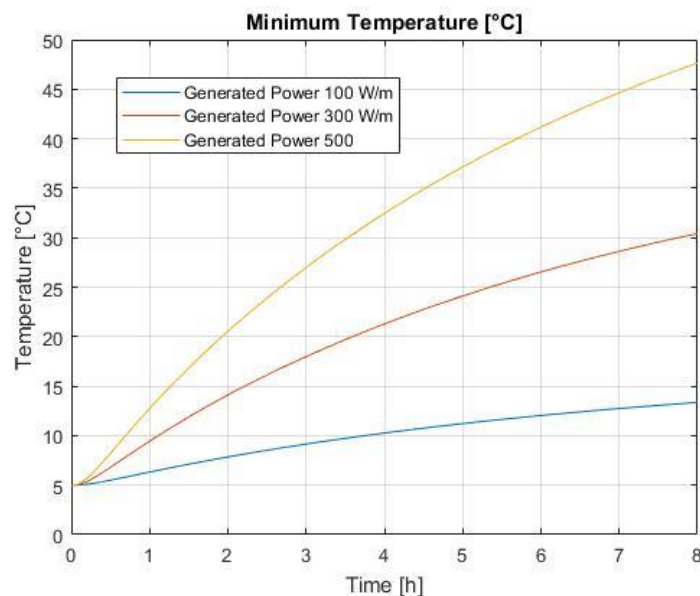


Figure 6.5.1 Minimum Temperature inside the Flowline, DEH technology

Visibly, the available time to start the production is related to power available for the start-up. Furthermore, the employment of the electrical heating technologies avoids the necessity of conventional flow assurance technologies. From the above figure is possible to obtain the minimum temperature as a function of the generated power. It has been assumed 8 hours as the available time to start the production. The chart obtained is reported in the figure 6.5.2.



Figure 6.5.2 Minimum Temperature after 8h as a function of the generated power, DEH technology

From the above figure is possible to see that a generated power of  $350 \frac{W}{m}$  is necessary to bring the fluid temperature from the sea water condition to  $35^{\circ}C$ , which is the critical temperature for solid deposition inside the flowline. The trends for the minimum temperature are obtained also for the EHTF technology. The results are reported in the figure 6.5.3.

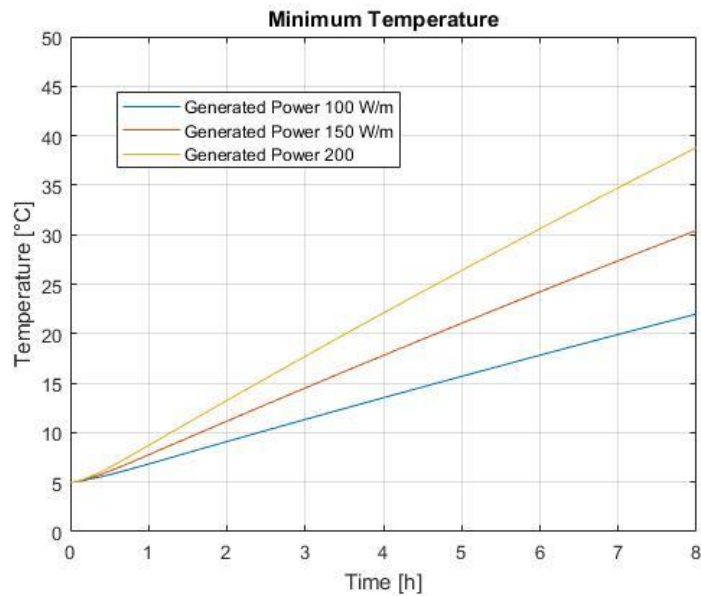


Figure 6.5.3 Minimum Temperature inside the Flowline, EHTF technology

Analogously, it is possible to obtain the minimum temperature after 8h as a function of the generated power. The chart is reported in the figure 6.5.4.

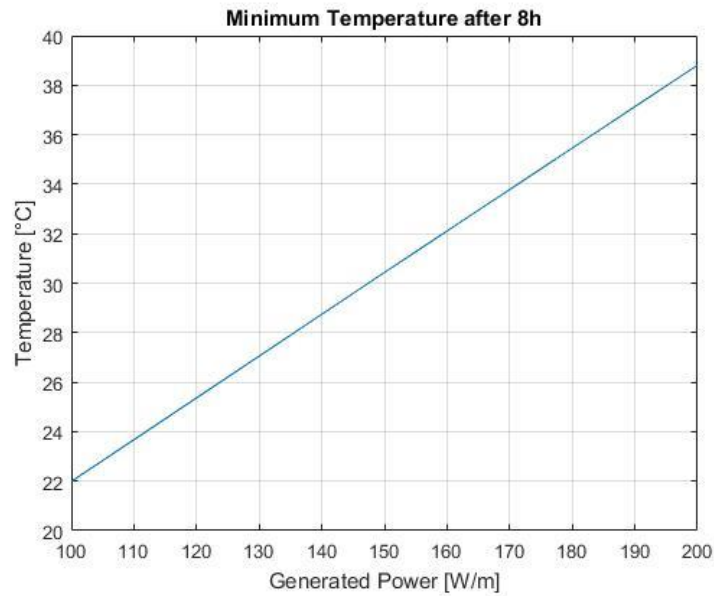


Figure 6.5.4 Minimum Temperature after 8h as a function of the generated power, EHTF technology

As can be expected the high level of insulation provided by the Pipe-in-Pipe configuration results in a smaller power requirement for the EHTF technology compared to the one of the DEH.

## 6.6 FINAL CONSIDERATIONS

The combination of high performance insulating materials and electrical heating is fundamental to ensure the transportation of hydrocarbon fluids from the reservoir to the platform. Furthermore, the electrical heating technology allows to maintain the flowline inside the shut-in operating region during a shut down. As a matter of fact, the employment of the electrical heating technologies increases the “no-touch”, providing to the operators enough time to solve the problem without the need to make operations on the flowline.

## 7 CONCLUSIONS

---

The scope of this study was to analyse the different electrical heating technologies from a flow assurance point of view. In general, the insulation of the pipe is enough to safely transport the hydrocarbon during normal operating conditions. However, if for any reasons the flow from the reservoir decreases or even stops conventional flow assurance technologies must be employed to operate the flowline. As already mentioned, conventional flow assurance technologies may be very expensive. For this reason, more cost-effective solutions have been investigated. The steady-state electrical heating models implemented in MATLAB® allow to simulate the trends of the thermodynamic variables for the different active heating technologies. The models are useful to compare the different solutions from a flow assurance point of view; however, they present some limitations. As already mentioned, the models require as an input the properties of the fluid as a function of pressure and temperature. In this work PVTsim has been used to obtain such properties starting from the fluid composition and employing the Peng-Robinson equation of state. Therefore, two different software must be employed to compare the different technologies. In order to obtain the average fluid properties of the multiphase system the models employ the homogeneous fluid theory, which introduces an approximation on the results. Furthermore, it has been assumed that the flowline is always surrounded by water, and for this reason only the water properties are used to calculate the external heat transfer coefficient. Despite the limitations, the models are useful to obtain general considerations about the different technologies. From the analysis in steady-state of the case study is possible to understand how the electrical heating technologies can be used to maintain the flowline inside the steady-state operating region. From a flow assurance point of view, it has been demonstrated that there is no difference between the employment of a direct current and the employment of an alternating current in the direct electrical heating technology. Furthermore, it has been seen that the combination of the high level of insulation provided by the Pipe-in-Pipe configuration and of the electrical heating is a key aspect for the future of the active heating technologies. As a matter of fact, the required power for the EHTF technology is an order of magnitude smaller than the one required for the DEH technology. The technologies are then also investigated during the shut-down. The passive insulation is only a temporary solution because a heat loss to the environment is inevitable. Hydrates may form during a shut-down as the flowline reaches the thermal equilibrium with the surrounding environment. One of the main advantages, of the electrical heating technologies is the possibility to maintain the flowline inside the shut-in

operating region. Hence conventional flow assurance technologies as depressurization of the line and dead oil displacement are not necessary to protect the pipeline. In addition, the “no-touch” time increases as the generated power increases. The “no-touch” time is the one in which the operators can try to correct problems without having to take any action to protect the subsea system from hydrates. As can be expected the level of insulation plays a crucial role in the calculation of the “no-touch” time. The technologies are then employed to simulate a cold start up, where cold implies that the flowline is initially in thermal equilibrium with the surrounding sea water. The active heating technologies can be used to warm up the fluids inside the flowline. Indeed, the level of generated power depends on the available time to start the production. Once more the combination of the high level of insulation and the active heating is crucial aspect for the operability of the flowline. The focus of this work has been to investigate the different technologies from a flow assurance point of view. From the analysis performed it is clear that the electrical heating technologies can be used to maintain the temperature above the critical level for wax and hydrates depositions. By providing a solution to these flow assurance challenges the electrical heating technologies enable the production from marginal fields that otherwise will result uneconomical. Furthermore, it has been demonstrated the advantages of the employment of the EHTF technology rather than the DEH technology. However, in order to have a complete characterization of the technologies it will be necessary to complete the study with an electrical and economical analysis

## LIST OF FIGURES

---

Figure 2.4.1 Schematic Open Loop Direct Electrical Heating .....	33
Figure 2.4.2 Schematic End-Fed Pipe-in-Pipe DEH.....	34
Figure 2.4.3 Skin and Proximity Effects.....	35
Figure 2.4.4 Schematic Center-Fed Pipe-in-Pipe DEH .....	35
Figure 2.5.1 Schematic of the EHTF Pipe-in-Pipe .....	36
Figure 3.2.1 Example of discretization of the line.....	40
Figure 3.2.2 Flow Diagram of the model.....	41
Figure 3.2.3 Flow Diagram of the simulator for the <i>ith</i> element .....	41
Figure 3.4.1 Control Volume for balance equations .....	44
Figure 3.5.1 Cross Section of the pipeline.....	50
Figure 3.5.2 Thermal Equivalent Circuit.....	50
Figure 3.5.3 Cross Section of the Flowline .....	52
Figure 3.5.4 Cross Section of the Flowline .....	55
Figure 3.5.5 Cross Section EHTF .....	59
Figure 3.5.6 Section of the element considered for the heat transfer .....	59
Figure 3.5.7 Section neglecting the curvature radius .....	60
Figure 3.5.8 Geometry of the simplified problem.....	60
Figure 3.5.9 Equivalent thermal circuit of the insulating layer and convective heat transfer with the surrounding water .....	61
Figure 3.5.10 Geometry of the carbon steel layer and relative properties .....	62
Figure 3.5.11 Equivalent thermal circuit from the cable to the surrounding water.....	65
Figure 4.2.1 Temperature variation inside the flowline.....	72
Figure 4.2.2 Pressure variation inside the flowline.....	73
Figure 4.3.1 Geometry of the Flowline .....	74
Figure 4.3.2 Temperature variation of the flowline.....	74
Figure 4.3.3 Pressure variation inside the flowline.....	75
Figure 4.4.1 Comparison of the Temperature distributions obtained with OLGA and with the Steady-State model.....	76
Figure 5.1.1 Geometry of the Case Study .....	77
Figure 5.1.2 Phase Envelope .....	78
Figure 5.1.3 Operating Phase Envelope .....	78
Figure 5.1.4 Steady-State Operating Region .....	79
Figure 5.2.1 Fluid Temperature of the 2 inches insulated flowline, nominal flowrate .....	80
Figure 5.2.2 Fluid Pressure of the 2 inches insulated flowline, nominal flowrate .....	81
Figure 5.2.3 Gas Volumetric fraction of the 2 inches insulated flowline, nominal flow rate .....	81
Figure 5.2.4 Fluid Temperature of the 2 inches insulated flowline, reduced flowrate .....	82
Figure 5.2.5 Fluid Temperature of the 2 inches insulated flowline .....	83
Figure 5.3.1 Fluid Temperature of the 1/2 inches insulated flowline, nominal flowrate .....	83

Figure 5.3.2 Fluid Temperature of the 1/2 inches insulated flowline, reduced flowrate .....	84
Figure 5.3.3 Fluid Temperature of the 1/2 inch insulated flowline .....	85
Figure 5.4.1 Effects of the level of insulation on the temperature distribution .....	85
Figure 5.5.1 Fluid Temperature of the pipeline with DEH technology, nominal flow rate .....	86
Figure 5.5.2 Outlet Temperature as a function of the generated power .....	87
Figure 5.5.3 Fluid Temperature of the pipeline with DEH (DC) technology, reduced flow rate .....	88
Figure 5.5.4 Fluid Temperature considering different flow rates, Power generated 700 W/m .....	89
Figure 5.6.1 Fluid temperature, nominal flow rate and 50 Hz alternating current .....	89
Figure 5.6.2 Fluid temperature, reduced flow rate and 50 Hz alternating current .....	90
Figure 5.6.3 Fluid Temperature considering different frequencies .....	91
Figure 5.7.1 Fluid Temperature according different current distributions .....	92
Figure 5.7.2 Temperature difference between direct current and alternating current .....	93
Figure 5.8.1 Fluid Temperature of the pipeline with EHTF technology, nominal flow rate .....	94
Figure 5.8.2 Fluid Temperature of the pipeline with EHTF technology, reduced flow rate .....	94
Figure 5.8.3 Fluid Temperature of the pipeline with EHTF technology, nominal flow rate, different activated wires .....	95
Figure 6.1.1 Geometry of the Problem .....	97
Figure 6.3.1 Shut-in Operating Region .....	101
Figure 6.3.2 Variation of the minimum fluid temperature considering different level of generation, DEH technology .....	102
Figure 6.3.3 Logarithmic variation of the minimum temperature inside the flowline, DEH technology .....	103
Figure 6.3.4 Variation of the minimum fluid temperature considering different level of generation, EHTF technology .....	103
Figure 6.3.5 Logarithmic variation of the minimum temperature inside the flowline, EHTF technology .....	104
Figure 6.4.1 Minimum Temperature Inside the flowline during a shutdown .....	105
Figure 6.4.2 Minimum Temperature Inside the flowline during a shutdown, logarithmic chart ..	105
Figure 6.5.1 Minimum Temperature inside the Flowline, DEH technology .....	106
Figure 6.5.2 Minimum Temperature after 8h as a function of the generated power, DEH technology .....	107
Figure 6.5.3 Minimum Temperature inside the Flowline, EHTF technology .....	107
Figure 6.5.4 Minimum Temperature after 8h as a function of the generated power, EHTF technology .....	108

## NOMENCLATURE

---

$A$	Matrix of the coefficients
$A_c$	Cross sectional area [ $m^2$ ]
$\mathbf{b}$	Vector of the known terms
$C_{1,2,3,4,5,6}$	Constants of integration
$C$	Chisholm Parameter
$\mathbf{c}$	Vector of the unknowns
$\bar{c}p_{mix}$	Average specific heat at constant pressure of the mixture [ $J/kgK$ ]
$D$	Hydraulic Diameter [ $m$ ]
$dA$	Infinitesimal area [ $m^2$ ]
$DEH$	Direct Electrical Heating
$dQ$	Infinitesimal heat flow [ $m^2$ ]
$e$	Internal energy per unit mass [ $J/kg$ ]
$\bar{e}_b$	Bulk internal energy per unit mass [ $J/kg$ ]
$EHTF$	Electrically Heat-Traced Flowline
$f$	Darcy- Weisbach friction factor
$F_p$	Flow pattern factor
$F_s$	Shape Factor
$G$	Mass Flux [ $kg/m$ ]
$g$	Acceleration due to gravity [ $m/s^2$ ]
$H$	Head [ $m$ ]
$H_{cs}$	Thickness carbon steel [ $m$ ]
$H_{ins}$	Thickness insulating material [ $m$ ]
$h$	Convective Heat transfer coefficient [ $W/Km^2$ ]
$I$	Inclination Factor
$k$	Thermal conductivity
$\bar{k}_b$	Bulk kinetic energy per unit mass [ $J/kg$ ]
$L$	Length of the section [ $m$ ]
$M$	Generic fluid Property
$m^2$	Fin Parameter
$Nu$	Nusselt Number
$p$	Pressure [ $Pa$ ]
$Pr$	Prandtl Number
$p_1, p_2$	Wetted Perimeter $m$ ]
$Q$	Heat Flow [ $W$ ]
$Q_{gen}$	Heat Generated [ $W$ ]
$Q_{loss}$	Heat loss to the environment [ $W$ ]
$R$	Thermal Resistance [ $K/W$ ]
$Ra$	Rayleigh Number
$Re$	Reynolds Number
$Re_L$	Liquid insitu Reynolds Number
$\bar{R}_b$	Dissipation of mechanical energy
$S$	Generated Power per unit volume [ $W/m^3$ ]

$s$	Slip ratio
$T$	Temperature [ $^{\circ}\text{C}$ ]
$X$	Lockhart-Martinelli Parameter
$x$	Mass quality
$\bar{u}$	Cross section averaged velocity [m/s]
$v$	Specific volume [ $\text{kg}/\text{m}^3$ ]
$\bar{v}_b$	Bulk specific volume [ $\text{kg}/\text{m}^3$ ]
$z$	Axial direction [m]
$\Delta P$	Pressure Variation [Pa]
$\Delta T$	Temperature Variation [ $^{\circ}\text{C}$ ]
$\Delta P/Dz$	Pressure Gradient [ $\text{Pa}/\text{m}$ ]

### Greek Symbols

$\alpha$	Void Fraction
$\beta$	Thermal expansion coefficient [ $1/\text{K}$ ]
$\Gamma$	Mass flow [ $\text{kg}/\text{s}$ ]
$\delta$	Skin Depth [m]
$\vartheta$	Inclination of the pipe to the horizontal [rad]
$\theta$	Excess Temperature [ $^{\circ}\text{C}$ ]
$\mu_G$	Dynamic Viscosity Gas [ $\text{Pa s}$ ]
$\mu_L$	Dynamic Viscosity Liquid [ $\text{Pa s}$ ]
$\mu_o$	Permeability void [ $\text{H}/\text{m}$ ]
$\mu_r$	Relative permeability
$\nu$	Kinematic Viscosity [ $\text{m}^2/\text{s}$ ]
$\rho$	Density [ $\text{kg}/\text{m}^3$ ]
$\bar{\rho}_b$	Bulk Density [ $\text{kg}/\text{m}^3$ ]
$\tau$	Central Angle for the calculation of the environmental losses [rad]
$\Phi^2$	Two-phase friction multiplier
$\psi$	Central Angle EHTF [rad]

### Subscripts

$cs$	Carbon steel
$eq$	Equivalent
$g$	Gas
$i$	Internal
$ins$	Insulating material
$JT$	Joule Thompson
$l$	Liquid
$o, eq$	Outer equivalent
$th$	Thermal
$tot$	Total
$tp$	Two Phase
$w$	Water

## BIBLIOGRAPHY

---

- [1] S. Denniel, J. Perrin, A. Felix-Henry, 'Review of flow assurance solutions for deepwater fields', OTC 16686. May 2004.
- [2] E.Louvet, S. Giraudbit, B. Seguin and R. Sathananthan, 'Active heated pipe technologies for field development optimization', OTC-26578-MS. March 2016.
- [3] [Petrowiki.org/hydrates](http://Petrowiki.org/hydrates)
- [4] <http://www.offshore-mag.com/articles/print/volume-70/issue-6/subsea/flow-assurance-chemical-inhibition-of-gas-hydrates-in-deepwater-production-systems.html>
- [5] J.Peytavy,P.Glènst,P.Bourg, 'Qualification of Low dose hydrate inhibitors field cases studies demonstrate the good reproducibility of the results obtained from flow loops', ICGH 2008. July 2008.
- [6] [http://petrowiki.org/index.php?title=Wax\\_problems\\_in\\_production&printable=yes](http://petrowiki.org/index.php?title=Wax_problems_in_production&printable=yes)
- [7] S. Easton, R. Sathananthan, 'Enhanced flow assurance by active heating within towed production systems'. January 2002.
- [8] R. Fisher Roth, R. Voigths, 'Direct Electrical Heating provides new opportunities for arctic pipelines', OTC 23732. December 2012.
- [9] L. Delebeque, E.Sibaud, M. Scocard, C. Rueda, P. Delbene , 'Active heating technologies for flowlines in deep water field development', OMC-2009-074. March 2009
- [10] S. Cherkaoui, J. Verdeil, S. Giraudbit, C. Geertsen, 'Electrically Heat-Traced Flowline Technology-Key Enabler for Optimized Field Architecture Developments and Operated Fields with High Thermal Performances Requirements', OTC-27100-MS,. May 2016.
- [11] F. Lirola, A. Pouplin, N. Settouti, J. Agoumi, 'Technical Assessment and Qualification of local and distributed active heating technologies', OMC-2017-554. March 2017.
- [12] <https://www.pvtsimnova.com>

- [13] L. Colombo, 'Lecture notes of the course: Multiphase systems and Technologies, Momentum and Energy Balance', 2017
- [14] Y. Xu, X. Fang, X. Su, Z. Zhou, W. Chen, 'Evaluations of frictional pressure drop correlations for two-phase flow in pipes', Nuclear Engineering and design 253 (2012) 86-97, . August 2012.
- [15] T.L. Bergaman, A.S. Lavine, F.P. Incropera, D.P. Dewitt, 'Fundamentals of heat and mass transfer, chapter 3 One-Dimensional Steady State Conduction: Thermal Resistances', 2011
- [16] T.L. Bergaman, A.S. Lavine, F.P. Incropera, D.P. Dewitt, 'Fundamentals of heat and mass transfer, chapter 3 One-Dimensional Steady State Conduction: Conduction with thermal energy generation-radial systems', 2011
- [17] T.L. Bergaman, A.S. Lavine, F.P. Incropera, D.P. Dewitt, 'Fundamentals of heat and mass transfer, chapter 3 One-Dimensional Steady State Conduction: Heat Transfer from extended surfaces', 2011
- [18] C. Tang, A. Ghajar, 'Validation of a general heat transfer correlation for Non-Boiling Two-Phase flow with different flow patterns and Pipe', HT2007-32219. January 2007.
- [19] K.G. Nayar, M.H. Sharqawy, L.D. Banchik, J.H. Lienhard, 'Thermophysical properties of seawater: A review and new correlation that include pressure dependence', V, 2016
- [20] M. H. Sharqawy, J.H. Lienhard V, S.M. Zubair, 'Thermophysical properties of seawater: A review of existing correlations and data', Desalination and Water Treatment, Vol. 16 pp.354-380. April 2010
- [21] T.L. Bergaman, A.S. Lavine, F.P. Incropera, D.P. Dewitt, 'Fundamentals of heat and mass transfer, chapter 9 Free convection: The long horizontal cylinder', 2011
- [22] T.L. Bergaman, A.S. Lavine, F.P. Incropera, D.P. Dewitt, 'Fundamentals of heat and mass transfer, chapter 7 External flow: The cylinder in cross flow', 2011
- [23] J.K. Lervik, M. Hoyer-Hansen, 'New Developments of Direct Electrical Heating for Flow Assurance', ISOPE. June 2012